

FINAL REPORT

Third-Generation (3G) Site Characterization: Cryogenic Core
Collection and High-Throughput Core Analysis -
An Addendum to Basic Research Addressing Contaminants in
Low Permeability Zones - A State of the Science Review

SERDP Project ER-1740

JULY 2016

Tom Sale
Saeed Kiaalhosseini
Mitchell Olson
Colorado State University

Richard Johnson
Oregon Health & Science University

Rick Rogers
Drilling Engineers Inc.

Distribution Statement A

This document has been cleared for public release



Page Intentionally Left Blank

This report was prepared under contract to the Department of Defense Strategic Environmental Research and Development Program (SERDP). The publication of this report does not indicate endorsement by the Department of Defense, nor should the contents be construed as reflecting the official policy or position of the Department of Defense. Reference herein to any specific commercial product, process, or service by trade name, trademark, manufacturer, or otherwise, does not necessarily constitute or imply its endorsement, recommendation, or favoring by the Department of Defense.

Page Intentionally Left Blank

REPORT DOCUMENTATION PAGE

Form Approved
OMB No. 0704-0188

The public reporting burden for this collection of information is estimated to average 1 hour per response, including the time for reviewing instructions, searching existing data sources, gathering and maintaining the data needed, and completing and reviewing the collection of information. Send comments regarding this burden estimate or any other aspect of this collection of information, including suggestions for reducing the burden, to Department of Defense, Washington Headquarters Services, Directorate for Information Operations and Reports (0704-0188), 1215 Jefferson Davis Highway, Suite 1204, Arlington, VA 22202-4302. Respondents should be aware that notwithstanding any other provision of law, no person shall be subject to any penalty for failing to comply with a collection of information if it does not display a currently valid OMB control number.
PLEASE DO NOT RETURN YOUR FORM TO THE ABOVE ADDRESS.

1. REPORT DATE (DD-MM-YYYY) 07/29/2016		2. REPORT TYPE Final Report		3. DATES COVERED (From - To) 05/17/2010 - 10/30/2015	
4. TITLE AND SUBTITLE Third-Generation (3G) Site Characterization: Cryogenic Core Collection and High-Throughput Core Analysis				5a. CONTRACT NUMBER W912HQ-10-C-0061	
				5b. GRANT NUMBER	
				5c. PROGRAM ELEMENT NUMBER	
6. AUTHOR(S) Dr. Tom Sale Colorado State University				5d. PROJECT NUMBER ER-1740	
				5e. TASK NUMBER	
				5f. WORK UNIT NUMBER	
7. PERFORMING ORGANIZATION NAME(S) AND ADDRESS(ES) 1320 Campus Delivery Department of Civil and Environmental Engineering Fort Collins, CO 80523-1320				8. PERFORMING ORGANIZATION REPORT NUMBER	
9. SPONSORING/MONITORING AGENCY NAME(S) AND ADDRESS(ES) Strategic Environmental Research and Development Program 4800 Mark Center Drive Suite 17D03 Alexandria, VA 22350-3605				10. SPONSOR/MONITOR'S ACRONYM(S) SERDP	
				11. SPONSOR/MONITOR'S REPORT NUMBER(S)	
12. DISTRIBUTION/AVAILABILITY STATEMENT Approved for public release; distribution is unlimited.					
13. SUPPLEMENTARY NOTES N/A					
14. ABSTRACT The overarching objective of this project is to advance new knowledge that will support comprehensive strategies for managing releases of chlorinated solvents and other persistent contaminants in groundwater in unconsolidated sediments.					
15. SUBJECT TERMS N/A					
16. SECURITY CLASSIFICATION OF:			17. LIMITATION OF ABSTRACT	18. NUMBER OF PAGES	19a. NAME OF RESPONSIBLE PERSON
a. REPORT	b. ABSTRACT	c. THIS PAGE			Dr. Tom Sale
U	U	U	UU	126	19b. TELEPHONE NUMBER (Include area code) 970-491-8413

Page Intentionally Left Blank

Abstract

Objectives

Modern contaminant hydrology has brought us to the realization that decisions regarding management of subsurface contamination at Department of Defense (DoD) facilities need to be based on an understanding of all contaminant phases (i.e., aqueous, non-aqueous-liquid, sorbed, and vapor) and the biogeochemical conditions in which the contaminants are present. The practical approach for collection and analysis of frozen-cores presented here represents an important new tool for improving that understanding. Uniquely, core samples frozen *in situ* before recovery can preserve pore fluids, volatile compounds, dissolved gases, redox conditions, mineralogy, microbial ecology, and pore structure. Furthermore, *in situ* freezing improves quality of recovered core by preventing materials from dropping out of sample liners during recovery to ground surface. Collectively, steps followed for collecting frozen cores are referred to here as cryogenic core collection (C₃).

Because freezing provides effective field preservation, frozen cores can be processed efficiently under controlled laboratory conditions to resolve a broad spectrum of chemical, physical and biological characteristics. Critically, processing core in the laboratory simplifies field work and improves the resources (e.g., anaerobic chambers) that can be utilized in preparation of samples for analysis. Furthermore, laboratory processing frozen cores allows “production line” processing and analysis of large quantities of samples, referred to here as high-throughput core analysis.

Building on these ideas, the overarching objectives of this research are to:

- Demonstrate the efficacy of cryogenic core collection and high-throughput core analysis for site characterization
- Develop standard operating procedure for cryogenic core collection and high-throughput core analysis

Technical Approach

Cryogenic Core Collection - C₃ has been considered by others, including most recently Johnson et al. (2012) as part of SERDP- ER-1559. One of the key limitations of previous cryogenic methods is their ability to collect large amounts of core in often-challenging media in support of site characterization. Necessary elements for large-scale site characterization using cryogenic core collection include fast freezing, operating procedures and equipment that are compatible with standard drilling techniques, the ability to penetrate hard formations and an efficient process for removal of frozen cores from core barrels. At the same time, cryogenic core collection has several potential advantages over conventional core collection in that it minimizes sample loss during the recovery process, facilitates high-throughput sampling, and can potentially help control problematic flowing sands.

Herein, standard hollow stem auger (HSA) drilling equipment (e.g., CME-55/75) and sampling systems (CME Continuous Sample Tube Systems) have been adapted to collect cryogenic core. Specifically, either a copper coil or dual-wall cooling cylinder are placed in a CME Continuous

Sample Tube System. Liquid nitrogen (LN) is circulated through the coil or dual-wall cooling cylinder to affect *in situ* freezing of core in polyvinyl chloride (PVC) sample liners.

Critical element of the freezing system include: a) using insulation in the sample barrel to maximize delivery of coolant to the core versus the drill pipe/formation, b) increasing back pressure on the LN line once freezing temperatures reach the LN discharge at grade to hold LN in the cooling coil/barrel, c) limiting sample drives to 2.5 feet to maximize recovery, d) using insulation on all LN lines to focus cooling capacities onto the sample, and e) using sample coring, versus driving, techniques to minimize sample disturbance.

The described methods were iteratively developed through seven field efforts, including work at the Drilling Engineers Inc. facility in Fort Collins, CO; Colorado State University's (CSU's) Agricultural Research Development & Education Center (ARDEC) facility near Fort Collins, CO; F.E. Warren (FEW) AFB in Cheyenne, WY; and a former refinery near Casper, WY. Work at the refinery was funded by Chevron.

High-Throughput Core Analysis (HTCA). High-throughput core analysis focused on the cores collected from FEW AFB. Cores were kept frozen from the time of collection until processing in the lab at CSU. Sub-samples were obtained by chopping the frozen cores into 1-inch thick disks, referred to as "hockey pucks". One sub-sample was recovered for every four inches of frozen core. Each 1-inch-thick frozen sub-sample was further divided into quarters for subsequent extractions and/or analyses. Sub-samples were analyzed for target contaminants, dissolved gases, inorganic ions (chloride, nitrate, and sulfate), pH, oxidation/reduction potential (ORP), and water content. Select subsamples were characterized for biological community, hydraulic conductivity and particle size distribution. In addition, funds provided by GE were used to explore the use of medical Computer Tomography (CT) and Magnetic Resonance Imaging (MRI) scanning equipment to characterize non-aqueous phase liquids (NAPLs) in the intact frozen core.

Results

Cryogenic core collection. Over the course of the field demonstrations, the efficiency of cryogenic core collection greatly improved. The time required to freeze a section of core was reduced from ~50 minutes to ~5 minutes. At FEW AFB, 52 feet of frozen-core were collected over two days of field effort. At the former refinery site, 36 feet of frozen-core were collected in one day. With the exception of caliche beds at FEW and large cobbles at the refinery, frozen cores with recoveries near 100 % were obtained.

High-throughput core analysis. High-throughput core analysis methods provided high-resolution definition of aqueous-, sorbed-, and gas-phase contaminants with detection limits as low as (10 µg/kg). In addition, frozen core was used to resolve geology, microbial ecology, mineralogy, and permeability. An intriguing result is that methane in the core was detected as well. In locations where both TCE and methane were present, inverse correlations were observed. With respect to use of medical scanning equipment funded by GE, CT scans were not useful for NAPL detection. However, MRI of frozen core was able to identify NAPLs when present in the cores. A key result was the realization that freezing water suppresses the MRI signal from the protons in the frozen water, while the signal from the NAPL (which remained a liquid at -20C) was not attenuated.

Benefits

The combination of cryogenic core collection and high-throughput sampling yielded high quality samples suitable for a wide range of chemical, physical and biological analyses. The protocols for sample collection and processing are sufficiently robust that they can now be used routinely at field sites.

Table of Contents

Abstract	2
List of Tables	8
List of Figures	9
List of Acronyms	12
Keywords	14
Acknowledgements	15
Chapter 1: Introduction	16
1.1 Problem Statement	16
1.2 Research Hypotheses	16
1.3 Objectives.....	17
1.4 Report Content.....	17
Chapter 2: Background	18
2.1 Limitations of 1G and 2G Site Characterization Methods	18
2.2 Factors Controlling Recovery of Representative Samples.....	18
2.3 Issues with Preservation of Subsurface Samples.....	20
2.4 Limitation of Advanced Core Collection Methods.....	21
Chapter 3: Cryogenic Core Collection	24
3.1 Methods.....	24
3.1.1 Locations and Dates of Cryogenic Coring Field Work	24
3.1.2 Drilling Methods.....	25
3.1.3 Modifications to Existing CME Continuous Sample Tube System.....	26
3.1.4 Cryogenic sampling systems	27
3.1.5 Critical Variables for Development of Cryogenic Coring Tools.....	29
3.1.6 Performance Assessment Metrics	30
3.2 Results and Discussion	34
3.2.1 Final Design of System Components and Methods.....	34
3.2.2 Performance with Respect to the Key Metrics	39
Chapter 4: High-Throughput Core Analysis -1- Frozen Core Sub-sampling	42
4.1 Materials and Methods	42
4.1.1 Materials and Equipment	42
4.2 Frozen Core Processing.....	43
4.3 Analytical Methods.....	45

4.3.1	Biological Analysis.....	45
4.3.2	Organic Compound Analysis.....	46
4.3.3	Dissolved Gases and Water-Extractable VOCs	47
4.3.4	Inorganic Analysis and Parameters.....	49
4.3.5	Total Petroleum Hydrocarbons (GRO, DRO and Benzene).....	50
4.3.6	Geologic Logging	51
4.3.7	Hydraulic Conductivity Testing.....	51
4.3.8	Fraction Organic Carbon.....	54
4.3.9	Density and Water Content.....	55
4.4	High-Throughput Core Analysis: Results	55
4.4.1	FEW Total VOC Concentration.....	55
4.4.2	FEW Dissolved Gases and Water-Extractable VOCs.....	57
4.4.3	FEW Aqueous and Sorbed Phases	58
4.4.4	FEW Inorganic Analytes.....	61
4.4.5	FEW pH and ORP.....	63
4.4.6	FEW AFB Geology	64
4.4.7	Hydraulic Conductivity.....	65
4.4.8	FEW AFB Density and Water Content.....	66
4.4.9	FEW Microbial Ecology.....	67
4.4.10	Data Panels.....	69
4.4.11	Comparison of “2G”, and “3G” Methods at FEW AFB.....	74
4.4.12	GRO, DRO and Benzene in Soils at the Former Refinery	75
Chapter 5:	High-Throughput Core Analysis. 2 – Frozen Core Scanning.....	76
5.1.	Frozen Core Scanning Methods.....	76
5.1.1	Materials and Sample Preparation.....	76
5.1.2	Magnetic Resonance Imaging.....	76
5.2	Frozen Core Scanning Results	79
5.2.3	Magnetic Resonance Imaging.....	80
Chapter 6:	Conclusions and Implications.....	82
6.1	Key Findings	82
6.1.1	An efficient method for cryogenic core collection was developed.....	82
6.1.2	Frozen core recovery was excellent.	82
6.1.3	Field processing of core samples is simplified.	82
6.1.4	Intact frozen core well is suited for geophysical scanning.....	82

6.1.5	Cores frozen <i>in situ</i> provide access to additional analyses.....	83
6.1.6	High-throughput core analysis represents a practical approach to obtain a high density of information from cores.	83
6.1.7	Data fusion adds value above and beyond the individual analyses	83
6.1.8	Confidence in accuracy of the depth interval sampled was significantly improved due to improved recovery.	83
6.2	Implications for Site Characterization.....	83
6.2.1	<i>In Situ</i> Frozen Core Samples Can Yield More Information.....	83
6.2.2	Improved retention of important sample intervals	84
6.2.3	Improved certainty of depth measurements	84
6.3	Future Work.....	84
6.3.1	Improved design of dual-wall cooling cylinder is needed.	84
6.3.2	Control of flowing sands needs additional demonstration and development.	84
6.3.3	Additional high-level thinking about best strategies for utilizing the newly available information is needed	85
6.3.4	Application of C ₃ at a broader range of sites would improve protocols.....	85
	Literature Cited.....	86
	Appendix A: Performance of Cryogenic Coring Systems – Developmental and Field Studies	88
	Appendix B: Protocol for Cryogenic Core Collection	98
	Appendix C: Protocol for High-Throughput Core Analysis.....	107
	Appendix D: K-Testing Particle Size Distribution Curves.....	114
	Appendix E: Geologic Log Data Table	115
	Appendix F. Calculation of Dissolved TCE Concentrations.....	121

List of Tables

Table 2-1. Potential Limitations of 1G Characterization Tools.....	18
Table 2-2. Potential Limitations of 2G Characterization Tools.....	18
Table 2-3. Attributes of Published Advanced Core Collection Methods	22
Table 2-4. Performance Relative to Objectives for Remediation Projects	22
Table 4-1. Hydraulic Conductivity Results	66
Table 5-1. Cores prepared for laboratory MRI experiment	77

List of Figures

Figure 2-1. Conceptual drawing of the flowing sands issue: During recovery of the sample to ground surface (a), non-cohesive materials may flow out of the bottom of the core barrel (b). At the same time, material can flow into the bottom of the auger (c) and be incorrectly collected as a portion of subsequent core samples. Finally, once at ground surface, core samples can continue to flow from the core liner and/or fluids can drain out of the core resulting in the introduction of oxygen into the sample.	20
Figure 3-1. Test Site at CSU's ARDEC.....	24
Figure 3-2. Test Site at Drilling Engineers Inc.....	24
Figure 3-3. Field Studies at F.E. Warren Air Force Base.....	25
Figure 3-4. Demonstration of cryogenic core collection methods at a former refinery near Casper, WY.....	25
Figure 3-5. Central Mining Equipment (CME) hollow-stem auger (HSA) drilling system.....	26
Figure 3-6. Modifications to the CME continuous sample tube system.....	27
Figure 3-7. Dimensioned drawing of modified drive shoe.....	27
Figure 3-8. Modified drive shoe.....	27
Figure 3-9. Dual-wall cooling cylinder, insulated cooling cylinder, and coil cooling system.....	28
Figure 3-10. Liquid nitrogen set up.....	28
Figure 3-11. Liquid nitrogen supply and exhaust lines.....	29
Figure 3-12. PIs evaluating data.....	29
Figure 3-13. Fabricated core samples.....	31
Figure 3-14. Temperature monitoring equipment for fabricated core.....	32
Figure 3-15. Frozen core.....	32
Figure 3-16. Downhole ice locking.....	33
Figure 3-17. Measuring LN use.....	34
Figure 3-18. Final coil system and coil system schematic (right).....	35
Figure 3-19. Dual-wall cooling cylinder.....	36
Figure 3-20. Dual-Wall cooling cylinder system design.....	36
Figure 3-21. Insulated stainless-steel tubes for delivery of liquid nitrogen to core barrels.....	37
Figure 3-22. Drilling and sampling sequence.....	38
Figure 3-23. Extraction of Sample Liner.....	38
Figure 3-24. Application of hot water to the cooling coils to release the sample liner.....	39
Figure 3-25. Temperature versus time data for freezing samples.....	40
Figure 3-26. Observed rates of change of temperature within the core liner.....	41
Figure 4-1. Materials and equipment used for high-throughput core processing. The following are shown: (A) cut-off saw, (B) stop blocks, (C) chisel, (D) hammer, (E) PVC pipe, cut to size, and (F) entire apparatus used for sub-dividing frozen core discs.	43
Figure 4-2. Packaging frozen core for shipping.....	43
Figure 4-3. Photograph of frozen-core cutting.....	44
Figure 4-4. Typical Sampling Pattern for Frozen Cores.....	45
Figure 4-5. Illustration of pattern used for sub-sectioning of frozen-core samples.....	45
Figure 4-6. Photographs of the aqueous-extraction transfer procedure. Aqueous transfer device shown (A) with parts labeled, (B) with clamp, (C) connected to headspace vial and aqueous-extract jar, (D) aqueous extraction vial/headspace vial assembly, with the headspace vial	

supported by a ring-stand clamp, (E) Tedlar bag, and (F) injection of water to complete the transfer of aqueous extract into the headspace vial	49
Figure 4-7. Components of core-in-liner K-testing apparatus: (A) collar, (B) end cap, (C) end cap overhead view, (D) filter disc, and (C) end cap overhead view with filter disc emplaced	52
Figure 4-8. Assembly of core-in-liner K-testing apparatus: (A) An empty core-sampling liner, (B) liner with one O-ring in place, (C) with collar, (D) with collar/end-cap assembly, loosely bolted with short bolts, (E) with second collar/end-cap assembly in place, and (F) with long-bolts in place	52
Figure 4-9. Falling head test station.....	54
Figure 4-10. TCE data (dry weight basis) in methanol extracts: linear (A) and log (B) scales....	56
Figure 4-11. PCE data (dry weight basis) in methanol extracts. Solid data points indicate detected values; hollow data points indicate estimated values for samples in which PCE was identified but was present below reporting limits	57
Figure 4-12. Methane concentration (dry weight basis) versus depth. Solid data points indicate detected values; hollow data points indicate lower detection limits for samples in which no methane was detected.	58
Figure 4-13. Geologic log, f_{oc} , and TCE concentration distribution between aqueous and sorbed phases for location MW173	59
Figure 4-14. Geologic Log, f_{oc} , and TCE concentration distribution between aqueous and sorbed phases for location MW-38C	60
Figure 4-15. Geologic Log, f_{oc} , and TCE concentration distribution between aqueous and sorbed phases for location MW700C	61
Figure 4-16. Anion data in aqueous extract (pore-water-volume basis).....	62
Figure 4-17. Ferrous iron data in aqueous extract (pore-water-volume basis). Solid data points indicate detected values; hollow data points indicate detection limits for samples in which Fe^{2+} was not detected.	63
Figure 4-18. pH and ORP data in aqueous extract.....	64
Figure 4-19. Geologic log summary	65
Figure 4-20. Water content and dry bulk density data for each core location	67
Figure 4-21. 16s rRNA Genes per gram of core for archaea and bacteria as a function of methane and TCE at MW- 700.....	68
Figure 4-22. Overall community composition.....	68
Figure 4-23. Geological sample legend	69
Figure 4-24. Comparison of data in core MW38C. (Side-by-side identifiers in the geologic log indicate interbedded layering on a scale too fine for this figure.)	70
Figure 4-25. Comparison of data in core MW173F.....	71
Figure 4-26. Comparison of data in core MW700C	72
Figure 4-27. TCE concentration data: comparison of 2G and 3G concentrations in borings collected from similar locations at FEW AFB.....	74
Figure 5-1. Styrofoam insulation for keeping the core frozen during MRI.....	78
Figure 5-2. Schematic of reference and core setting in mri probe for the one-dimensional quantification	79
Figure 5-3. Predicted intrinsic signal intensity of measured fid using a regression method	79
Figure 5-4. MRI images of the scanned cores. (a) sand and water at 20°C, (b) sand and water at -20°C, (c) sand and TCE (100% pore saturation) at -20°C, and (d) sand, water, and TCE (variable pore saturation) at -20°C.....	80

Figure 5-5. One-dimensional quantification results of a TCE-contaminated core. a) detected signals from the field of view b) quantification curve within the core. 81

List of Acronyms

AFB	Air Force Base
ARDEC	Agricultural Research, Development and Education Center
bgs	Below Ground Surface
C ₃	Cryogenic Core Collection
CCH	Center for Contaminant Hydrology
CIL	Core-In-Liner
CSU	Colorado State University
CT	Computer Tomography
DEI	Drilling Engineers Inc.
DI	De-ionized
DNA	Deoxyribonucleic Acid
DNAPL	Dense Non-Aqueous Phase Liquid
ER	Environmental Restoration
ERD	Enhanced Reductive Dechlorination
FEW AFB	Francis E. Warren AFB
GC	Gas Chromatograph
GC/ECD	GC/Electron Capture Detector
GC/FID	GC/Flame Ionization Detector
GC/MS	GC/Mass Spectrometric Detector
GE	General Electric
HSA	Hollow-Stem Auger
HTCA	High-Throughput Core Analysis
IC	Ion Chromatograph
ID	Inner Diameter
k	Permeability
LN	Liquid Nitrogen
LNAPL	Light Non-Aqueous Phase Liquid
MIP	Membrane Interface Probe
MRI	Magnetic Resonance Imaging
NAPL	Non-Aqueous Phase Liquid
OD	Outer Diameter
ORP	Oxidizing-Reducing Potential
PCE	Perchloroethene
PCR	Polymerase Chain Reaction
PRB	Permeable Reactive Barrier
psi	Pounds per Square Inch
PVC	Polyvinyl Chloride
qPCR	Quantitative Polymerase Chain Reaction
RNA	Ribonucleic Acid
SOP	Standard Operating Procedure
SERDP	Strategic Environmental Research and Development Program
STELA	Sustainable Thermally-Enhanced LNAPL Attenuation
SVE	Soil Vapor Extraction

SSR	State-of-the-Science Review
TCE	Trichloroethene
USGS	United States Geological Survey
VOC	Volatile Organic Compound
ZVI	Zero Valent Iron
1G	First Generation
2G	Second Generation
3G	Third Generation

Keywords

Cryogenic Core Collection

High-Throughput Core Analysis

Sample Preservation

Core Recovery

Medical Scanning

Acknowledgements

This project has been a collaborative effort with many supporting participants. The authors wish to gratefully acknowledge the support of:

- SERDP staff including Katie O'Toole, Deanne Rider, Hans Stroo, and Andree Leeson
- Staff at FEW including Ernesto Perez and Wanda Gershmel
- Chevron staff supporting the work at the former refinery in WY former including Bob Conlin and Mark Lyverse
- Drilling Engineers field staff including Dustin Coy and Andy Lozano
- Staff at Colorado State University including Helen Dungan and Maria Irrani Renno
- Financial support for complementary research provided by:
 - GE
 - University Consortium for Field-Focused Groundwater Contamination Research
 - Chevron

Chapter 1: Introduction

This report is an addendum to “Management of Contaminant Stored in Low Permeability Zones – State-of-the Science Review” (“SSR”, SERDP Project ER-1740). The motivation for this work is that coupled cryogenic core collection and high-throughput core analysis has the potential to provide a “third-generation” (3G) approach to site characterization that has significant advantages over current “first-generation” (1G) and “second-generation” (2G) site characterization methods. 1G site characterization methods involve analyzing water samples from wells and grab samples of subsurface solids. 2G site characterization methods include Membrane Interface Probes (MIPs), Hydraulic Profiling Tools (HPTs), Waterloo^{APS}™ and Subsampling Standard Soil Core, and Multiple Level Sampling Systems (MLSs). The merits of 2G site characterization methods, as compared to 1G methods, is a primary theme in the SSR. Work described in this addendum to the SSR was completed by Colorado State University, Dr. Rick Johnson, and Drilling Engineers Inc. from July 2013 to July 2015.

1.1 Problem Statement

Over time, site characterization methods based on conventional monitoring wells and subsurface grab samples (1G methods) have proven to be inadequate in many ways (see SSR Section 1.1). Briefly, monitoring wells provide depth-averaged groundwater data that are typically biased toward highly-transmissive zones, and traditional solids grab sampling (e.g., from auger cuttings) can have consequential limitation with respect to preservation of pore fluids, volatile compounds, dissolved gases, redox conditions, mineralogy, microbial ecology, and pore structure.

As documented in the SSR, the small-scale spatial discretization of data provided by vertically-resolved samples (i.e., 2G technologies) has provided a major improvement over the 1G site characterization methods. However, limitations of the 2G technologies were noted. For instance, preservation of *in situ* conditions in cores can be difficult, even during the initial step of removing the core from the subsurface. Also, the efficacy of 2G methods varies widely from site to site. Commonly, 2G site characterization tools are best applied in combinations with the hope that one of the methods will prove to be effective. The potential need to employ multiple 2G methods can lead to high costs.

The research discussed herein presents third-generation (3G) cryogenic core sampling techniques, which are designed to improve upon the limitations of the 2G methodologies listed above and described in detail in the SSR.

1.2 Research Hypotheses

The following research hypotheses are addressed in the addendum:

1. *In situ* freezing of core can improve the recovery of core by limiting losses of core from sample tubes during sample recovery.
2. *In situ* freezing of core can preserve pore fluids including water, non-aqueous phase liquids (NAPLs), and gases.
3. Cryogenically-collected cores can be stored at low temperatures, which will preserve key parameters during transported to a laboratory and storage before analysis.

4. A laboratory-based system can be devised that will allow for high-throughput analysis of frozen cores, providing a larger amount of data that more accurately represents *in situ* conditions than data generated from field-processing of unfrozen cores.
5. Medical scanning methods (e.g., MRI) can be used to provide continuous data from frozen cores.

1.3 Objectives

The objective of the research presented in this addendum is to demonstrate the combination of cryogenic core collection and high-throughput core analysis for site characterization. Included in this addendum are standard operating procedures for C₃ and HPCA.

1.4 Report Content

This report is divided into six chapters. Background information is presented in Chapter 2. Subsequent chapters present detailed methods and results for cryogenic core collection (Chapter 3), high-throughput core analysis using frozen-core subsampling techniques (Chapter 4), and high-throughput core analysis using scanning methods (Chapter 5). Finally, conclusions are presented in Chapter 6.

The methods developed as part of the research have been compiled into protocols to guide future users of the approaches developed herein. The protocol for cryogenic core collection is provided in Appendix B. The protocol for high-throughput core analysis is provided in Appendix C.

Chapter 2: Background

This chapter presents foundational background information, including:

- Limitations of 1G and 2G site characterization methods
- Factors controlling recovery of representative samples
- Issues with preservation of core samples
- Limitations of advanced core collection methods

2.1 Limitations of 1G and 2G Site Characterization Methods

The efficacy of 1G and 2G site characterization methods are described at length in the SSR. Summaries of the limitations of the 1G and 2G methods, which were the motivation for this work, are presented in Tables 2-1 and 2-2.

Table 2-1. Potential Limitations of 1G Characterization Tools

1G Tools	Limitations
Monitoring Wells	<ul style="list-style-type: none"> - In-well mixing of water from different depths obfuscates plume structure - Not effective for identification of impacted low-<i>k</i> zones - Leads to an incorrect conceptual model (i.e., large-and-dilute plumes rather than structured plumes, only captures water samples from transmissive zones)
Grab Soil Samples	<ul style="list-style-type: none"> - Loss of volatile compounds - Loss of soil structure - Drainage of pore fluids

Table 2-2. Potential Limitations of 2G Characterization Tools

2G Tools	Limitations
Membrane Interface Probes (MIPs)	<ul style="list-style-type: none"> - Limited accuracy below 100 µg/L - Provides little insight regarding sorbed or non-aqueous liquid phases - Infeasible to drive sample system in many geologic settings
Waterloo Profiler™	<ul style="list-style-type: none"> - Recovery of water samples difficult in sediments with fines (plugging) - Provides little insight regarding sorbed or non-aqueous liquid phases - Infeasible to driving sample system in many geologic settings
Analysis of Subsample from Core	<ul style="list-style-type: none"> - Recovery of representative core is difficult in non-cohesive materials - Redistribution of fluids during extraction and handling of cores - Difficult to preserve target analytes during sampling - Difficult to preserve biogeochemical conditions during core recovery

2.2 Factors Controlling Recovery of Representative Samples

Collection of subsurface unconsolidated media (core) is common in geotechnical, mining, agricultural, geologic, and remediation practices. Sample tubes of varying diameters are advanced either by driving or vibration, or “over drilling” using a hollow-stem auger. The ratio of the length of the collected core to the depth over which the sample tube is advanced is referred to as “**recovery**”. Factors controlling recovery include:

- **Diameter of the sample tube** – The diameter of the core sampling system constrains the sizes of the material that can enter the sample tube. Large material will limit entry of sediments into the sample liners (Zapico et al. 1987). In addition, smaller-diameter liners present more wall resistance compared to their cross-sectional area, and complete filling of the liner becomes more difficult.
- **Length of the sampled interval** – Friction inside sample liners also increases with sample length. Friction associated with pushing longer sample intervals into sampling systems can again lead to conditions where the length of the recovered sample is less than the length of the sampled interval (poor recovery).
- **Losses while withdrawing sampling tools** - During extraction of the sampling tools from the subsurface, a vacuum can form below the sample system (particularly a problem in saturated media – see (a) and (b) in Figure 2-1). Also, during extraction, samples can be mechanically jarred by lifting and/or impacts with drilling systems. Both vacuum and mechanical jarring commonly cause core samples to fall out of the sample tubes compromising recovery (Murphy and Herkelrath 1996).
- Another critical challenge in saturated media is “**flowing sands**” (see Figure 2-1 (c) below). As drilling/sampling proceeds, removal of solids and water often leads to conditions where the effective stress inside the drilling system is less than the effective stress in the adjacent formation. Imbalanced forces between the formation and the interior of drill system often cause 1) liquefaction of low-cohesion materials and 2) flow of sands (fluff) into the drill systems. Flowing sand often leads to collection of samples that are not representative of the formation.

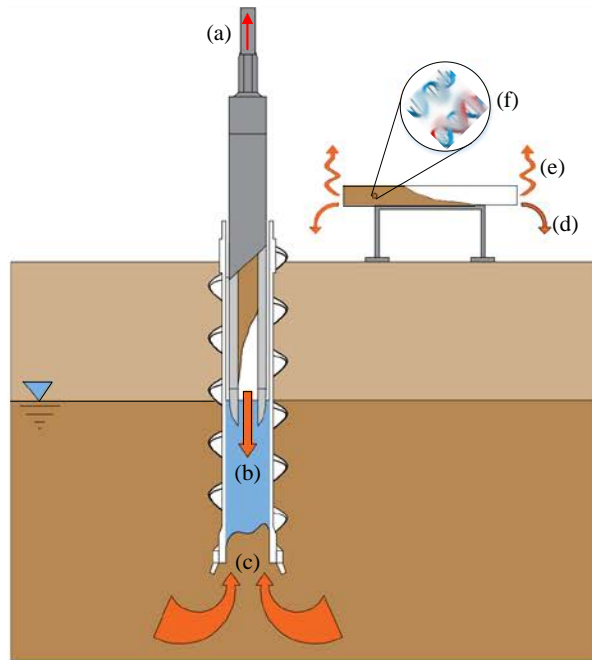


Figure 2-1. Conceptual drawing of the flowing sands issue: During recovery of the sample to ground surface (a), non-cohesive materials may flow out of the bottom of the core barrel (b). At the same time, material can flow into the bottom of the auger (c) and be incorrectly collected as a portion of subsequent core samples. Finally, once at ground surface, core samples can continue to flow from the core liner and/or fluids can drain out of the core resulting in the introduction of oxygen into the sample.

2.3 Issues with Preservation of Subsurface Samples

Ideally preservation of subsurface samples (see (d) through (f) in Figure 2-1) for remediation efforts includes:

- Retaining pore fluids including water, NAPLs, and gases
- Preventing consequential losses of volatile compounds
- Not altering aqueous oxidation/reduction conditions, mineralogy, or microbial ecology through the introduction of atmospheric oxygen
- Preserving RNA for characterization of the active microbial ecology
- Maintaining the arrangement of particles for the determination of porous media properties

Uniquely, freezing cores *in situ*, before recovery, holds the promise of preserving all of the above subsurface properties, because:

- Drainage of fluids from sample can be prevented. Commonly during recovery of samples, pore fluids drain and are replaced by atmospheric air. Drainage biases estimates of water, NAPL, and gas saturations. Furthermore, drainage can bias estimates of contaminant mass associated with aqueous, NAPL, and gas phases.

- Introduction of atmospheric oxygen into samples can be limited. Introduction of oxygen can alter sample redox conditions, lead to losses of volatile compounds, alter sample mineralogy, and alter anaerobic microbial ecology.
- Losses of volatile compounds in water and NAPL, and sorbed phases can be limited. Particularly for compounds with large Henry's coefficient (i.e., chlorinated solvents), losses through volatilization can be large.
- Common aqueous phase chemical reactions can be prevented. Primary chemical reactions of concern require free liquid water molecules for a reaction to proceed, as opposed to immobile water molecules in frozen water.

2.4 Limitation of Advanced Core Collection Methods

Leading efforts to address the concerns noted in the previous section are reviewed in this section. Table 2-1 presents key attributes of advanced coring system developed to date. Table 2-2 describes the efficacy of each of the methods with respect to recovery and sample preservation.

Core Freezing Followed by Coring - Early work on sampling saturated unconsolidated cores using freezing techniques was conducted for liquefaction analysis at Fort Peck Dam. Forty hours of injecting liquid nitrogen (at -196°C) through a pipe (73-mm diameter) froze the formation radially to diameter of about 60 cm and depth of 10 meters. Subsequent coring of frozen cores required a giant core barrel and heavy crane (Yoshimi et al. 1984).

Wireline Piston Core Barrel – Zapico et al. (1987) describes the use of the WaterlooTM aquifer piston core barrel (without freezing). A piston is installed on the inside of a solid body drive sample barrel. The piston moves to the top of the sample barrel as the sample system is driven into the targeted interval. Upon extraction, the piston (held by a wire) holds a vacuum at the top of the sample system reducing losses of solids and pore fluids. Drilling mud can be used to increase the effective stress inside the drill system to control flowing sands. While the wireline piston core barrel improves recovery and retention of pore fluids, many of the issues described in the previous section remain as issues. Also, use of drilling mud to control flowing sands can complicate the sampling process and may raise concerns with cross contamination of samples.

CO₂ Cooled Drive Shoe - Durnford et al. (1991) employs a solid body drive sampler with a gas expansion chamber located in the bottom 3 inches of the drive sample system. Liquid CO₂ is allowed to expand in the gas expansion chamber sampler, freezing the core sample at the base of the solid body drive sampler. Freezing at the drive shoe limits losses of solids and fluids and improves recovery. To the negative, 1) CO₂ gas is discharged downhole potentially biasing samples, 2) the CO₂ line on the outside of the drive sampler is vulnerable to damage during driving, 3) only a portion of the sample is frozen *in situ*, slow cooling is observed in the saturated zone, and 4) issues remain with flowing sands.

Piston Core Barrel and Liquid CO₂ Cooled Drive Shoe – Murphy and Herkelrath (1996) combined the piston core barrel approach of Zapico et al. (1987) and the liquid CO₂ cooled drive shoe of Durnford et al. (1991). Results, both positive and negative, are similar to those of Durnford et al. (1991).

Liquid N₂ Cooling Coil Using Direct Push Tools – Johnson et al. (2012) wrapped a copper coil around an aluminum sample liner in a GeoProbe Dual Tube sampler (GeoProbe 2011). Liquid

nitrogen reduces the potential coolant temperature from -79°C for CO₂ to -196°C for liquid nitrogen. Importantly, in the Johnson et al. design the gas lines are on the inside of the drive sampler to protect them from mechanical damage. An approximate 3-foot core sample could be frozen *in situ* prior to recovery. Many of the issues related to recovery and sample preservation are addressed by this method. Limitations of Johnson et al. (2012) are that a) a small diameter sample tube is employed limiting the size of the material that can be recovered, and b) the likelihood of friction inside the sample liner will limit recovery. Furthermore, Geoprobe direct push sampling systems are prone to refusal at shallow depth in many settings, drive sample systems can be prone to compaction of cores, and no resolution is provided for flowing sands.

Table 2-3. Attributes of Published Advanced Core Collection Methods

	Core Freezing Followed by Coring	Wireline Piston Core Barrel	CO₂ Cooled Drive Sampler	CO₂ Cooled Drive Sampler	LN Cooled Direct Push Tool
Reference	Yoshimi et al. (1984)	Zapico et al. (1987)	Durnford et al. (1991)	Murphy and Herkelrath (1996)	Johnson et al. (2012)
Sample Type	Coring	Dive	Drive	Drive	Drive
Coolant	Liquid Nitrogen	None	Liquid Carbon Dioxide	Liquid Carbon Dioxide	Liquid Nitrogen
Potential drive length (feet)	30	5	2	5	3
Sample Diameter			1.25 inch	1.88 inch	1.25 inch
Coolant discharge	Downhole	None	Downhole	Downhole	Grade
Freezing	Total prior to coring	None	Partial	Partial	Total

Table 2-4. Performance Relative to Objectives for Remediation Projects

	Core Freezing Followed by Coring	Wireline Piston Core Barrel	CO₂ Cooled Drive Sampler	CO₂ Cooled Drive Sampler	LN Cooled Direct Push Tool
Freezing	Total	None	Partial	Partial	Total
Retention of pore fluids	Yes	Partial	Yes	Yes	Yes
Potential for loss of volatile	Low	Yes	Yes - Reduced	Yes - Reduced	Low
Invasion of atmospheric oxygen	Unlikely	Likely	Possible	Possible	Unlikely
Penetration of hard formations	Possible	Drive system limited by refusal in hard soil or cobbles	No – vulnerable exterior gas line	No – vulnerable exterior gas line	Drive system limited by refusal in hard soil or cobbles
Control of Flowing sand	Yes	Yes w/mud	No	No	Unlikely

Potential sample bias due to down hole gas discharge	No	No	Yes	Yes	No
Time to freeze core	Days	NA - No Freezing	Performance degrades with depth and in the saturated zone	Performance degrades with depth and in the saturated zone	Limited data
Overall practically for wide use	Low given time to freeze and cost	Low given no freezing &	Low given above limitations	Low given above limitations	Moderate – limited to easy geologic settings
Historical use	One application	Multiple applications	One application	Multiple applications	One sand tank application
Commercially available	No	No	No	No	No

Chapter 3: Cryogenic Core Collection

The following chapter describes cryogenic core collection (C₃), including:

- Methods
 - Locations and dates of cryogenic core collection field work
 - Drilling methods
 - Modifications to existing CME Continuous Sample Tube System
 - Cryogenic sampling systems
 - Critical variables for the development of cryogenic coring tools
 - Performance assessment metrics

- Results
 - Final resolution of system components and methods
 - Performance with respect the key metrics

3.1 Methods

3.1.1 Locations and Dates of Cryogenic Coring Field Work

Development of the cryogenic core collection methods has involved sequential testing of different sampler designs and protocols to arrive at a robust, rapid, and practical approach. Initial designs were tested at **Drilling Engineers Inc.** in Fort Collins, CO, allowing for refinement of techniques with shop resources close-at-hand in uncontaminated media. Dates of work at Drilling Engineer’s facility included May 13 to 14, 2014, June 22 to 23, 2014, and September 15, 2014.

Developmental studies were also conducted at **CSU’s Agricultural Research Development & Education Center (ARDEC)** in Fort Collins, CO. ARDEC is underlain with fluvial deposits that grade from silt at ground surface to coarse sand at approximately 20 feet below ground surface (bgs). ARDCEC is also an uncontaminated site. The silt is an easy formation to drill, while the underlying coarse sand is more challenging because it flows into the augers during the



Figure 3-2. Test Site at Drilling Engineers Inc.



Figure 3-1. Test Site at CSU’s ARDEC

sampling process. Dates of work at ARDEC included March 10 to 11, 2014 and July 7 to 8, 2014.

Following development work in Fort Collins, field studies were conducted at **F.E. Warren Air Force Base (FEW AFB)**, located west of Cheyenne, WY (September 22 to 23, 2014). FEW is an approximately 7,000-acre facility, consisting of shallow of eolian and fluvial deposits. Eolian deposits include local beds of caliche. Eolian and fluvial deposits are underlain by the Ogallala Formation. Locally, the Ogallala Formation consists of interbedded gravel, sand, and silt beds with varying clay content. Through historical maintenance and disposal activities, chlorinated solvents (primarily TCE) have been inadvertently released to the subsurface. A primary concern associated with releases is the risk posed to surface waters, including Diamond Creek and Crow Creek. Previously, CSU conducted ESTCP/SERDP field work at FEW in 2001 to 2004 (CU-0112) and 2010 (ER-1740).

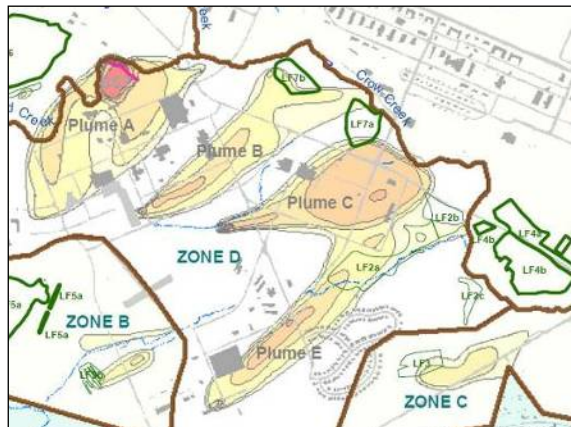


Figure 3-3. Field Studies at F.E. Warren Air Force Base

Our vision in going to FEW AFB was to test cryogenic core collection at the same location that 2G methods were demonstrated in 2010 (See SSR). Drill locations at FEW duplicated CSU's studies at FEW in 2010 at MW -173, MW-700, and MW 38. Repeating investigations at the same locations provides an opportunity to compare 2G and 3G site characterization methods. MW -173 and MW-700 are located at Spill Site 7. At Spill Site 7 sequential applications of excavation, soil vapor extraction (SVE), iron permeable reactive barrier (PRB), and enhanced reductive dechlorination (ERD) have failed to address TCE concentrations in excess of maximum contaminant levels (MCLs) in a down-gradient creek.

Former Refinery in Wyoming – Building on successes at FEW, Chevron funded a demonstration of cryogenic core collection at a former refinery located near Casper, WY. Work was conducted on October 30, 2014. The site covers approximately 200 acres and is adjacent to the North Platte River. Petroleum refining occurred at the site from 1923 to 1982. The site is underlain by North Platte River alluvium. Sediments grade from fine-grained overbank deposits (sand and silts) at ground surface into point bar sands and channel gravel with depth. In the study area, a weathered petroleum smear zone extends from 5 to 15 feet below grade. CSU has been conducting field research at the former refinery since 2001.



Figure 3-4. Demonstration of cryogenic core collection methods at a former refinery near Casper, WY

3.1.2 Drilling Methods

Central Mining Equipment (CME) hollow-stem auger (HSA) drilling systems were employed in the project. All work was conducted using

4.25-inch ID auger flights and a 4-inch OD CME Continuous Sample Tube System. HSA drilling and sampling equipment is widely available, are generally inexpensive to operate, and has the advantage over direct push coring methods because it is applicable to a broad range of geologic settings. Details regarding CME equipment are available in their product catalog - http://www.cmeco.com/cat/cme_product_catalog_catalog.pdf.

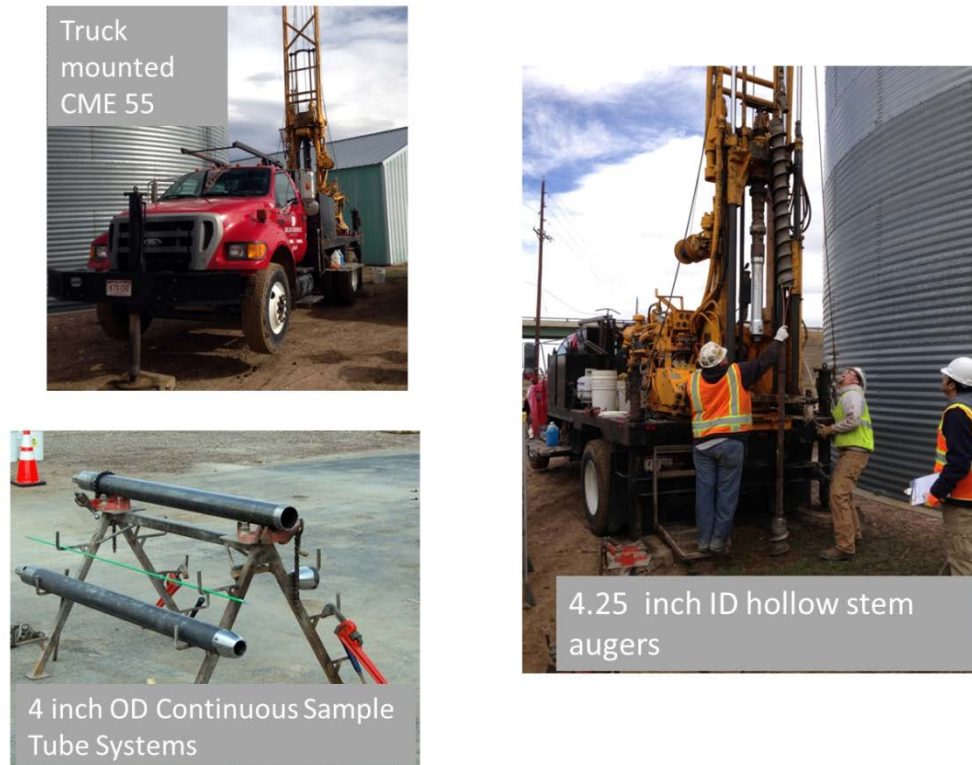


Figure 3-5. Central Mining Equipment (CME) hollow-stem auger (HSA) drilling system

3.1.3 Modifications to Existing CME Continuous Sample Tube System

Two modifications were made to the CME standard 4-inch Continuous Sample Tube System.

Core-Barrel Drive Head. To allow LN delivery and exhaust lines to enter and exit the top of the sample system, two 3/4-inch holes were drilled in the top of the drive head for the core barrel.

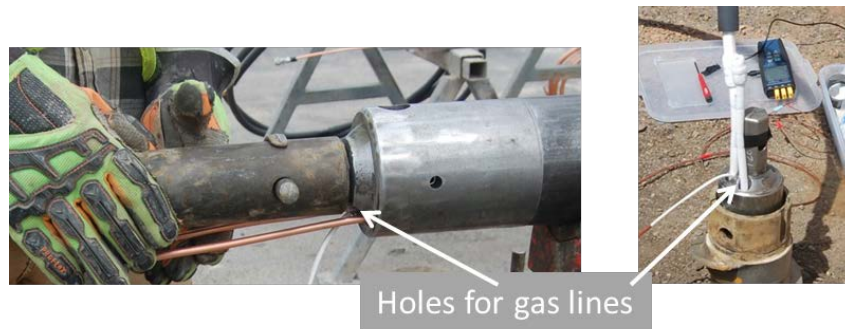


Figure 3-6. Modifications to the CME continuous sample tube system

Drive Shoe Modification. Custom-designed drive shoes were purchased from CME. A dimensioned drawing of the design is shown in Figure 3-7. The custom design was necessary because 2 1/2-inch OD sample liners were used to allow more clearance in the core barrel for cooling coils/cylinder and insulation.



Figure 3-8. Modified drive shoe

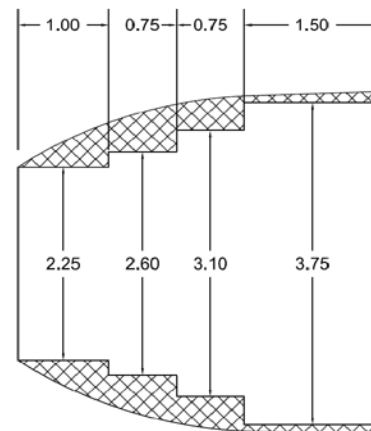


Figure 3-7. Dimensioned drawing of modified drive shoe

3.1.4 Cryogenic sampling systems

Cryogenic sampling systems - Two cryogenic sampling systems were developed, a **dual-wall cooling cylinder** and a **cooling coil**. Both systems fit into the 4-inch CME Continuous Sample Tube System.

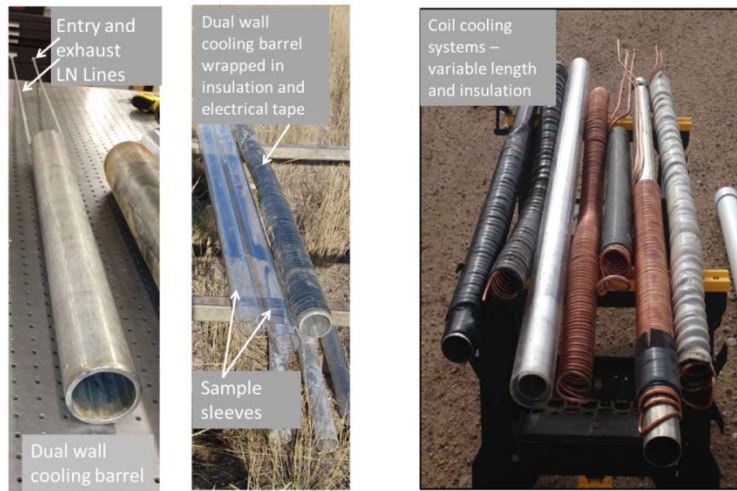


Figure 3-9. Dual-wall cooling cylinder, insulated cooling cylinder, and coil cooling system

Liquid Nitrogen - A central element of cryogenic core collection is use of liquid nitrogen as a coolant. LN was delivered using a commercial liquid nitrogen dewar and back-pressure control. The pressure of the LN within the dewar is controlled by a valve that regulates the rate of warming in the LN tank. “High-pressure” (~200 psi) tanks are preferred for C₃.



Figure 3-10. Liquid nitrogen set up

LN delivery and exhaust lines consisted of two parts. The first was an insulated length of 3/8” copper tube extending from the dewar to the top of the drill system. Second, 5 foot sections of 3/8-inch stainless steel tubing fitted with ~1/4” insulation and heat shrink tubing. These extend from grade down the core cooling section. The 5-foot sections were connected with stainless steel Swagelok™ fittings.



Figure 3-11. Liquid nitrogen supply and exhaust lines

3.1.5 Critical Variables for Development of Cryogenic Coring Tools

A key element of this project was the iterative evaluation of the efficacy of different combinations of design variables for cryogenic core collection systems. These combinations were accomplished through seven separate field events. This section introduces key variables and briefly notes outcomes. Details regarding outcomes are presented in the following results section. A summary of tested systems is presented in Appendix A.



Figure 3-12. Pls evaluating data

Tank pressure – Liquid nitrogen comes in dewars that range in size and discharge pressure. High-pressure (230 psi - 160L) dewars were needed to achieve the desired rates of cooling and to provide sufficient LN for one day of coring using a single dewar.

Cooling tubing diameter – Limited space in core sample systems (e.g., CME Continuous Sample Tube Systems) constrains the size of LN lines used for cooling coils/barrels in the sample barrels. After considering 1/4- and 3/8-inch tubing, 3/8-inch tubing was required to achieve the desired cooling rates.

Cooling coil tubing length and diameter – Consideration was given to cooling coils ranging from 50 to 200 feet. Lengths greater than 50 feet adversely restricted coolant delivery rates. Final coil cooling systems employ 50-foot cooling systems. Again, both 1/4 and 3/8” diameter tubing was considered for the coils. 3/8” tubing proved to be the most effective.

Sample lengths – Consideration was given to collection of 5- and 2.5-foot long core samples. Five-foot samples frequently yielded poor recovery due to excess friction associated with

pushing samples into the sample liners in lengths greater than 2.5 feet. Core freezing systems and sample drives were limited to 2.5 feet.

Sample diameter – All work was based on collecting 2.5-inch OD core samples. 2.5-inch samples systems facilitate collection of large sediments and collection of enough core from distinct intervals for a broad range of analytes.

Cooling coil/barrel insulation – If insulation was not present between the cooling coils/barrel, much of the cooling capacity of the LN was lost to the drilling systems and the formation. Losses of cooling capacity to the drilling system and the formation increased the time to freeze samples (dramatically), tended to cause the drill/sampling system to become frozen in place, and to consume excessive amounts of LN. Iterative testing of different types and thicknesses of insulation lead to wrapping cooling systems (coil and dual-wall cylinder) in 1/4-inch closed cell foam.

LN delivery/exhaust lines – Proper insulation of LN delivery/exhaust lines is an essential element of rapid freezing and efficient use of LN. The final resolution was use of 3/8 stainless steel tubing, 1/4-inch thick closed-cell insulation cover by heat-shrink tubing, and steel Swagelok™ fittings.

Sample Liners – Cores are collected in liners. Consideration was given to aluminum, acetate, and clear PVC liners. Aluminum was rejected due an inability to see the samples in the field and conduction of heat along the aluminum when cutting the core into subsections. Acetate tended to fail under the extremely low temperatures. Clear PVC performed well and facilitated visual inspection of the samples in the field.

LN feed/exhaust line insulation - Absent insulation on the LN feed/exhaust lines caused cooling capacity loss to the drill systems between the cooling coils/barrels.

LN discharge backpressure – Back pressure in the subsurface cooling systems can be controlled with a throttle valve. Optimal cooling was achieved by a) applying zero back pressure on the LN discharge line until 0 °C was observed in the LN exhaust line and b) after 0 °C exhaust was observed, using a throttle value to apply approximately 100 psi back pressure at the LN exhaust.

3.1.6 Performance Assessment Metrics

Primary performance metrics for evaluating for cryogenic systems included sample recovery, control of flowing sands, time to freeze, limiting downhole ice locking of tools (i.e., core barrel freezing to auger flights or auger flights freezing to subsurface granular materials, efficient use of LN, and core production rates. The ability to use frozen core to characterize critical core attributes is addressed under the topic of high-throughput core analysis.

Recovery was determined as the length of the recovered sample divided by the sampled interval.

Control of flowing sands was evaluated by observing the elevation of the sample system at the beginning of a sample drive versus the elevation of the bit at the base of the hollow-stem auger flights. (i.e., flowing sand inside the auger flight prevented placement of the leading edge of the core barrel at the bottom of the auger.)

Time to freeze was evaluated using 5-foot core sections constructed in that laboratory that were equipped with three K-type thermocouples (top, middle, and bottom). These cores were placed in pre-drilled holes in the field in a manner to simulate actual field conditions. This allowed temperature within the core at depth to be monitored in real time during the cooling process. We could also assess the effectiveness of freezing by inspecting the state of cores collected at the field sites.

Fabricated cores were 1) filled with water-saturated medium sand, 2) placed inside the Continuous Sample Tube System, and 3) placed inside *in situ* hollow-stem auger flights located both above and below the water table (see image below).



Figure 3-13. Fabricated core samples

Temperatures inside the fabricated cores were monitored using an Omega HH378 temperature meter and Omega data logging software.



Figure 3-14. Temperature monitoring equipment for fabricated core

Temperatures of frozen core from field drilling were evaluated using a MicroTemp MT 250 infrared temperature monitor and through direct physical inspection.



Figure 3-15. Frozen core

Downhole ice locking was revealed by an inability to pull either the cryogenic sampling tool out of the hollow stem augers or by ice on the outside of the sampling systems.



Figure 3-16. Downhole ice locking

Efficient use of LN – During developmental field work in Fort Collins, the amount of liquid nitrogen used in freezing samples was determined by weighing the LN dewar before and after sample freezing. Initially, the Dewar was placed on a pallet underlain by four analog bathroom scales. Subsequently, an electronic scale interfaced to a laptop computer was employed. During field work at FEW and the former refinery, the status of the dewar was tracked (more simply, but less reliably) using the level and pressure gauges on the dewar.



Weight by analog scales



Weight by digital scale

Figure 3-17. Measuring LN use

Core Production – Core product at FEW and the former refinery was recorded in terms of feet of core recovered per day.

3.2 Results and Discussion

The most significant result of this work was the development of a practical downhole cryogenic sampling system and ancillary equipment and methods. The following describes:

- The final design of cryogenic sampling tools, ancillary equipment, and methods
- Performance with respect to the key metrics

Note: further elucidation of many of the point in the following section can be found in the SOP for cryogenic core collection, presented in Appendix B.

3.2.1 Final Design of System Components and Methods

The following section describes the developed cryogenic core collection tools.

3.2.1.1 Cooling Coil and Dual-Wall Cooling Cylinder

Two different systems were developed for *in situ* freezing of samples, cooling coil and dual-wall cooling cylinder. Both are designed to collect frozen samples in 2.5-foot long, 2.5-inch diameter liners. Critical to both systems is:

- Extending the cooling system into the drive shoe without insulation, improved freezing at the front of the core and probably reducing the effects of heaving sands by freezing the formation ahead of the drive shoe
- Insulation around the reaming sections of the cooling coils/cylinder was critical for achieving rapid freezing and limiting downhole ice locking of tools

Critical elements of the **cooling coil** system (Figure 3-18) consists of:

- 50 feet of 3/8-inch copper tubing wrapped over 2.5-foot sample intervals
- 1/4-inch closed-cell foam insulation wrapped around the copper coils and covered with electrical tape. Note: future studies should consider use of large diameter heat shrink tubing in lieu of electrical tape.
- PVC liners for core collection

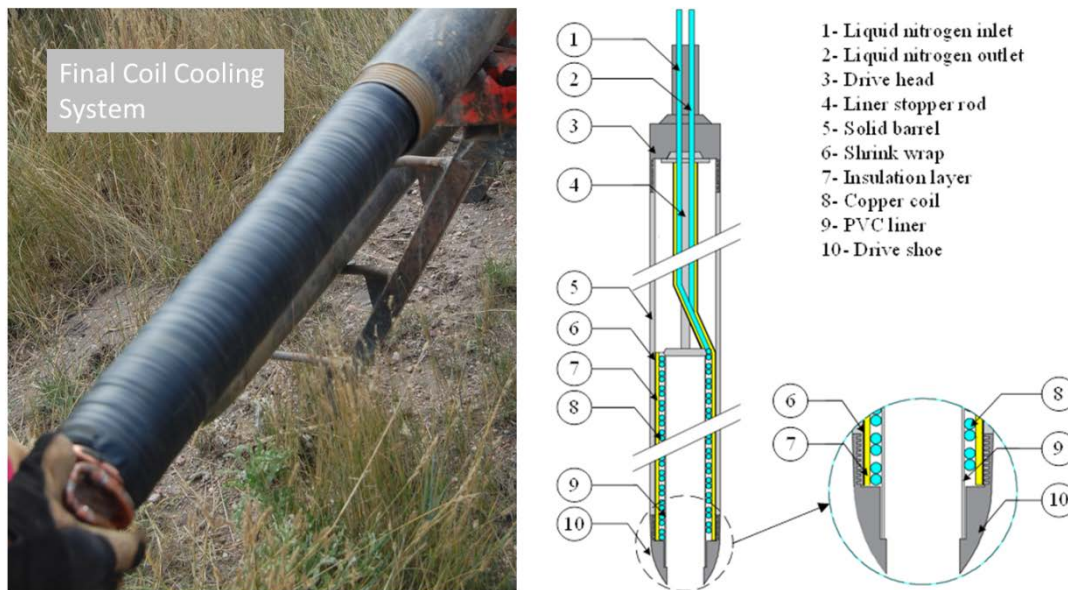


Figure 3-18. Final coil system and coil system schematic (right)

The **dual-wall cooling cylinder** system (Figures 3-19 and 3-20) attributes include:

- The barrel is composed of two stainless-steel tubes
- The delivery LN line enters the base of the barrel to maximize cooling at the drive shoe
- The LN exhaust line exits at the top of the barrel
- The cooling cylinder is wrapped in 1/4-inch closed-cell foam insulation covered by heat shrink tubing
- PVC liners for core collection



Figure 3-19. Dual-wall cooling cylinder

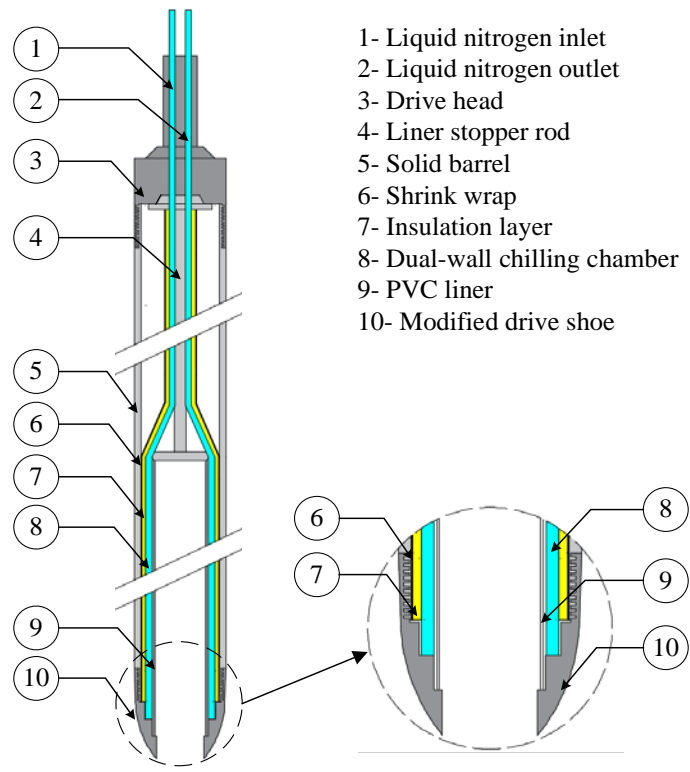


Figure 3-20. Dual-Wall cooling cylinder system design

3.2.1.2 Liquid Nitrogen Systems

230 psi/160 L LN dewars proved to be an effective coolant source including:

- Exhaust temperatures as low as -196 C°

- Sufficient cooling capacity for a full day of coring
- Reasonable costs
- Wide availability

Based on field experience, the preferred control for field studies was to:

- Maintain a pressure at the dewar of ~ 200 psi
- Leave the discharge valve open until freezing temperature (0 C°) was achieved on the LN discharge line
- Use a manual discharge throttle valve to create 100 psi back pressure after 0 C° was achieved at the LN discharge line
- Achieve total cooling times of 5-10 minutes:
 - Larger times for large depths or low tank pressure
 - Shorter times for unsaturated media and high tank pressure

Delivery of LN from the surface to the core barrel is a critical step for *in situ* freezing. 3/8-inch OD, 5-foot long stainless-steel tubes were used for this purpose (Figure 3-21). To minimize losses of cooling capacities, the tubes were wrapped with closed-cell foam and covered with heat-shrink tubing. The diameters of these insulated tubes needed to be kept small to avoid interference with the augers spinning around the hex rod and LN-riser tubes. The connections between the tubes must be able to handle LN at greater than 200 pounds per square inch (psi) pressure. Stainless-steel Swagelok™ unions were used to connect the riser tubes together and to connect to the LN supply, pressure control system, and cooling coils/cylinder.



3.2.1.3 Core Liners

Figure 3-21. Insulated stainless-steel tubes for delivery of liquid nitrogen to core barrels

Three types of 2.5-inch OD core liners were used for this project: acetate, PVC, and aluminum. Of the three, PVC provides the best combination of heat conduction, ease of use, and transparency. The tubes were cut to 5 feet in length to fit snugly into the cooling coil or dual-wall cylinder. As discussed above, our conclusion was that 2.5-foot cores were preferred over 5-foot pushes due to better recovery.

3.2.1.4 Drilling and Sampling Sequence

Figure 3-22 describes the ideal drilling and sampling sequence. Specifically, a) concurrent advancement of the augers and sample barrel fills the sample liner with 2.5 feet of solids and associated fluids, b) liquid nitrogen is used to freeze the sample, c) the frozen sample is recovered and a frozen plug below the bit controls flowing sands, and steps a), b) and c) are repeated to the desired final sampling depth.

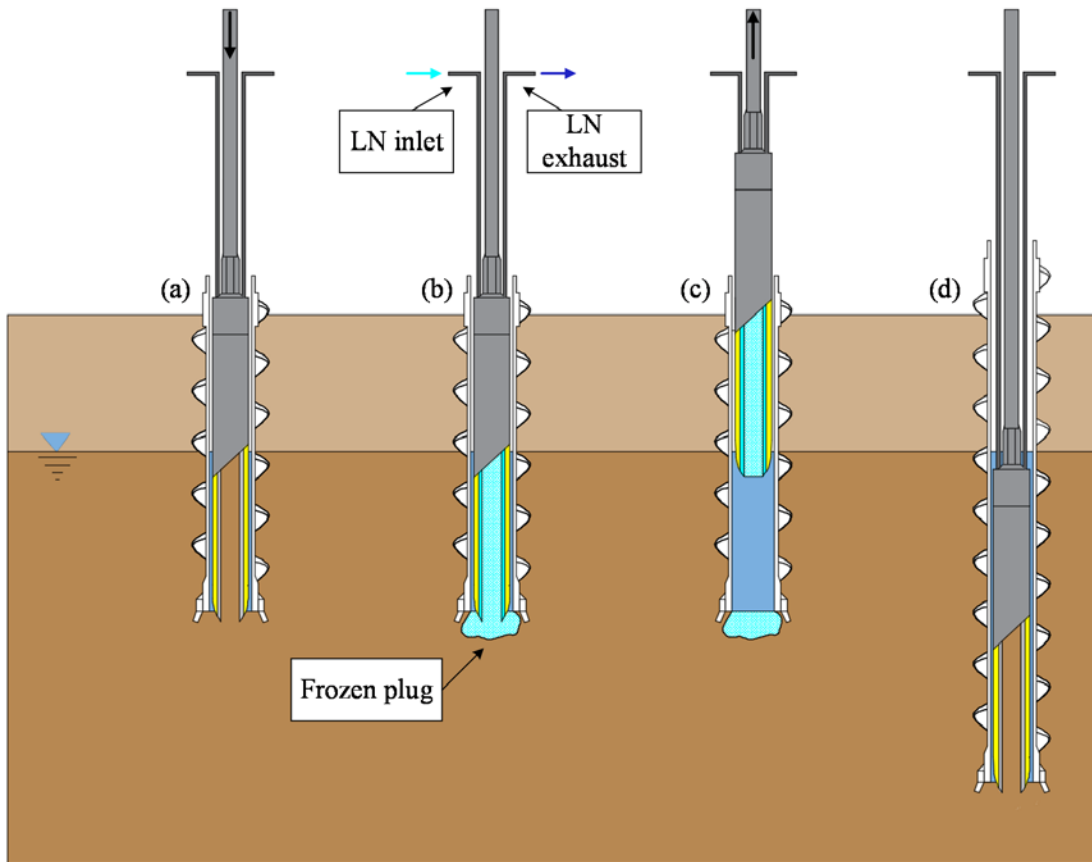


Figure 3-22. Drilling and sampling sequence

3.2.1.5 Extraction of Core from Continuous Sample Tube System

One of the greatest difficulties with the developed systems was extraction of the sample liners from the cooling coils/dual-wall cylinder due to buildup of ice and/or sediments between the liner and the cooling system.



Figure 3-23. Extraction of Sample Liner

Developed solutions for liner removal included:

- Using a hot-water power washer to clear sediments from the cooling system between uses.
- When necessary, using hot water in the cooling system to thaw the frozen contact between the sample liner and the cooling system.
- Applying food-grade oil to the outside of the sample liner to limit direct contact of water with the sample liner.



Figure 3-24. Application of hot water to the cooling coils to release the sample liner

While the developed method for removing the samples from the cooling coil/cylinder is practical, more effective approaches would help reduce the level of effort associated with cryogenic core collection. A second set of core sampling equipment would also improve the process by allowing the drilling team to hand the core barrel to a second field crew and to quickly return down hole with the second core barrel.

3.2.2 Performance with Respect to the Key Metrics

The following sections describe performance of the developed system and methods with respect to key metrics.

3.2.2.1 Recovery

Tabulated recovery data from field work at FEW AFB and the former refinery site are presented in Appendix A. At **FEW AFB**, excepting caliche beds that required a center head in lieu of the continuous sample tube system, recovery was close to 100%. At the **former refinery**, except where gravel size exceeded the diameter of the sample liner, recovery was 85%. An attempt to collect core samples at the former refinery site using the 2.5-inch sample system without freezing yielded extremely poor recovery (<15%).

3.2.2.2 Time to Freeze

Figure 3-25 presents temperature versus time data acquired using fabricated cores equipped with thermocouples in the center of the cores. The initial cooling coil system employed 200 feet of ¼-inch copper tubing and no insulation. The final optimized cooling coil system employed 50 feet of 3/8-inch copper tubing with insulation. The data show four phases of cooling: 1) cooling the lines leading to the core sample, 2) cooling the core, 3) a temperature plateau associated with the heat of freezing water (heat of fusion), and 4) cooling the fully-frozen core.

Based on the data in Figure 3-26, the time to reach full freeze of the core samples (temperature below 0C°) was reduced by 400%, from 35 to 9 minutes. Note: the percent improvement in time to freeze would have been higher if the starting temperatures for the initial and optimized systems had been the same. Using optimized system time to freeze sample at FEW and the former refinery was on the order of 5 minutes, given initial dewar pressures close to 200 psi (see Appendix A).

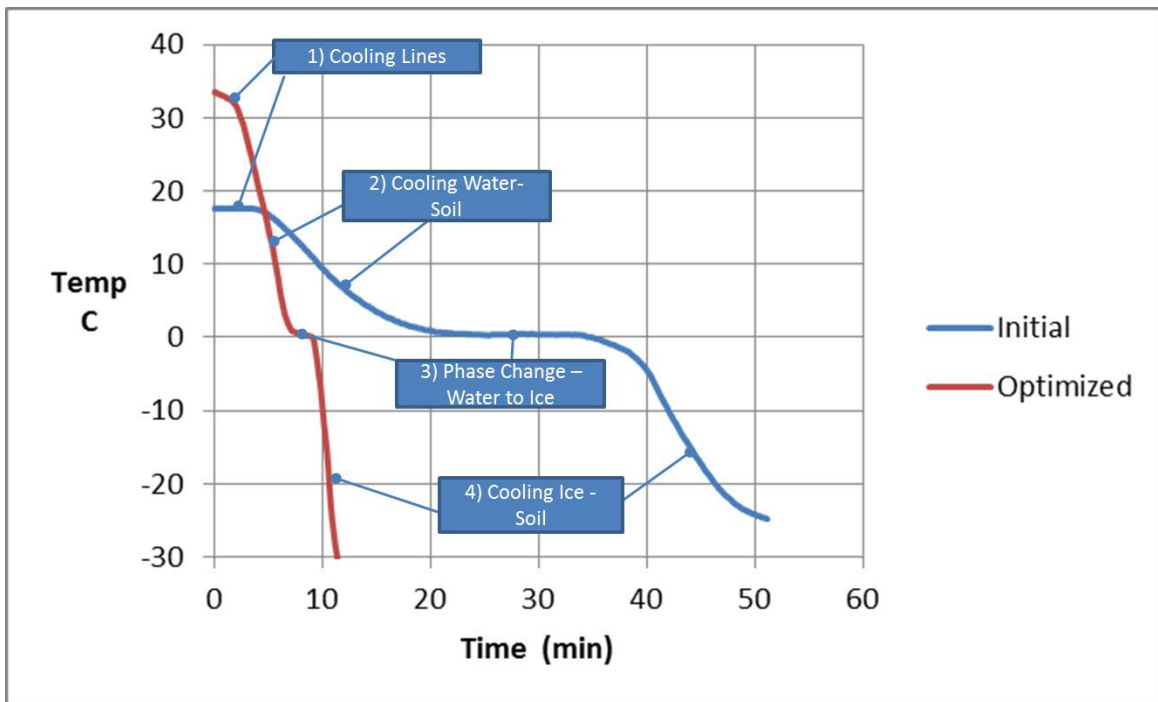


Figure 3-25. Temperature versus time data for freezing samples

An alternative way to consider the data is observed rates of change of core temperatures, shown in Figure 3-26 below. The rates of change data provides further insight regarding processes associated with *in situ* freezing of core.

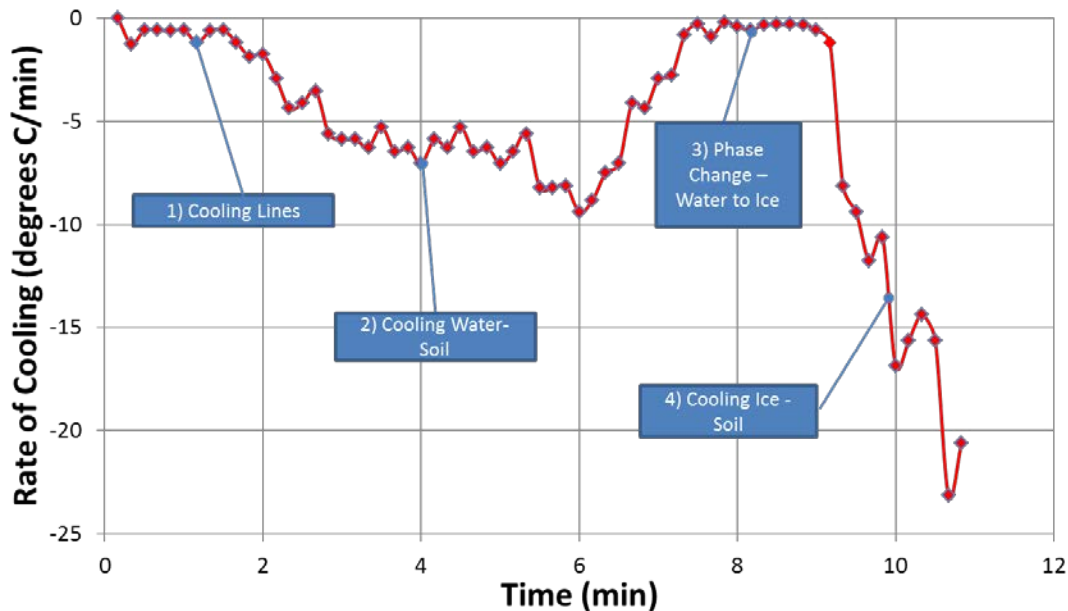


Figure 3-26. Observed rates of change of temperature within the core liner

3.2.2.3 Downhole ice locking of the core barrel in the auger flights

During field work at FEW and the former refinery, no problems were encountered with freezing of the sampling system in the auger flights. This result can be attributed to the use of insulation on the outside of all cooling systems and the resulting short periods of time used to freeze the samples.

3.2.2.4 Efficient Use of LN

Initial development studies used as much as 60 lbs of LN per foot of frozen core. Correspondingly, issues arose with respect to freezing tools inside the HSAs. Optimized systems using field protocol reduced LN use by 600 % to 9 lbs of LN per foot of frozen core. Considering a saturated core with a porosity of 27.5%, the theoretical amount of liquid nitrogen needed to drop solid/water system to 0 C° and freeze the water is 7.5 lbs LN per foot of frozen core. As such, at 9 lbs of LN per foot of frozen core, the cryogenic coring systems are 83% efficient.

3.2.2.5 Core Production

At FEW AFB, 52 feet of frozen core was collected over two days of field work. At the former refinery, 36 feet was collected in one day. As such, core production rates ranged from 26 to 36 feet of core per day. Per input from Drilling Engineers, including *in situ* freezing required approximately 1.5 times the level of effort that would have been required absent of cryogenic core collection. We believe that further refinement of the technique and, in particular, use of a second core barrel and cooling system, will result in levels of effort that are only slightly greater than for conventional coring and when expressed in terms of length of core recovered, could even represent less effort.

Chapter 4: High-Throughput Core Analysis 1- Frozen Core Sub-Sampling

As a complement to cryogenic core collection, laboratory methods were developed to rapidly process a large number of samples from the frozen cores. Parameters of interest included: contaminants (aqueous, sorbed and gas-phase), dissolved gases, redox conditions, mineralogy, microbial ecology, and hydraulic properties. This chapter presents methods for high-throughput core analysis (HTCA) along with demonstrative analytical results. Analytical results are recorded from frozen core collected at FEW and the former refinery.

4.1 Materials and Methods

This section presents materials and methods used for HTCA methods involving subsampling of frozen cores. Processing was conducted at the Center for Contaminant Hydrology (CCH) in a laboratory at Colorado State University, Fort Collins, Colorado.

4.1.1 Materials and Equipment

Photographs of select materials are shown in Figure 4-1. Methods are described in the following sections. Materials and equipment used for the processing of frozen cores are as follows:

- Hitachi cut-off saw with a Diablo “Metal Cut-Off” blade, with nominal dimensions of a 14-inch diameter and 1/8-inch thickness
- Hand-held stop-blocks, fabricated from scrap wood, cut to lengths of 1 inch and 3 inches
- Dremmel[®] 200-Series hand-held tool with a 1½-inch Cut-Off Wheel
- Stanley 4-lb “engineer hammer” with 12-inch handle
- Dasco Brick Set chisel, 4-inch wide × 7-inch long
- 3-inch PVC pipe, cut to a length of 2 inches, and with a 5/8-inch notch cut in the pipe wall
- Off-the-shelf aluminum foil and sealable plastic bags (Ziploc[®] or similar)



Figure 4-1. Materials and equipment used for high-throughput core processing. The following are shown: (A) cut-off saw, (B) stop blocks, (C) chisel, (D) hammer, (E) PVC pipe, cut to size, and (F) entire apparatus used for sub-dividing frozen core discs.

4.2 Frozen Core Processing

In the field, frozen cores were typically cut to a length of 2.5 feet (the initial liner length was 5 feet to be compatible with the CME core barrel, but the core barrel was only advanced 2.5 feet). Caps were placed on the ends, the cores were labeled, and stored on dry ice. Subsequently, cores were placed in the freezer at CSU: a) $-80\text{ }^{\circ}\text{C}$ freezer for RNA samples and b) $-20\text{ }^{\circ}\text{C}$ freezer for all other samples. Processing of frozen core was conducted in the CCH laboratory at CSU.

Prior to the processing of frozen cores, several preliminary tasks were conducted. Extraction jars were prepared with prescribed amounts of methanol or water, and weights were recorded. Sample log sheets were printed (Appendix C). Shortly before frozen-core processing, the cut-off saw and sampling equipment (described previously) were placed in a fume hood. Off-the-shelf aluminum foil and sealable plastic bags (Ziploc[®] or similar) were also gathered for collection of the cut-off core pieces.

At the time of processing, each frozen core was cut and processed as quickly as possible to minimize thawing. From our experience, the typical time requirement to process a 2.5-foot core section was about 30 minutes (some took longer due to unforeseen delays, such as rocks in the core). This processing rate appeared to be sufficient for the completion of processing without more the minor surficial thawing of the frozen cores. For processing of the frozen cores, one



Figure 4-2. Packaging frozen core for shipping

section of core was removed from the freezer (or cooler containing dry ice) and placed in a fume hood. Each core section was measured for length and recovery (i.e., percentage of tube containing core); this information was recorded on the log sheet. Next, each core was stripped of extraneous materials (labels, end-caps, and tape) and then transferred into the fume hood for processing.

Cores were divided into smaller cylindrical discs using a cut-off saw (A). Hand-held stop-blocks were used to quickly gauge lengths of frozen core for each cut (B). Cutting of each core section proceeded from the top (i.e., the end of the core that, in place, was nearest to the ground surface) to bottom. A short section of about 1 inch was cut from the top of the column and discarded. Thus, the first sample from each core occurred at a depth interval of about 1 to 2 inches from the top of the core. In general, one sample was collected for every 4 inches of core. Samples were 1-inch in thickness, and the distance between each sample was about 3 inches. The typical core sampling pattern is shown in Figure 4-5.

Immediately after each frozen sub-sample was cut from the frozen core, the following processing steps were completed as quickly as possible: (a) the plastic liner was cut from the outer rim of the sample, using a hand-held Dremmel[®] tool; (b) the frozen-core disc was placed in the splitting device (F); (c) the hammer and chisel were used to cut the frozen-core disc into three sub-samples, according to the pattern shown in ; (d) the core sub-samples were removed for microbial analysis, extraction in methanol, or extraction in water. Specific details regarding handling of each of these samples are provided subsequently. The time required to conduct these steps was about one minute per sample; performing these steps with minimal delays was necessary to prevent thawing of frozen cores before extraction and/or re-freezing was complete.

After completion of sampling, approximately 75% of the cores remained (i.e., the 3-inch segments from between the 1-inch-thick samples for each 4-inches of frozen core). These segments were placed in sealable plastic bags and returned to the freezer.



Figure 4-3. Photograph of frozen-core cutting

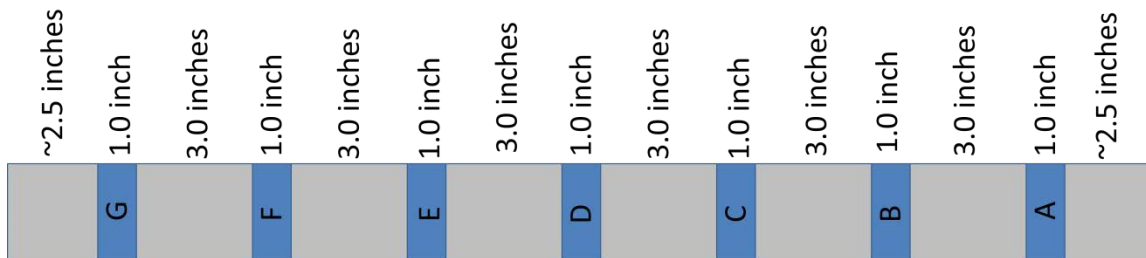


Figure 4-4. Typical Sampling Pattern for Frozen Cores

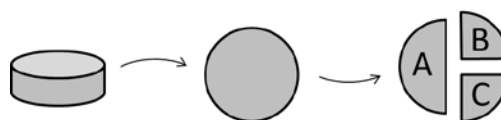


Figure 4-5. Illustration of pattern used for sub-sectioning of frozen-core samples

A = microbiological analysis

B = methanol extraction

C = water extraction

4.3 Analytical Methods

4.3.1 Biological Analysis

For microbiological analysis, half of each sample disk was wrapped in aluminum foil and returned to the freezer (-80°C) until DNA extraction. Note low DNA yields did not justify doing RNA analyses. DNA microbial analysis was performed in triplicate on the core samples following similar procedures previously described in Irianni Renno et al (2015). To remove potential contaminants (e.g, humic substances), which can negatively affect nucleic acid extraction yields as well as inhibit polymerase chain reaction (PCR) and pyrosequencing reactions, core samples were pretreated as previously described (Whitby and Lund, 2009) with a few modifications. 120 ng of skimmed milk was added per gram of pretreated core sample instead of 80 ng, polydeoxinocinic deoxycytidilic was added as an aqueous solution, and the core sample combined with the polydeoxinocinic-deoxycytidilic solution, the skimmed milk and 1 mL of distilled water were vortexed (1 minute) and centrifuged prior to proceeding with the wash steps as indicated by the published protocol.

DNA was extracted from the pretreated core samples using the Powerlyzer™ Powersoil DNA isolation kit (Mobio, Carlsbad, CA) per the manufacturer's specifications with the following modifications: DNA yield was maximized by using 0.5 g of core instead of 0.25 g, and duplicate extractions for each core subsample were pooled and processed with a single Powersoil™ spin filter. Additionally, the volume of elution buffer was limited to 50 µl instead of the recommended volume of 100 µl to increase DNA concentrations in the recovered volume. DNA was quantified via optical density at 260 nm with a Nanodrop™ 2000 reader (Thermoscientific, Wilmington, DE). DNA was extracted in triplicate from each core subsample and stored at -20°C prior to qPCR and pyrosequencing analysis.

qPCR assays. SYBR greenTM (Life Technologies, Grand Island, NY) qPCR assays were used to quantify the bacterial and archaeal 16S rRNA genes. Genomic DNA extracted from *Desulfivibrio desulfuricans* (ATCC #: 277740-5) and *Methanosarcina acetivorans* (ATCC #: 3595) was used to generate calibration curves for the bacterial and archaeal assays, respectively. The primer sets 27F/388r and 931AF/1100Ar were used for amplification of bacterial and archaeal 16SrRNA genes, respectively. All assays were performed using an ABI 7300 real-time PCR system (Applied Biosystems, Foster City, CA). Each 25- μ l SYBR greenTM qPCR reaction contained: 1X Power SYBR greenTM 567 (Life Technologies, Grand Island, NY), forward and reverse primers (2.5 μ M), magnesium acetate (10 μ M), PCR-grade water and 1 ng of DNA template. Thermocycling conditions were as follows: 95°C for 10 min, followed by 40 cycles of 95°C for 45 s, 56°C for 30 s, and 60°C for 30 s. Dissociation curve analysis was conducted to confirm amplicon specificity.

Pyrosequencing analysis. Pyrosequencing analysis was performed by Research and Testing Laboratory, LLC (Lubbock, TX), using an Illumina MiSeq/HiSeq Sequencer (Illumina, San Diego, CA). 16S community profiling was performed targeting bacterial 16S rRNA genes with primers 28F and 519r and archaeal 16S rRNA genes with primers 519wf and 519r.

4.3.2 Organic Compound Analysis

For VOC analysis, core sub-samples were extracted into methanol. These extractions took place in 120-mL glass jars with PTFE-lined caps. The extraction jars were initially prepared with 80 mL of high-purity (99.9%) methanol (Burdick & Jackson), and the preliminary weight of each extraction vial with methanol was recorded.

Approximately one quarter of each sample disc (fragment “B” in Figure 4.5) was extracted into the methanol for VOC analysis. After the frozen core sample was added to each jar, the cap was replaced. The weight of the jar with sample was then recorded (typical sample weights were about 25 g). The sample jars were placed on a vortex shaker for about 15 minutes to disperse cores. The jars were then stored in a refrigerator (about 4°C) for at least 4 days, providing time for slowly-desorbing contaminants to partition into the methanol. Finally, an aliquot of the methanol extract was transferred into a GC vial for analysis.

The methanol extract was subjected to two analyses: the first analysis (method 1) provides low detection limits for the more highly-chlorinated compounds (TCE and PCE); the second method (method 2) provides higher detection limits but is more sensitive to degradation products (VC and DCE isomers). Details for each method are as follows:

- Method 1 is conducted on an Agilent 6890 GC with an electron-capture detector (ECD). The GC is equipped with a J&W Scientific DB-5 column with the following dimensions: length = 30 m, ID = 0.32 mm, and film thickness = 0.25 μ m. Injection parameters consisted of a 5:1 split ratio and a column flow rate of 3.0 mL/min. The GC temperature program is as follows: initial temperature of 40°C, hold for 3 min, ramp at 10°C/min to 50°C, ramp at 40°C/min to 120°C, hold for 1 min.
- Method 2 is conducted on an Agilent 6890 GC with mass spectrometric (MS) detector. The GC/MS is equipped with a Restek RXi[®]-624Sil MS column with the following dimensions: length = 30 m, ID = 0.25 mm, and film thickness = 1.4 μ m. Injection

parameters consisted of a 4:1 split ratio and a column flow rate of 3.0 mL/min. The GC temperature program is as follows: initial temperature of 40°C, hold for 2 min, ramp at 8°C/min to 100°C, ramp at 40°C/min to 160°C, hold for 1 min. The MS detector was operated in single-ion mode (SIM) for this analysis.

For both methods, calibration standards for TCE, PCE, cDCE, tDCE, 11DCE, and VC were prepared in high-purity methanol. Five-point calibration curves were included with each analytical sequence.

4.3.3 Dissolved Gases and Water-Extractable VOCs

Aqueous extraction was conducted for volatile organic compound analysis, primarily targeting the lower-molecular weight products, including methane, ethane, and ethene.

Aqueous extraction jars were prepared ahead of time with de-aired, de-ionized (DI) water. Deionized (DI) water, with a resistivity of 18.3 MΩ, was obtained from a Barnstead Thermolyne NanoPure®Diamond™ UV ultrapure water system. The DI water was de-oxygenated by sparging with N₂ and then stored in an anaerobic chamber. Inside of the anaerobic chamber, water was distributed into 120-mL borosilicate glass jars with PTFE-lined septa caps; jars were filled with the de-aired, DI water to the top, such that no headspace existed. Jars were then re-sealed and stored anaerobically until shortly before processing of the frozen cores.

For this extraction, approximately one-quarter of the sample disc (“C” in Figure 4.5) was placed in an extraction jar, which was prepared as described in the previous paragraph. Because the jars initially were completely filled with water, the core sample displaced water from the jar. The jar lids were then replaced, thus re-sealing the jars with no headspace (with the exception of gas phases that may have been entrapped in the frozen-core subsample). Weights recorded included the extraction jar before sampling, the extraction jar with sample and displaced water, and the displaced water (the displaced water weight was used to estimate sample density). The sample jars were placed on a vortex shaker for about 15 minutes to disperse solid materials. The jars were then stored in a refrigerator (about 4°C) for an equilibration time of at least 4 days.

Water extract was transferred into 20-mL headspace vials for analysis. The headspace vials are constructed of borosilicate glass and were sealed with crimp-style PTFE-lined septa caps. A transfer method (described below) was employed that allowed for transfer of water from water-extract jars into the headspace vials with no atmospheric exposure.

A transfer device, consisting of coupled syringe needles, was constructed as shown in (C). Second, a 5-mL plastic syringe was fitted with a ½-inch, 27-gauge disposable needle. A Tedlar® bag was filled with de-aired water and then suspended from a ring stand. Finally, headspace vials were pre-sealed with crimp caps. The list of transfer steps we employed were as follows:

1. Record the tare weight of the headspace vial.
2. Place clamp in the middle (Viton tubing portion) of the transfer device (B).
3. Hold transfer device with the 2-inch needle pointed down and the ½-inch needle pointed up; insert the 2-inch needle through the septum of the aqueous-extract jar. Invert

headspace vial, then insert ½-inch needle through septum. Place inverted headspace vial in ring-stand clamp (C).

4. Remove the clamp from the transfer device (D).
5. Collect 5 mL of water from the Tedlar[®] bag in 5-mL syringe (E). Place ½-inch needle on syringe.
6. Insert 5-mL-syringe needle through septum of aqueous-extract jar (as shown in F).
7. Inject the 5 mL of DI water into the aqueous extract vial, displacing water from the aqueous-extract jar into the headspace vial.
8. When all of the water has been injected into the aqueous-extraction jar and pressure has equilibrated (i.e., no more water is flowing into the headspace vial), remove the injection syringe/needle from the aqueous-extract jar septum.
9. Re-clamp the transfer-device Viton tubing to eliminate water flow out of the headspace vial or aqueous-extract jar, both of which are now under pressure. Remove transfer-device needles from aqueous extraction jar and headspace vial.
10. Record the final weight (with sample) of the headspace vial.

Note: the water remaining in the extract vial was subsequently used for inorganic analysis and parameter measurement); the aqueous-extract jars were returned to the refrigerator to preserve conditions for these analyses. The headspace vials were analyzed within 24 hours of transfer.

Analysis for dissolved organic gases and water-extractable VOCs was conducted on an Agilent 6890 GC with flame ionization detector (FID) with a Tekmar 7000 headspace autosampler. Samples were equilibrated in the autosampler at 80°C for 15 minutes. The GC/FID was equipped with a Restek RT[®]-Q-BOND column with dimensions of length = 30 m, ID = 0.32mm, and film thickness = 10 µm. Injection parameters consisted of a 20:1 split ratio. A ramped column flow profile was implemented as follows: initial flow of 1.0 ml/min, hold for 5.5 min, ramp at 12 mL/min² to 4.0 mL/min. The GC temperature program is as follows: initial temperature of 45°C, hold for 5 min, ramp at 20°C/min to 250°C.

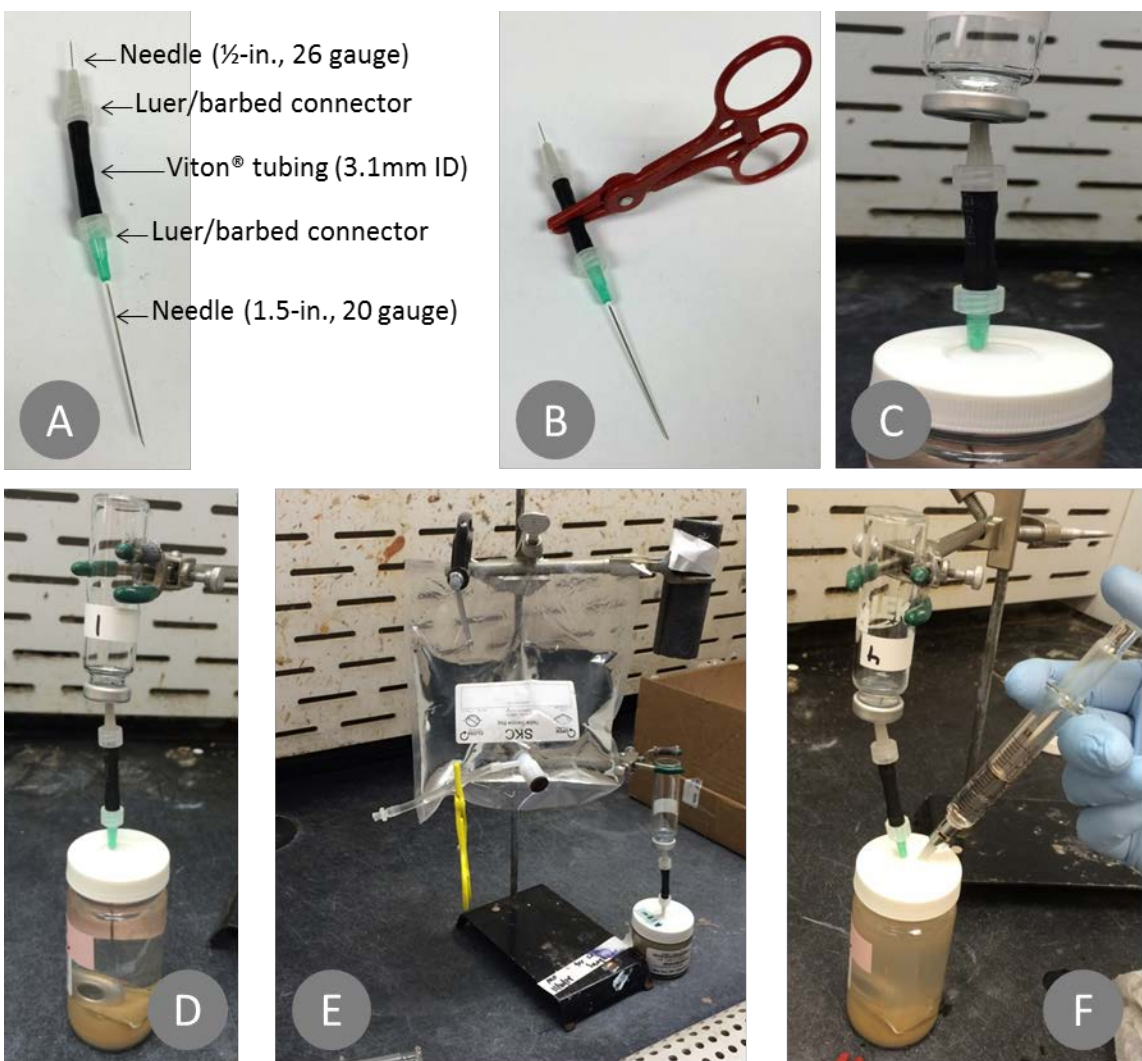


Figure 4-6. Photographs of the aqueous-extraction transfer procedure. Aqueous transfer device shown (A) with parts labeled, (B) with clamp, (C) connected to headspace vial and aqueous-extract jar, (D) aqueous extraction vial/headspace vial assembly, with the headspace vial supported by a ring-stand clamp, (E) Tedlar bag, and (F) injection of water to complete the transfer of aqueous extract into the headspace vial

4.3.4 Inorganic Analysis and Parameters

Inorganic analysis included anions and dissolved ferrous iron (Fe^{2+}). Methods are described below.

Anions Analysis. Analysis for anions was completed using an aqueous-extract solution (see Section 4.2.4); after 10 days, 10 mL of the aqueous extract solution was removed from select samples and transferred to the instrument-specific IC vials. Analysis for anions was conducted on a Metrohm 861 Advanced Compact Ion Chromatograph (IC), equipped with a Metrohm A Supp 5 – 250 column. Calibration standards for chloride, bromide, nitrate, phosphate, and sulfate were included in the analysis.

Ferrous Iron Analysis. The aqueous extract was also analyzed for dissolved ferrous iron (Fe^{2+}) using colorimetric methods. A modified version of the Hach Ferrous Iron method (1,10-phenanthroline) was used. The manufacturer's instructions state to dissolve the contents of 1 reagent pillow (Hach part #103769) in 25 mL of aqueous sample (i.e., 0.04 pillows/mL). Due to the smaller volume of water available, a concentrated reagent solution was prepared with 1 reagent pillow per 2.5 mL of DI water (0.4 packets/mL). Next, in a clear-plastic cuvette, 200 μL of the concentrated reagent solution were added to 1800 μL of aqueous sample. This combination provided 2 mL of sample for analysis, at a reagent concentration of 0.04 packets/mL, which is equivalent to the manufacturer's instructions. Cuvettes were placed in a Thermo Scientific Genesys 10uv spectrophotometer for analysis. Calibration solutions were included in the analysis.

pH and ORP Analysis. The aqueous extract left over after completion of work was analyzed for pH and ORP. Note that dilution of pore water, which occurs during the aqueous-extraction procedure, is likely to affect measured pH and ORP values. All other analyses of pore water parameters used dilutions factors to correct diluted constituent concentrations back to pore water concentrations.

The pH values represent a concentration, $[\text{H}^+]$, which can be corrected to a pore-water value by a simple dilution relationship, $C_1V_1=C_2V_2$ (where C and V refer to concentration and volume, respectively; subscripts 1 and 2 refer to the stock and diluted solutions, respectively). However, ORP refers to a potential, not a concentration, so dilution-based correction is not possible. Thus, although the reported ORP values may not directly indicate in situ conditions, the relative ORP values provide an indication of regions in the subsurface where conditions are relatively oxidizing or reducing.

Value for pH and ORP were measured in each of the aqueous-extract jar shortly after samples were collected for VOC analysis. Vial lids were opened in a fume hood, and were thus exposed to oxygen, which could affect ORP. Measurements were taken quickly (i.e., within 5 minutes) after opening the vial caps to minimize impact of atmospheric oxygen.

pH and ORP were measured using combination electrodes (VWR 89231-604 and VWR 89231-640, respectively) with Ag/AgCl as the internal reference. For both pH and ORP, the electrodes were connected to Denver Instruments UP-25 meters. The pH meter was calibrated in 4, 7, and 10 buffer solutions prior to sample measurements.

4.3.5 Total Petroleum Hydrocarbons (GRO, DRO and Benzene)

Concentration of total petroleum hydrocarbons (C_{TPH}) of samples were determined using liquid-solid extraction followed by gas chromatography (GC) method. Sub-samples were agitated in SMI multi-tube vortex, (SMI, Midland, ON, Canada) for one hour. One micro liter (μl) of the extract was injected into gas chromatograph (Hewlett Packard, Model 5890 Series II) with a flame ionization detector (FID). The GC was equipped with an automatic sample injector (Hewlett Packard, Model 7673) and a Restek (Bellefonte, PA) RTX-5TM column (30 m length x 0.32 mm ID x 0.25 μm film thickness). The GC temperature was kept at 45 $^{\circ}\text{C}$ for 3 minutes, increased to 120 $^{\circ}\text{C}$ by rate of 12 $^{\circ}\text{C}/\text{min}$, increased to 300 $^{\circ}\text{C}$ by rate of 20 $^{\circ}\text{C}/\text{min}$, and kept at 300 $^{\circ}\text{C}$ for 3 min. The injection port and detector temperatures were 250 $^{\circ}\text{C}$ and 300 $^{\circ}\text{C}$, respectively. The supply rate for the carrier gas (Helium) was 3 ml/min. A nine-component gasoline range organic

(GRO) EPA/Wisconsin mix standard (Restek, Bellefonte, PA) was used for GRO components including BTEX. A-component diesel range organic (DRO) EPA/Wisconsin mix standard (Restek, Bellefonte, PA) was used for DRO components. All calibration curves were characterized by coefficient of determination greater than 0.99 ($R^2 > 0.99$). At least two calibration standards were measured with each GC run. Total petroleum hydrocarbon (TPH) results are reported as the sum of GRO and DRO on a dry weight sediment basis. The dry weight of each sample was determined by removing excess liquids from sub-sample 1 and using microwave oven heating method according to ASTM D4643.

4.3.6 Geologic Logging

Geologic logging was conducted based on visual observation of the cores residing in the methanol-extract bottles. Cores were visually logged for properties including sediment type (sand, silt, clay) particle size, sorting, description, color, and cementation. Visual observations on mineralogy were noted for select samples as well. The geologic logging was led by Dr. Tom Sale, a Wyoming Professional Geologist - #1954.

4.3.7 Hydraulic Conductivity Testing

To facilitate high-throughput analysis of hydraulic conductivity, K (cm/s)¹, in cryogenically-collected cores, a Core-In-Liner (CIL) method was developed. The CIL method is designed to measure K directly in the liner. After sub-sampling of the frozen cores (Section 4.1.2), the unsampled intermediate sections of core, which are about 3 inches in length, remained intact and were returned to the freezer. The CIL method was designed to test K directly on these specimens, without the need to remove cores from the liner. In addition to reducing the time requirement and uncertainty associated with handling and re-packing of core specimens, the CIL method allows for K measurement under in situ conditions (e.g., with particle sorting and layering); these conditions are generally well-preserved in cryogenically-collected cores.

To implement the CIL method, fittings were designed to attach directly to the plastic core-sampling liner, using bolts to provide compression and O-rings to provide water-tight seals. The fittings consisted of collars that bolted onto end caps (both constructed of acrylic). The end caps are designed such that the short bolts (2 inch) can be tightened to compress Viton O-rings, thus creating seals between the liner, collar, and end cap. Furthermore, long bolts (5 inch) were employed to compress the core sample, thus reducing the chance of side-wall leakage occurring. Components of the CIL system are shown in Figure 4-7; assembly is shown in Figure 4-8.

¹ metric units are used here because they are more-widely used in K testing than imperial units)

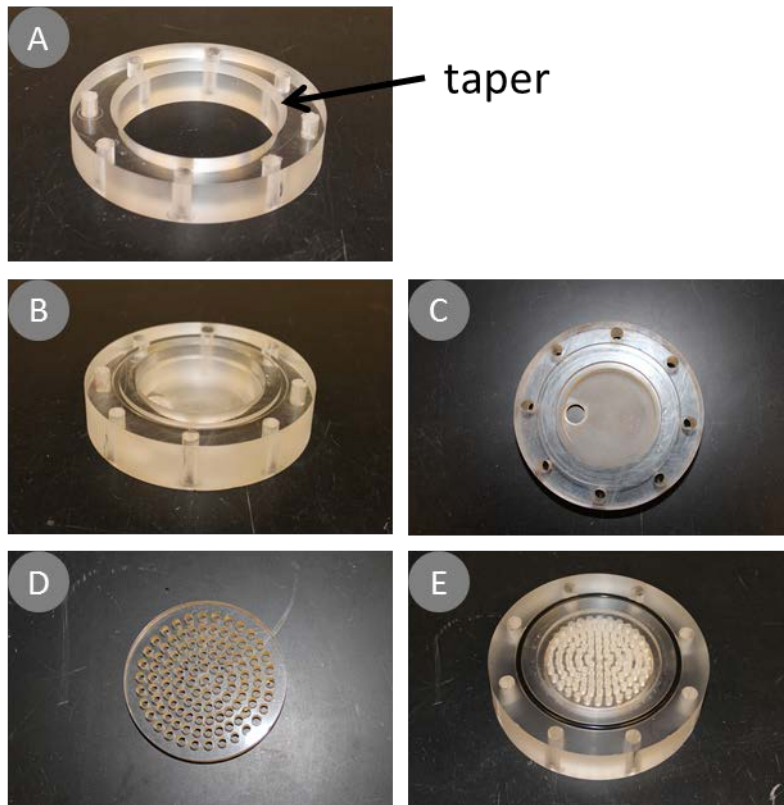


Figure 4-7. Components of core-in-liner K-testing apparatus: (A) collar, (B) end cap, (C) end cap overhead view, (D) filter disc, and (E) end cap overhead view with filter disc emplaced

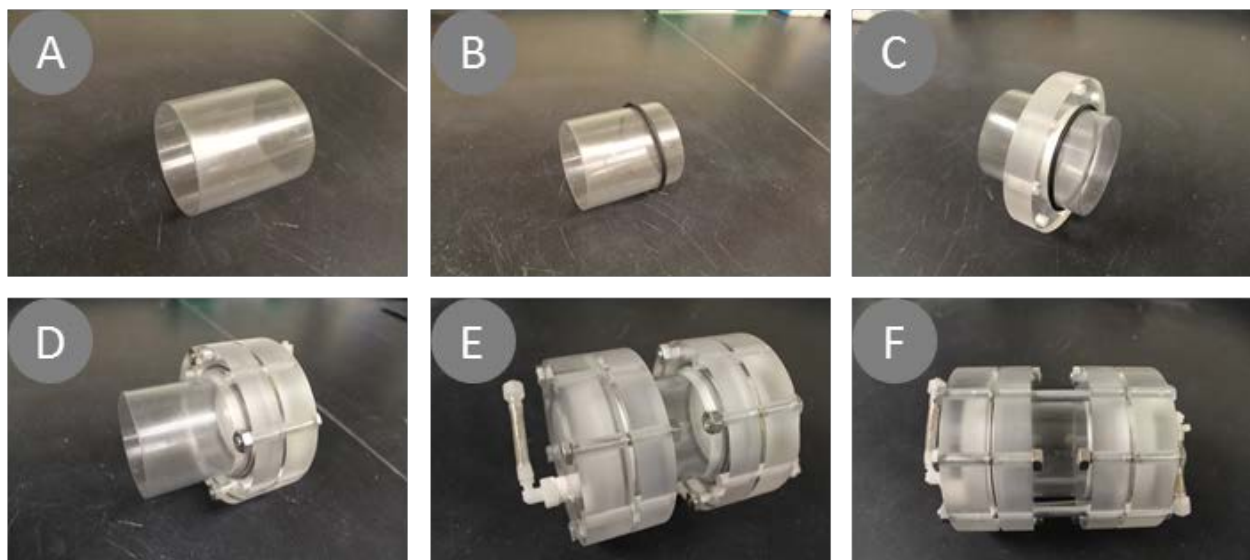


Figure 4-8. Assembly of core-in-liner K-testing apparatus: (A) An empty core-sampling liner, (B) liner with one O-ring in place, (C) with collar, (D) with collar/end-cap assembly, loosely bolted with short bolts, (E) with second collar/end-cap assembly in place, and (F) with long-bolts in place

Testing was completed on eight of the intermediate core sections. The samples were selected based on the geologic logging (Section 4.1.7), as being representative of different geologic regions observed in the samples. Particle size distribution curves for each of the samples used for K testing are shown in Appendix D.

In preparation for K testing, core sections were removed from the freezer and then mounted into the CIL device. Filter paper was placed on both ends of the sample to limit discharge of solid particles. For loading the CIL device, the collars and end caps were loosely placed on both ends of the sample. The long bolts were then installed and tightened, thus providing compression on the core sample. Finally, the short bolts were tightened to provide a seal. After the sample was loaded, the CIL device was connected to a hydraulic testing station for analysis. The device was allowed to sit at room temperature for at least six hours to allow the sample to thaw before testing.

Constant-flow and/or falling head methods were used to measure K . Samples were initially tested using falling head, and high-permeability samples ($K > 10^{-5}$ cm/sec) were analyzed using a constant flow test. For all K testing, tap water (City of Fort Collins) was used as a permeating fluid.

Constant-Flow Methods. For constant-flow testing, a peristaltic pump was used to conduct flow through the specimens at flow rates ranging from about 0.5 to 12 mL/min. Flow rates were calculated by collecting discharge water over a known time period. At each flow rate, the steady-state head drop across each sample, Δh (cm), was recorded.

For constant-flow K testing, values of K for each sample were calculated by linear regression of Q versus $\Delta h \cdot A/L$, based on the following form of Darcy's Law:

$$Q = -K \left(\frac{\Delta h}{L} A \right)$$

where L (cm) is the sample length, and A (cm²) is the cross-sectional area. The value of L was measured for each specimen; typical values were between 2.8 and 3.0 inches (7.0 and 7.5 cm). For all specimens tested, $A = 4.2$ square inches (27 cm²).

Falling Head Methods. For low-conductivity samples ($K < 10^{-5}$ cm/sec), K values were estimated using falling-head methods. The falling head testing station is shown (). For falling head testing, the initial head drop (Δh) values were approximately 1.1 m of water. Head values versus time were manually recorded and also logged using a Solinst 3001 Levelogger, which recorded a pressure value every 5 min. Pressure values recorded by the datalogger were corrected for atmospheric fluctuations based on readings recorded from a Solinst Barologger. K values were calculated from experimental data by linear regression, based on the following equation:

$$\ln \left(\frac{\Delta h_0}{\Delta h_t} \right) = -K \frac{At}{aL}$$

where Δh_0 (cm) is the initial head drop across the specimen, Δh_t (cm) is the head drop across the specimen at time t , and a (cm²) is the cross-sectional area of the falling head reservoir.



Figure 4-9. Falling head test station

Additional Testing. After completion of hydraulic conductivity testing, specimens were tested for porosity, water content, and particle size distribution. Porosity and water content were calculated based on weight measurements before and after oven drying at 80°C, overnight. Particle size distribution was determined by conducting sieve analyses.

4.3.8 Fraction Organic Carbon

The core-sample fraction organic carbon (f_{oc}) is defined as the mass of organic carbon per mass of total solids. For analysis of FEW AFB cryogenic core collection samples, the f_{oc} was measured using core from the water-extract samples after all other analyses were complete. To obtain f_{oc} data, all samples were analyzed for total- and inorganic-carbon fractions; organic carbon was then calculated by difference.

In preparation for the analyses, excess water was decanted from the water-extract jars. The samples were oven-dried at 80°C overnight. The dry weight was measured to determine sample water content. Next, all of the dried samples were ground to a fine powder using a ball mill. Subsamples of the powder were then removed for total carbon and inorganic carbon analysis.

Total carbon was measured at the EcoCore facility (Colorado State University, Fort Collins, CO) using a LECO Tru-Spec CN analyzer (Leco Corp., St. Joseph, MI). Inorganic carbon was measured using an acid-digestion method.

4.3.9 Density and Water Content

Core parameters including dry-bulk density, ρ_b (g/cm³), and gravimetric water content, w (g water / g dry solids), were determined for water-extract samples after other analyses were complete. The total sample masses and volumes were measured at the time of sample collection (Section 4.1.5). To calculate w , the dry-soil mass was needed for each sample. To obtain dry-soil values, each sample was oven-dried at 80 °C overnight, and the resulting dry-soil weight was recorded. Values for ρ_b and w were calculated as follows:

$$\rho_b = \frac{\text{sample dry mass (g)}}{\text{total sample volume (cm}^3\text{)}}$$

$$w = \frac{\text{sample water mass (g)}}{\text{sample dry soil mass (g)}}$$

4.4 High-Throughput Core Analysis: Results

Cryogenically collected cores from FEW and the former refinery were analyzed to provide depth-discrete data that demonstrate the efficacy of cryogenic coring. For FEW, analytes included contaminants (aqueous and sorbed phases), dissolved gases, aqueous phase inorganic constituents, pH, ORP, microbial ecology, geology, and hydraulic properties. For the former refinery, analytes included gasoline range organics, diesel range organics, and benzene. The following sections review results by site. Results from studies evaluated the use of medical scanning equipment to characterize core are presented in the following Chapter.

4.4.1 FEW Total VOC Concentration

FEW subsamples were analyzed for the following VOCs: PCE, TCE, DCE isomers, and VC. The primary VOC detected was TCE, which was present in all three cores. The highest TCE concentrations were present in the core samples from MW700C. PCE, tDCE, cDCE, 11DCE, and VC were not detected in any of the core samples.

TCE concentrations versus depth in each of the three core locations are shown in Figure 4-10. Given the low concentrations and large distances from release areas, we assumed that no nonaqueous phase liquids (NAPL) were present in any of the samples. Observations from Figure 4-10 include:

- For MW173F, TCE concentrations ranged from non-detect (<5 µg/kg) to 110 µg/kg; the average of detected values was 38 µg/kg. Minor elevated TCE concentrations (>50 µg/kg) were noted at depths of 14.4, 19.2-20.1, 27.2, 30.8-33.6, and 37.2-39.0 feet.
- For MW38C, TCE concentrations ranged from <5 to 41 µg/kg and averaged 21 µg/kg. No elevated TCE concentrations (>50 µg/kg) were observed in MW38C.
- For MW700C, TCE concentrations ranged from 6 to 400 µg/kg and averaged 110 µg/kg. Elevated TCE concentrations were observed between 13.9 and 17.0 feet bgs.

In general, the results indicate fairly smooth trends with variable concentrations versus depth. These results are not surprising considering typical heterogeneous subsurface environments. The earliest documentation of TCE at FEW dates back to work conducted by the U.S. Geological

Survey (USGS) in May and June 1987. Given this information, TCE has persisted at FEW at detectable levels for more than 28 years.

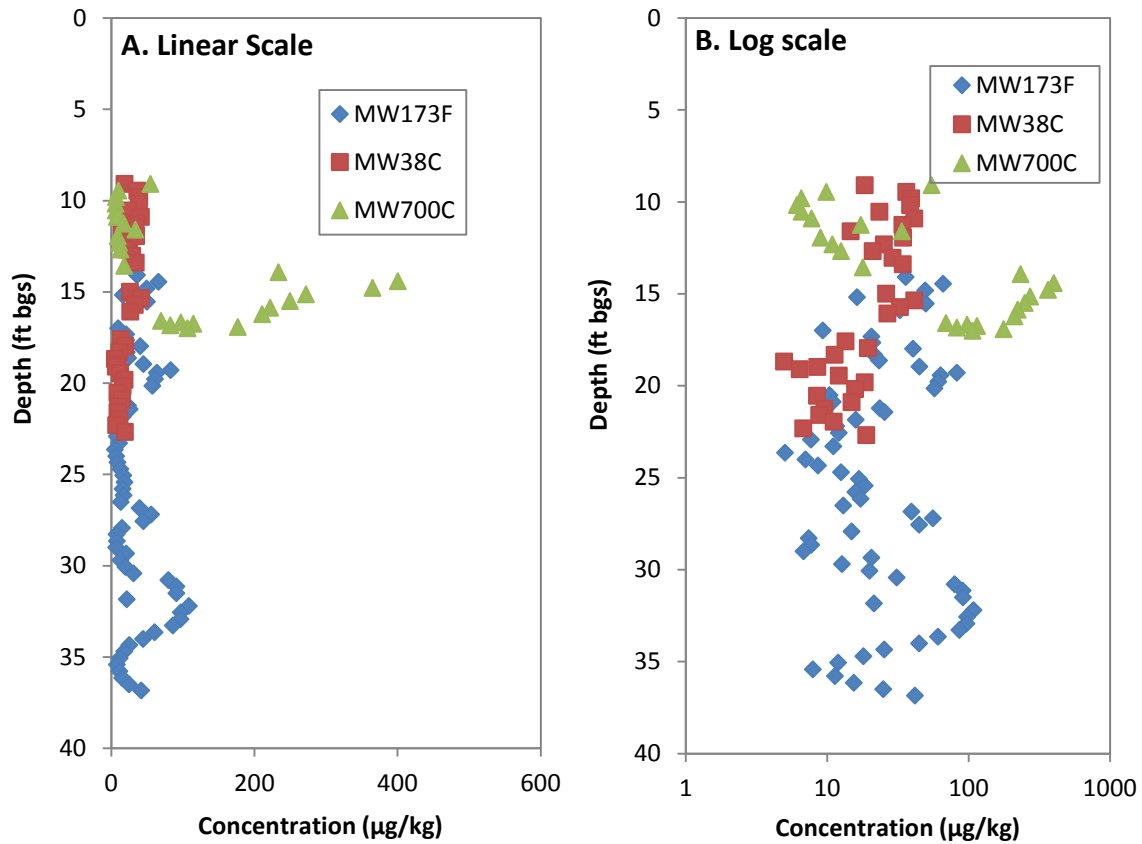


Figure 4-10. TCE data (dry weight basis) in methanol extracts: linear (A) and log (B) scales

Samples were also analyzed for PCE. PCE was detected above reporting limits (about 7.0 µg/kg) in only one sample: MW173F, at a depth of 14.80 feet (14.5 µg/kg). PCE was present below reporting limits in several samples. Estimated quantities for these samples are shown in Figure 4-11.

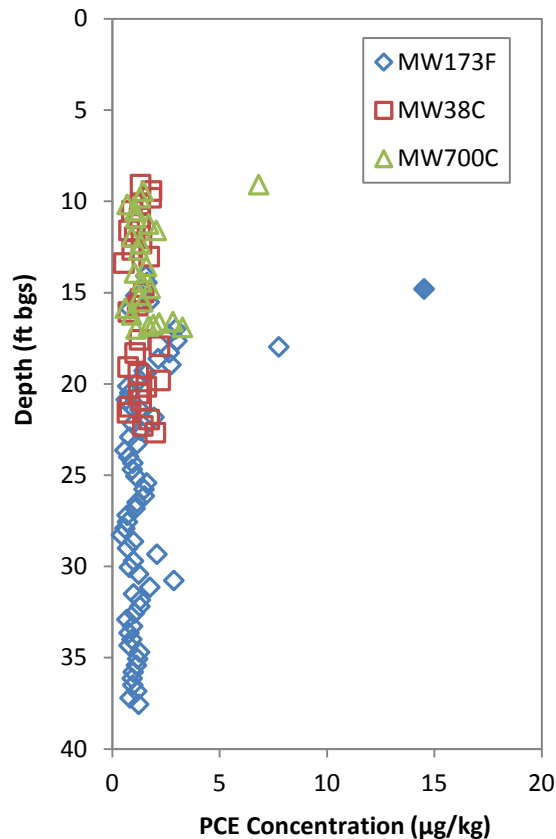


Figure 4-11. PCE data (dry weight basis) in methanol extracts. Solid data points indicate detected values; hollow data points indicate estimated values for samples in which PCE was identified but was present below reporting limits.

4.4.2 FEW Dissolved Gases and Water-Extractable VOCs

Water-extract samples were analyzed using a GC/FID method that is capable of providing data for a wide range of compounds, including methane, ethane, ethene, acetylene, vinyl chloride, DCE isomers, TCE, and PCE. Of these, the only compound regularly detected in samples was methane (Figure 4-12). Methane was detected in MW 173F and MW700C, at concentrations that varied considerably with depth. In MW173F, methane concentrations ranged from non-detect (about 900 µg/kg) to 17,000 µg/kg; higher concentrations of methane were generally detected at greater depths (i.e., greater than 27 feet bgs). In MW700C, methane concentrations ranged from 4900 to 21,000 µg/kg. No methane was detected in MW38C.

Ethane was detected in every sample, including blanks, implying that cross-contamination with ethane occurred. The assumed source of ethane cross-contamination was the anaerobic chamber in which headspace vials were prepared. None of the experimental samples contained ethane at levels much higher than those detected in the blanks. The presence of methane, a potential electron donor for reduction of chlorinated solvents was a surprise. Interestingly, lactate was injected near MW173F as part of an effort to enhance reductive dechlorination in the Spill Site 7 area in the late 2000s. The sampled interval at MW700C is located in alluvium associated with No Name Creek and may have elevated levels of recent natural organic materials.

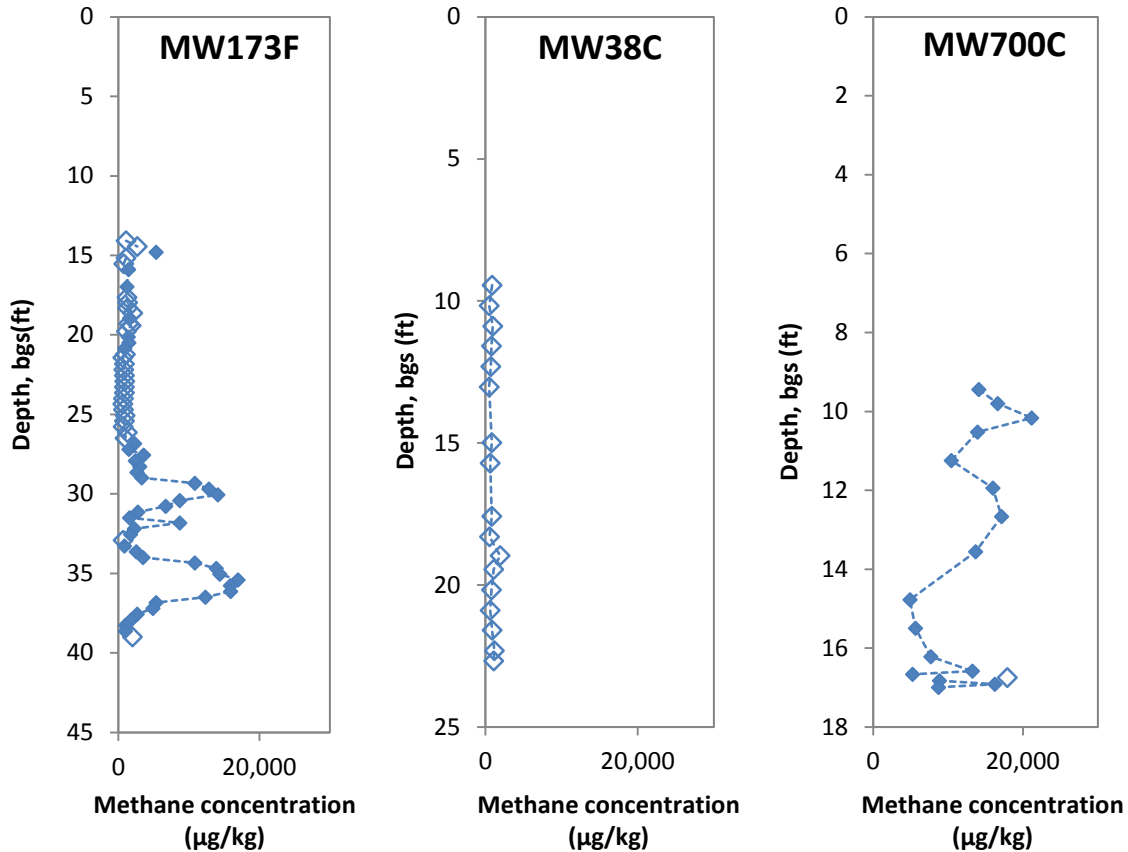


Figure 4-12. Methane concentration (dry weight basis) versus depth. Solid data points indicate detected values; hollow data points indicate lower detection limits for samples in which no methane was detected.

4.4.3 FEW Aqueous and Sorbed Phases

The fraction of organic carbon (f_{oc}) was measured using all the core subsamples. Fraction of organic carbon results are presented in Figures 4-13 to 4-15 and Appendix F. Report values range from 0 (below detection limits) to 4.0%, with an average value of 0.11%. By location, average f_{oc} values were 0.057% (MW173F), 0.14% (MW38C) and 0.18% (MW700C).

Aqueous phase concentrations (C_{aq}) and sorbed phase concentrations are also presented in Figure 4-13, Figure 4-14, and Figure 4-15 for locations MW173F, MW38C, and MW700C, respectively. Values for C_{aq} were estimated using the above total contaminant concentrations (C_t), the equations below, and the assumptions of no NAPL, water saturation $S_w=1$, and an organic carbon water partitioning coefficient (K_{oc}) value of 126 mL/gm (Pankow and Cherry 1996). Bulk density and porosity values were calculated for each sample based on measured sample volumes and water contents.

$$C_{aq} = \frac{C_T}{\frac{\phi S_w}{\rho_b} + f_{oc} K_{oc}} \quad C_{sorbed} = f_{oc} K_{oc} C_{aq}$$

Stick figures of the geology, based on visual inspection of cores are included with the concentrations plots. Results suggest that generally:

- The vast majority of the contaminant mass is in the aqueous phase at FEW
- Pore water concentrations are as high as 250 to 500 ug/L
- MW 38C and MW173F have the highest concentrations in transmissive zones while MW700C has the highest concentrations in the low k zones.
- Plausible explanation can be developed for the observed distributions of chlorinated solvents can be gained from local histories of remedial action and other measured parameters as discussed subsequently in the section on data panels.

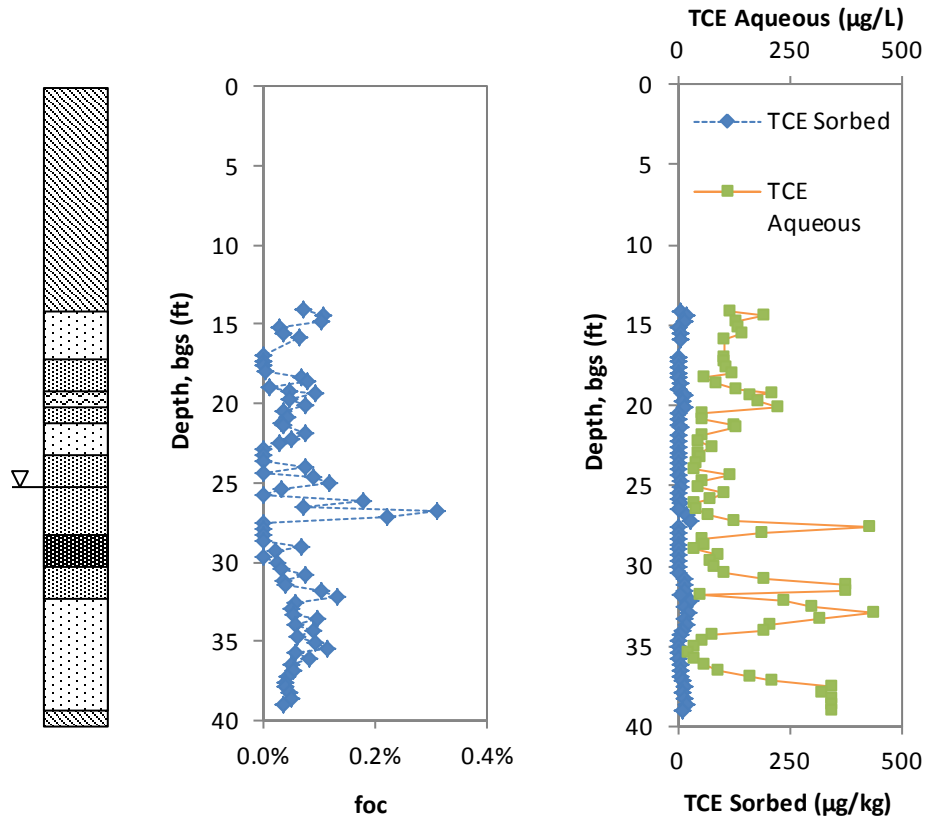


Figure 4-13. Geologic log, f_{oc} , and TCE concentration distribution between aqueous and sorbed phases for location MW173

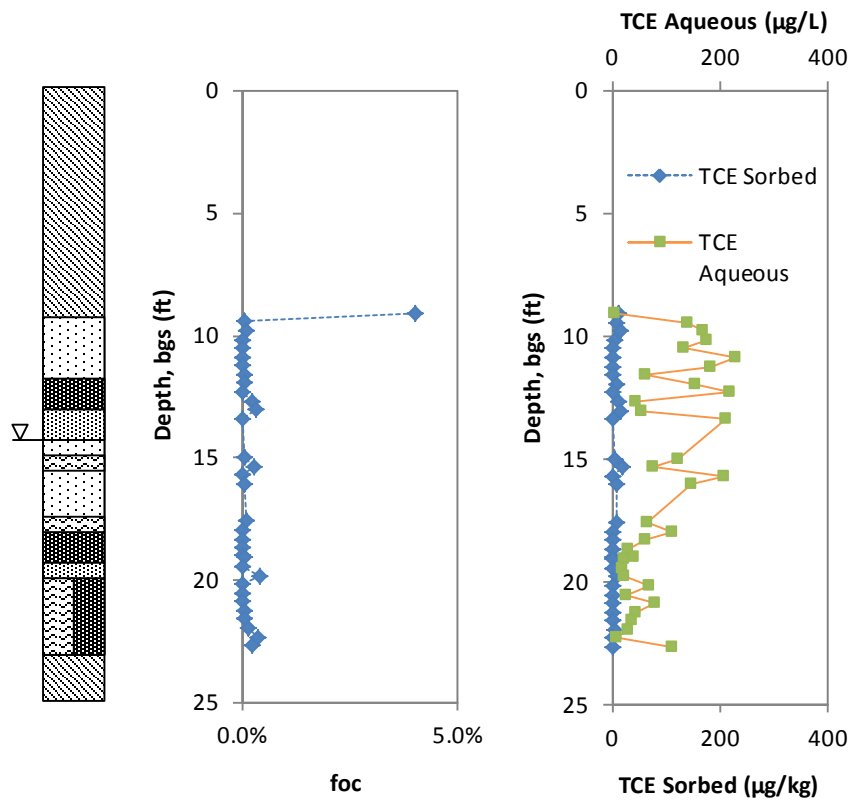


Figure 4-14. Geologic Log, f_{oc} , and TCE concentration distribution between aqueous and sorbed phases for location MW-38C

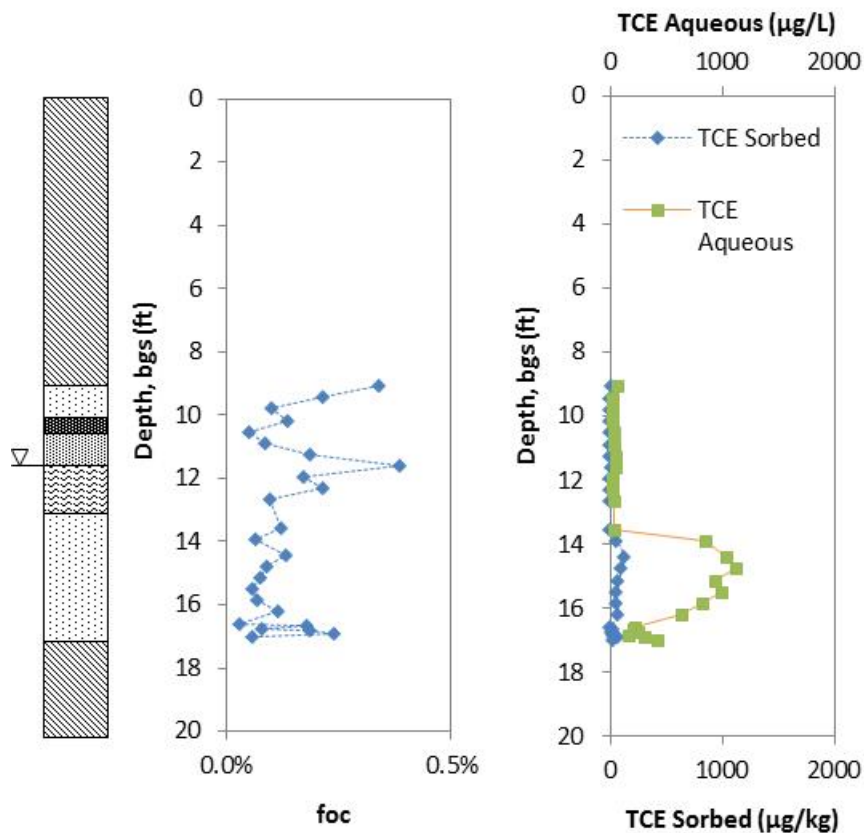


Figure 4-15. Geologic Log, f_{oc} , and TCE concentration distribution between aqueous and sorbed phases for location MW700C

4.4.4 FEW Inorganic Analytes

Inorganic Analyses: Anions. Inorganic parameters included chloride, bromide, nitrate, phosphate, and sulfate are presented in Figure 4-16. Measured aqueous-phase concentrations were converted to a total-sample-mass basis in term of mg per L water.

In MW173F, results were as follows:

- Chloride concentrations ranged from 10 to 490 mg/L and averaged 130 mg/L.
- Nitrate concentrations ranged from non-detect (< 2 mg/L) to 11 mg/L and averaged 5.4 mg/L.
- Sulfate concentrations ranged from 7.7 to 890 mg/L and averaged 137 mg/L.
- Bromide and phosphate were not detected in any samples.

In MW38C, results were as follows:

- Chloride concentrations ranged from 13 to 390 mg/L and averaged 100 mg/L.
- Nitrate concentrations ranged from non-detect (<2.0 mg/L) to 26 mg/L and averaged 15 mg/L.
- Sulfate concentrations ranged from 14 to 150 mg/L and averaged 51 mg/L.
- Bromide and phosphate were not detected in any samples.

In MW700C, results were as follows:

- Chloride concentrations ranged from 8.4 to 120 mg/L and averaged 37 mg/L.
- Nitrate concentrations ranged from non-detect (<2.0 mg/L) to 5.0 mg/L and averaged 3.3 mg/L.
- Sulfate concentrations ranged from 3.3 to 48 mg/L and averaged 17 mg/L.
- Bromide and phosphate were not detected in any samples.

Potential implications of the above analyses include:

- Elevated chloride levels may reflect historical reductive dechlorination of chlorinated solvents in select intervals.
- The presence of nitrate suggests a plume that is not strongly reduced from a redox perspective (no favoring reductive dechlorination).
- High levels of sulfate may indicate intervals where reductive dechlorination is inhibited by preferential reduction of sulfate.

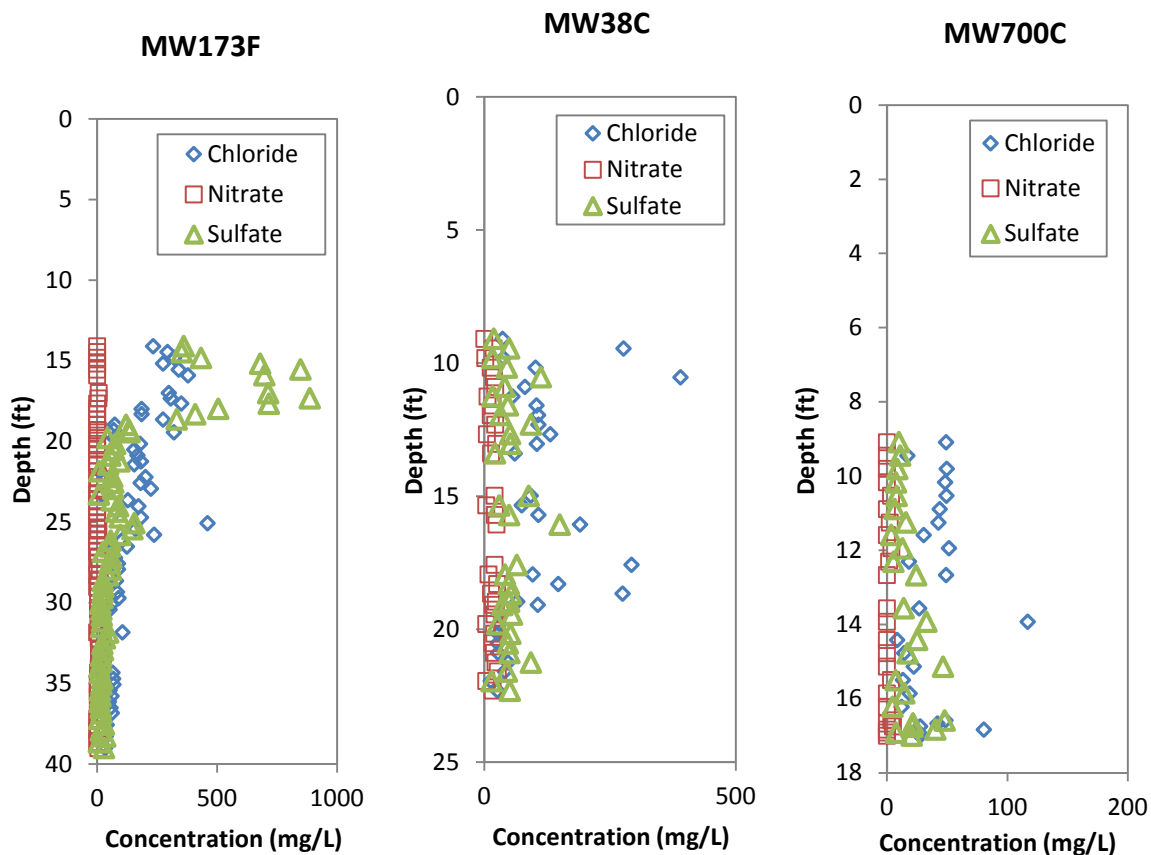


Figure 4-16. Anion data in aqueous extract (pore-water-volume basis)

Inorganic Analyses: Ferrous Iron (Fe^{2+}). Ferrous iron data are shown in Figure 4-17. A summary of statistics by core locations are as follows:

- In MW173F, ferrous iron ranged from non-detect (< about 0.04 mg/L) to 7.2 mg/L.

- In MW38C, ferrous iron ranged from non-detect (< about 0.04 mg/L) to 10 mg/L.
- In MW700C, ferrous iron ranged from 1.1 to 110 mg/L. In general, Fe²⁺ concentrations were higher at shallower depths (i.e., < 14.5 feet bgs).

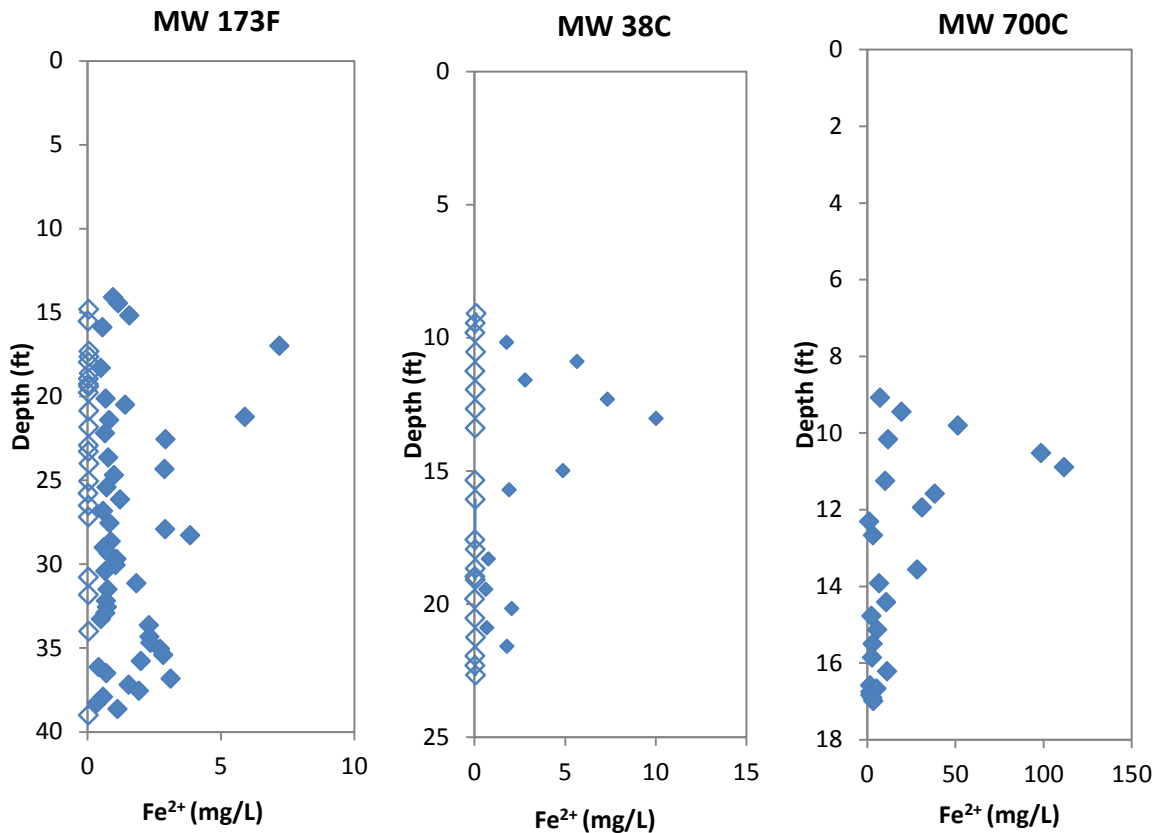


Figure 4-17. Ferrous iron data in aqueous extract (pore-water-volume basis). Solid data points indicate detected values; hollow data points indicate detection limits for samples in which Fe²⁺ was not detected.

4.4.5 FEW pH and ORP

Parameters included pH and ORP. pH and ORP were measured in core samples that had been diluted in water. Reported pH and ORP values are measured in the diluted aqueous-extract water.

- In MW173F, pH ranged from 8.2 to 8.7 and ORP ranged from -80 to 150 mV.
- In MW38C, pH ranged from 8.2 to 8.8 and ORP ranged from 140 to 400 mV.
- In MW700C, pH ranged from 7.8 to 9.0 and ORP ranged from -230 to 120 mV.

Overall, pH values are constant near 8 in all cases. ORP values suggest:

- An absence of reducing condition at MW38
- More reduced conditions at NW173F
- Shallow strongly reducing conditions at MW700C

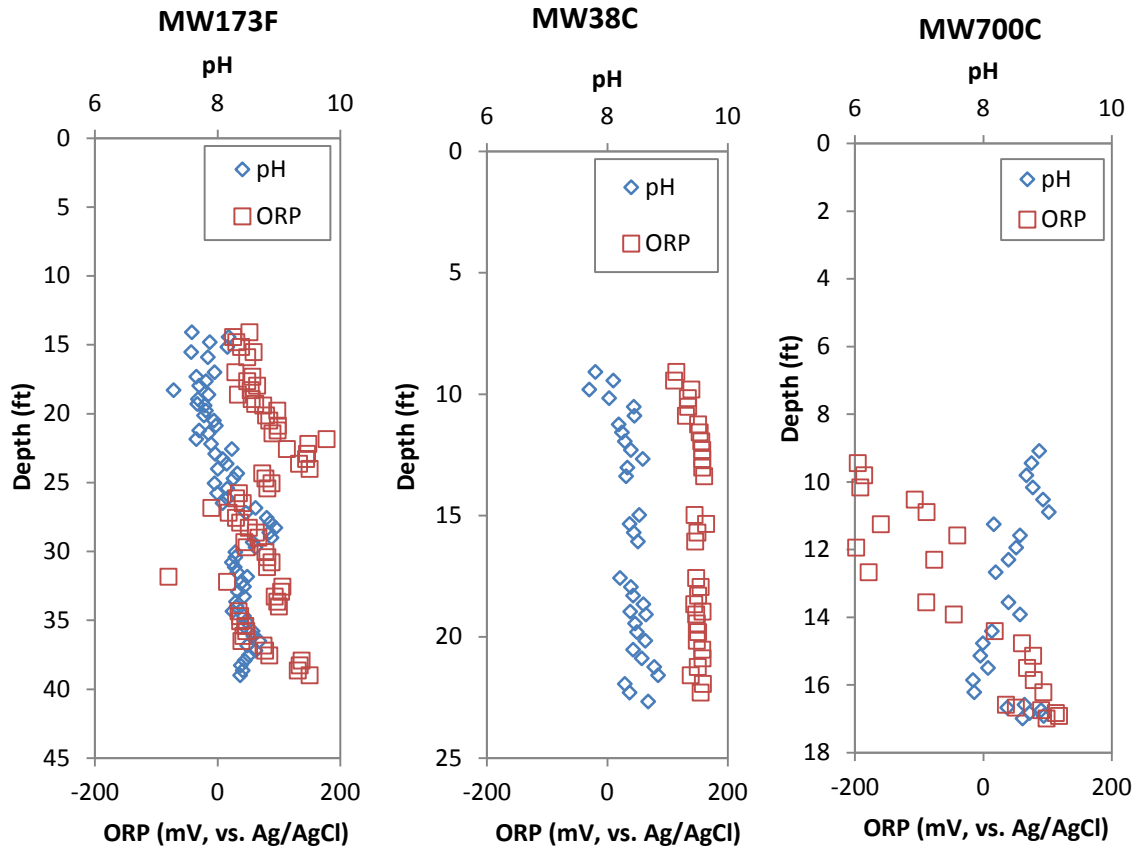


Figure 4-18. pH and ORP data in aqueous extract

4.4.6 FEW AFB Geology

A summary of the geologic logging of cores is shown in Figure 4-19, and the complete log is shown in Appendix E. In general, site geologic media was comprised of fine-grained materials, with particle sizes primarily ranging from fine-sand to silt. One of the key features of the site geology is the degree of heterogeneity. Most of the geologic layers consisted primarily of fine sand with varying degrees of sorting (well- to poorly-sorted). Layers of well-sorted to poorly sorted silt were identified, interbedded within the fine sand. Perhaps most significantly insight from this work is that geologic heterogeneity can be correlated to spatial variations in contaminants, redox conditions, and f_{oc} in ways that holds promise for novel insight into governing processes.

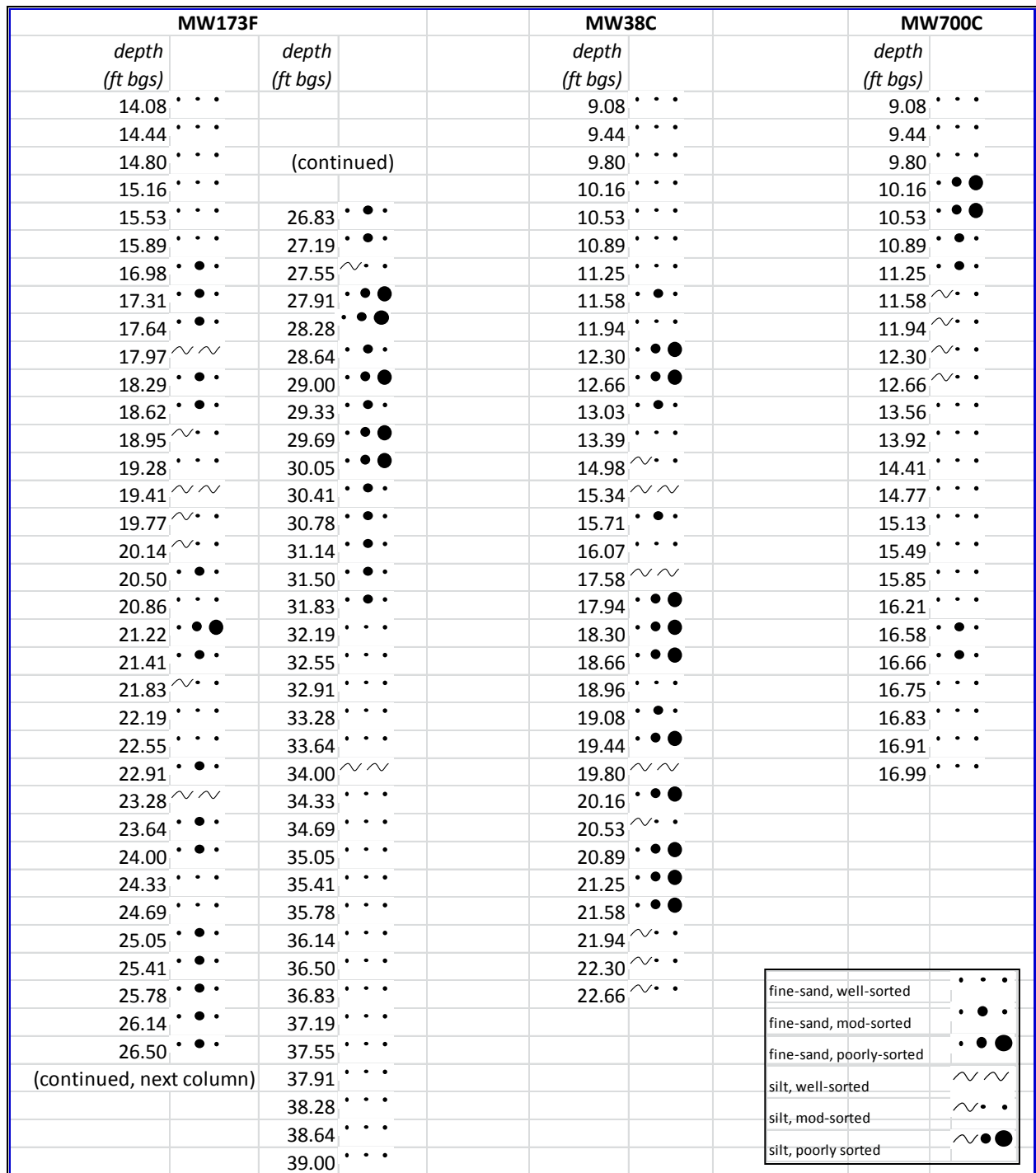


Figure 4-19. Geologic log summary

4.4.7 Hydraulic Conductivity

Results of hydraulic conductivity testing are shown in Table 4-1. The data indicate nearly a 3 order of magnitude variation in hydraulic conductivity values for the studied materials (7.8×10^{-3} to 1.9×10^{-5} cm/sec). Logically, the materials with larger hydraulic conductivity values are sand versus silt and well sorted versus moderately or poorly sorted.

Table 4-1. Hydraulic Conductivity Results

Sample ID	Core location	Depth (ft)	Description	Water content (g/g)	K, CF ¹ (cm/s)	K, FH ² (cm/s)
110	MW 38C	15.34	Silt, well-sorted	0.205		5.2x10 ⁻⁵
118	MW 38C	19.08	Sand, moderately sorted, fine-to-medium grained	0.208	7.8x10 ⁻³	1.2x10 ⁻³
79	MW700C	9.80	Sand, well-sorted, fine-grained	0.240	2.3x10 ⁻³	
81	MW700C	10.53	Sand, poorly-sorted, fine-to-coarse grained	0.180	1.6x10 ⁻³	
82	MW700C	10.90	Sand, moderately-sorted, silt-to-fine grained	0.149	7.3x10 ⁻⁴	
126	MW38C	21.94	Silt, moderately-sorted, with fined sand			2.2x10 ⁻⁵
122	MW38C	20.53	Silt, moderately-sorted, with fined sand			3.5x10 ⁻⁶
104	MW38C	11.94	Sand, well-sorted, fine-grained			1.9x10 ⁻⁵

¹ Constant flow testing methods (K > 10⁻⁴ cm/s)

² Falling head testing methods (K < 10⁻⁴ cm/s)

4.4.8 FEW AFB Density and Water Content

Results for bulk density (ρ_b) and water content (w) are shown in Figure 4-20. Values for ρ_b ranged from 1.1 to 2.4 g/cm³ and averaged 1.8 g/cm³. Values for w ranged from 0.08 to 0.52 (g/g) and averaged 0.21. Measured water content values were used to convert measured concentrations for organic compounds (TCE and methane) to a dry-weight basis.

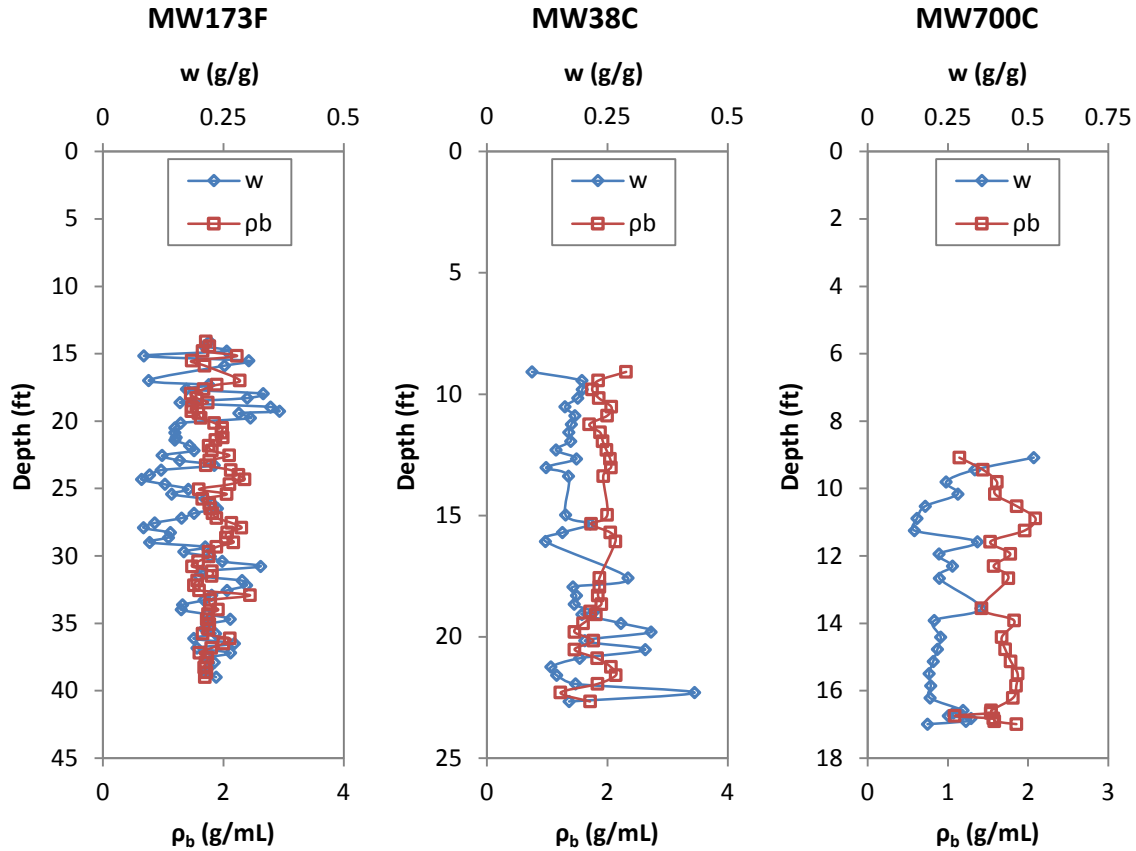


Figure 4-20. Water content and dry bulk density data for each core location

4.4.9 FEW Microbial Ecology

Figure 4-21 presents the number of 16s rRNA genes per gram of solids for archaea and bacteria as a function of methane and TCE at MW- 700. Overall, the number of expressed genes is low. Two distinct intervals are identified:

- A) A moderately sorted silt (low k zones) with low TCE, high methane, and higher levels of 16s rRNA genes
- B) A fine-grained well-sorted sand (transmissive zone) with high TCE, low methane, and low levels of numbers of 16s rRNA genes

Noted conditions would be consistent with the low zones acting as a diffusive/reactive sink for TCE.

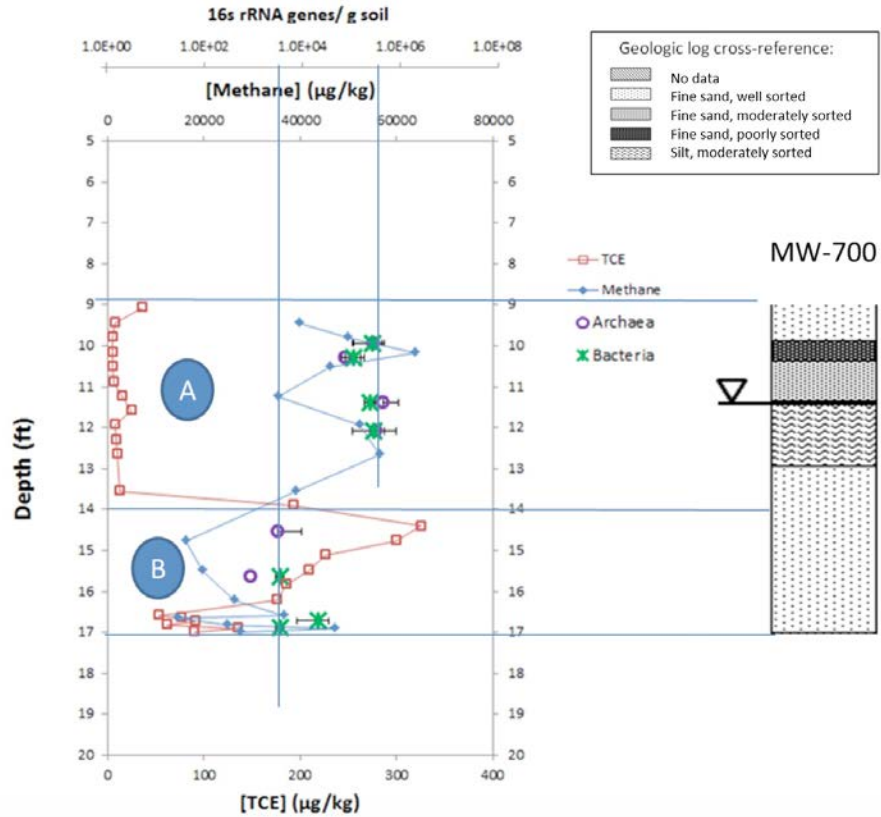


Figure 4-21. 16s rRNA Genes per gram of core for archaea and bacteria as a function of methane and TCE at MW- 700

Figure 4-22 describes the overall microbial community at MW700 based on five samples. The data suggest distinct microbial communities in A) the low k zone and B) the transmissive zone.

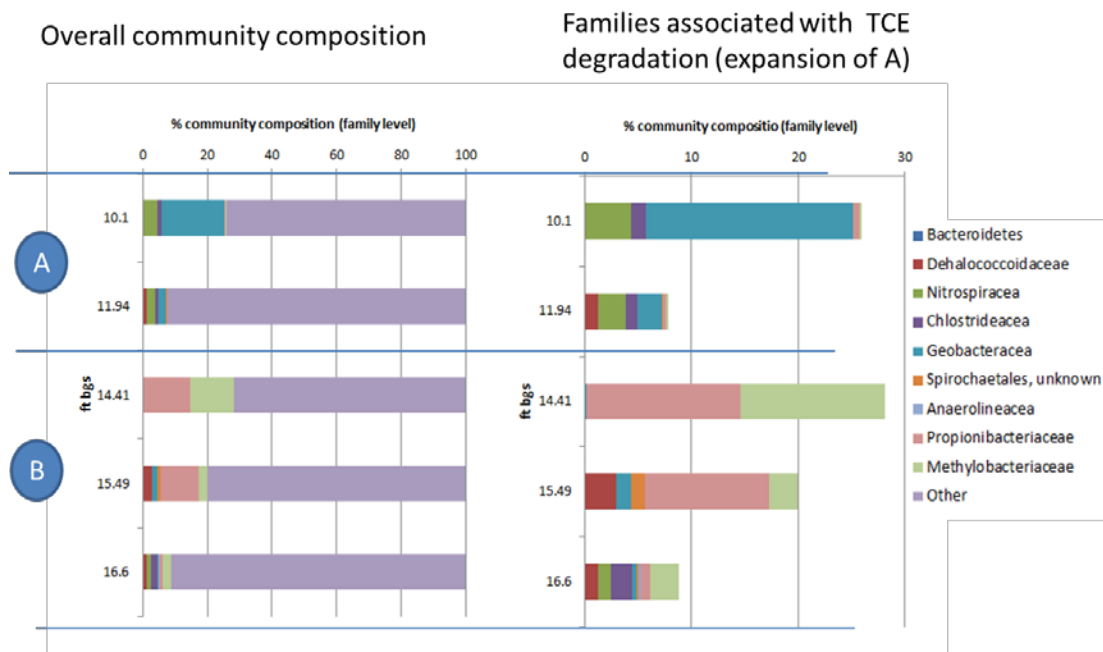


Figure 4-22. Overall community composition

4.4.10 Data Panels

The greatest insight from the data can be generated by creating data panels. A legend for geologic samples is presented in Figure 4-23. Data panels are shown for locations MW38C, MW173F, and MW700C are shown in Figure 4-24, Figure 4-25, and Figure 4-26, respectively. A discussion of the data follows.

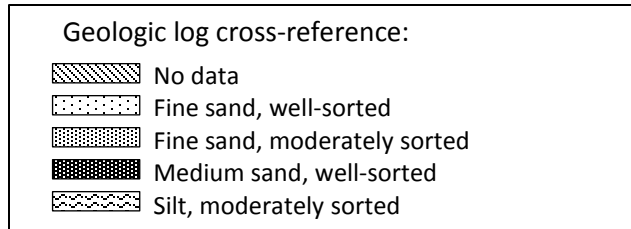


Figure 4-23. Geological sample legend

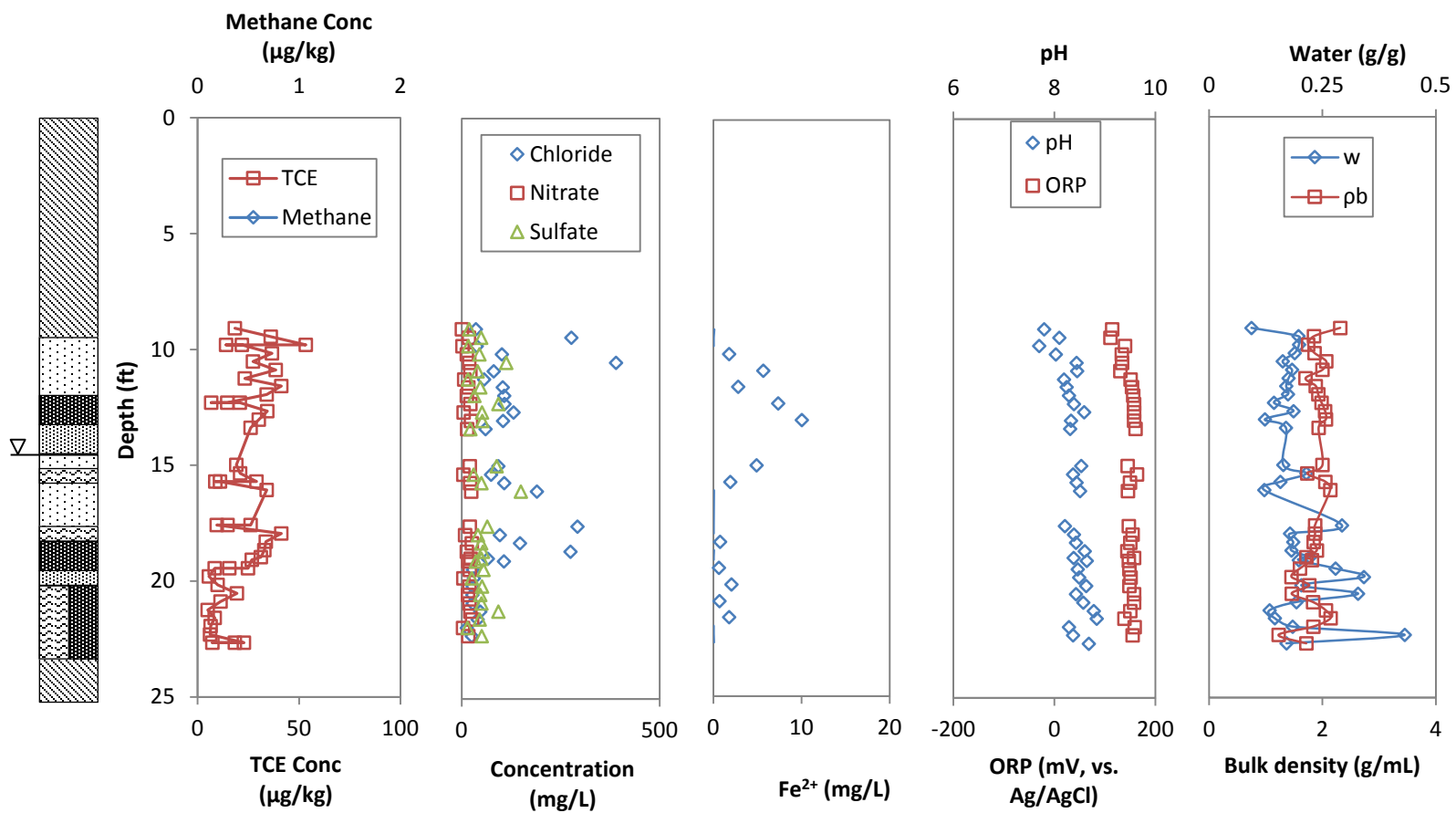


Figure 4-24. Comparison of data in core MW38C. (Side-by-side identifiers in the geologic log indicate interbedded layering on a scale too fine for this figure.)

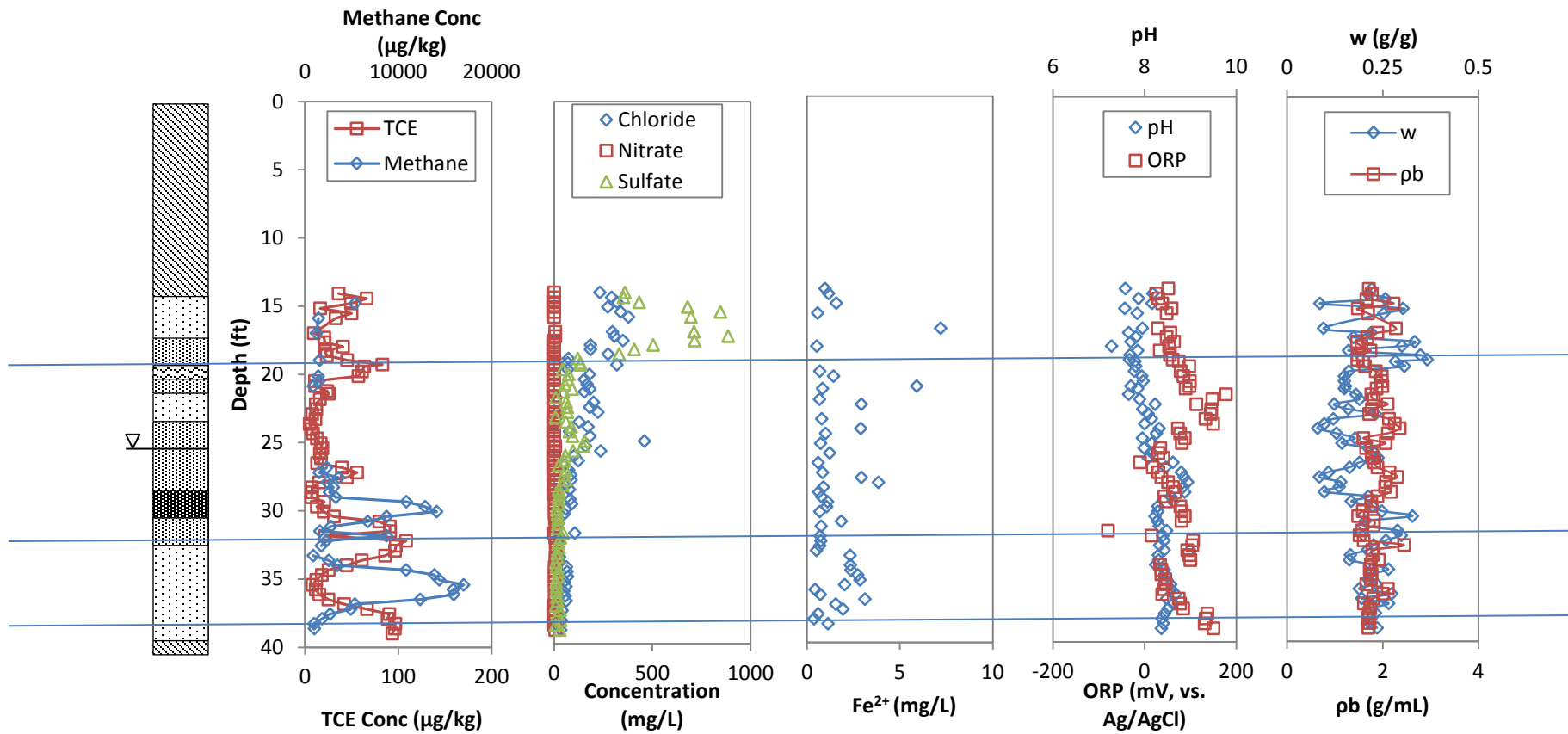


Figure 4-25. Comparison of data in core MW173F

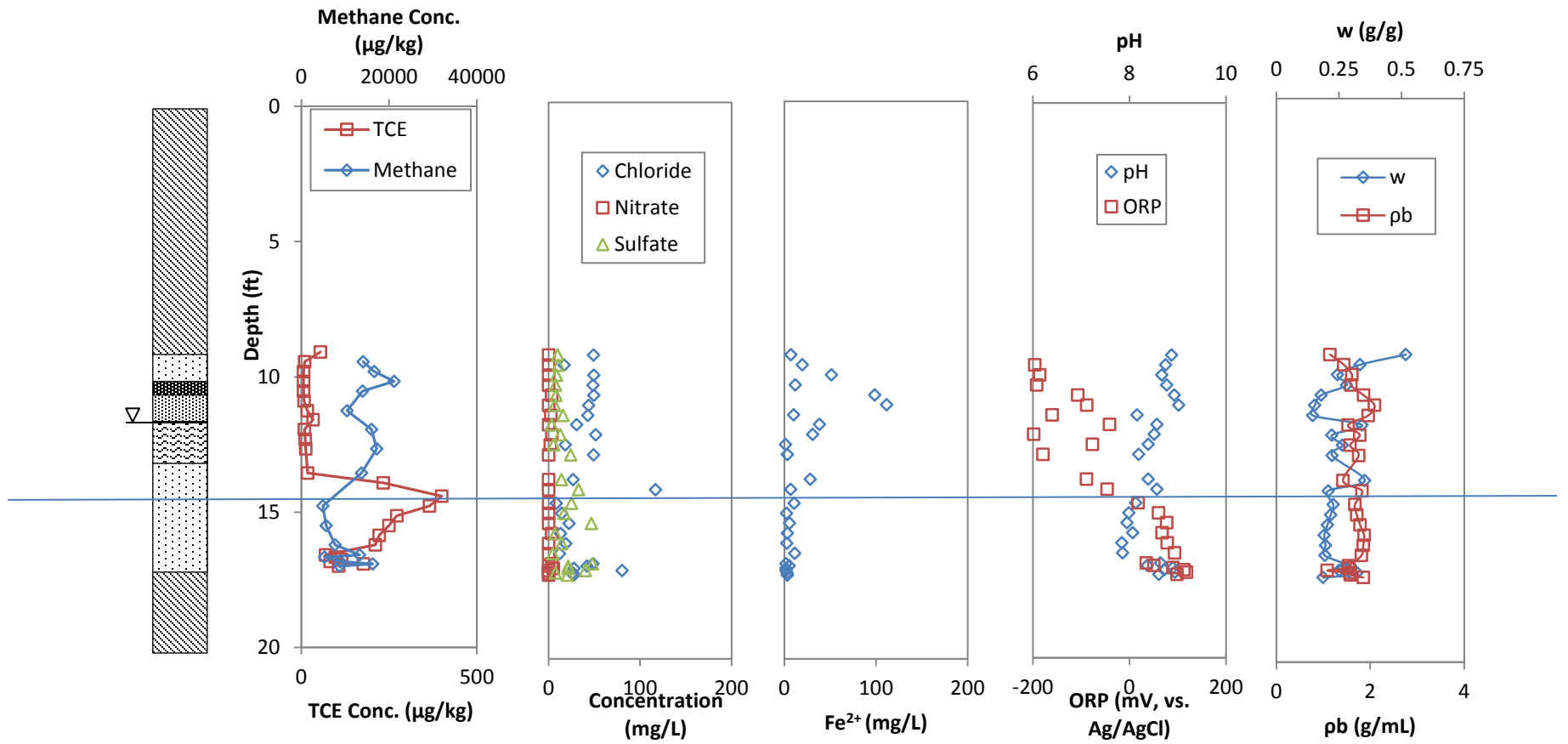


Figure 4-26. Comparison of data in core MW700C

Location: MW38C. Key points:

- The water table is 14.5 feet below ground surface (bgs).
- TCE was detected, but concentrations were lower than 50 µg/kg.
- There are no clear correlations between TCE and sediment type.
- No methane was detected at this location.
ORP values are higher than MW700 and MW173.

Location: MW173F. Key points:

- The water table is 25 feet bgs.
- TCE was detected at concentrations as high as 100 µg/kg.
- Methane was observed in transmissive zones, potentially associated with lactate injection near the well in the late 2000s.
- TCE concentrations are generally lower in transmissive versus low-k zones, perhaps reflecting preferential delivery of lactate to the transmissive zones.
- ORP values were lower than MW38 and follow observed methane values.

Location: MW700C. Key points:

- The water table is 11.5 feet bgs.
- Highest detected TCE concentrations were at this location (~400 µg/kg) is in a transmissive zone.
- Highest detected methane concentrations were also at this location (~22,000 mg/kg) in a low-k zone.
- Below the water table, inverse correlation between methane and TCE suggests active treatment in low-k zones.
- Note: methane is about 100 times higher in concentration than TCE.

4.4.11 Comparison of “2G”, and “3G” Methods at FEW AFB

In 2010, “2G” site characterization tools, including Membrane Interface Probes (MIPs), Hydraulic Profiling Tools (HPTs), Waterloo^{APS}™ and Subsampling Standard Soil Core, and Multiple Level Sampling Systems (MLSs), were employed at FEW at MW38, MW173, and MW700. In 2014, cryogenic core was collected at 5-foot offsets from the locations of the 2010 test holes. The purpose of returning to the same locations in 2014 was a desire to compare the performance of “2G” and “3G” site characterization methods.

Of the four methods employed in 2010, only field Subsampling Standard Soil Core provided meaningful insight. The shortcomings of the other methods at FEW are described at length in the SSR. Figure 4.27 plots total TCE concentrations as a function of depth at MW38, MW173, and MW700, using field Subsampling Standard Soil Core (2G) and cryogenic core collection with laboratory high-throughput analysis (3G). Results show consistently higher TCE concentrations at all three locations using the 3G methods. Many factors could account for higher contaminant concentrations using cryogenic coring techniques. The most obvious is drainage of pore water from the unfrozen 2G samples.

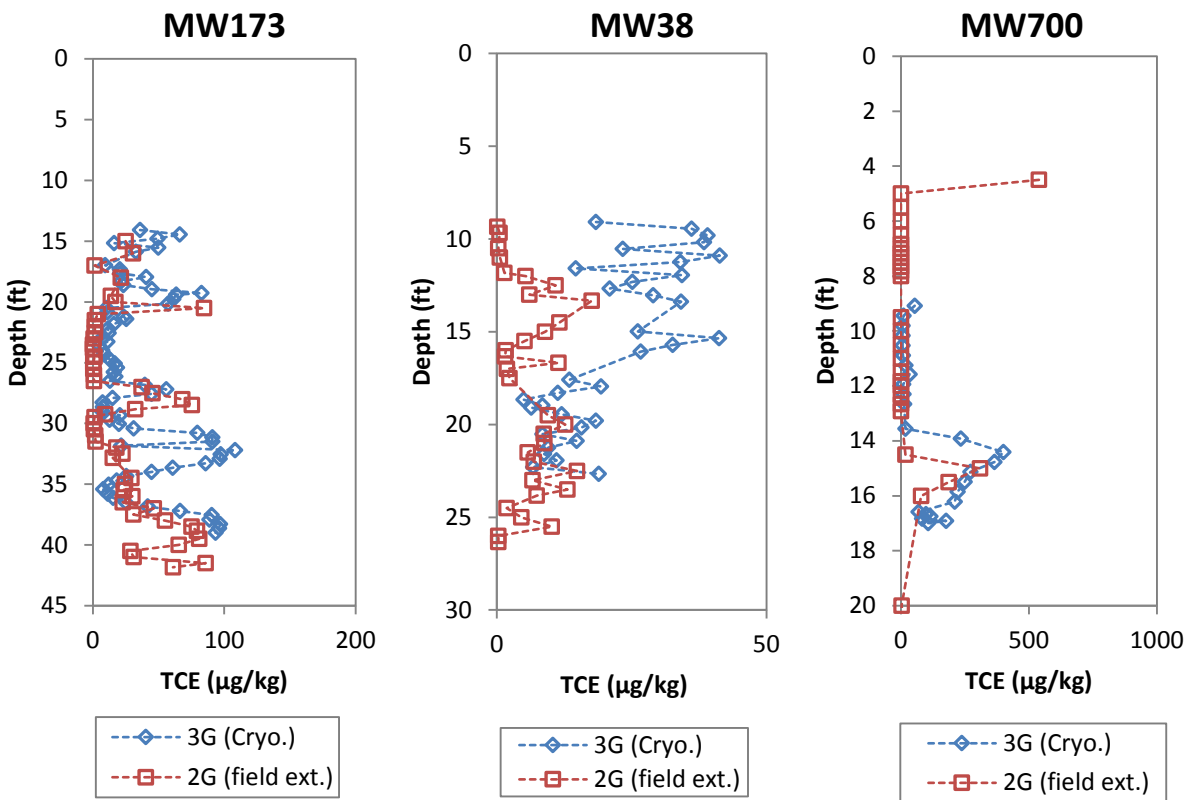


Figure 4-27. TCE concentration data: comparison of 2G and 3G concentrations in borings collected from similar locations at FEW AFB

4.4.12 GRO, DRO and Benzene in Soils at the Former Refinery

Figure 4-28 presents GRO, DRO and benzene in soil from four borings (E1D, B3D, B2D, and D4D). Missing section are due to incomplete recovery in section with cobbles that blocked entry of the samples into the liner.

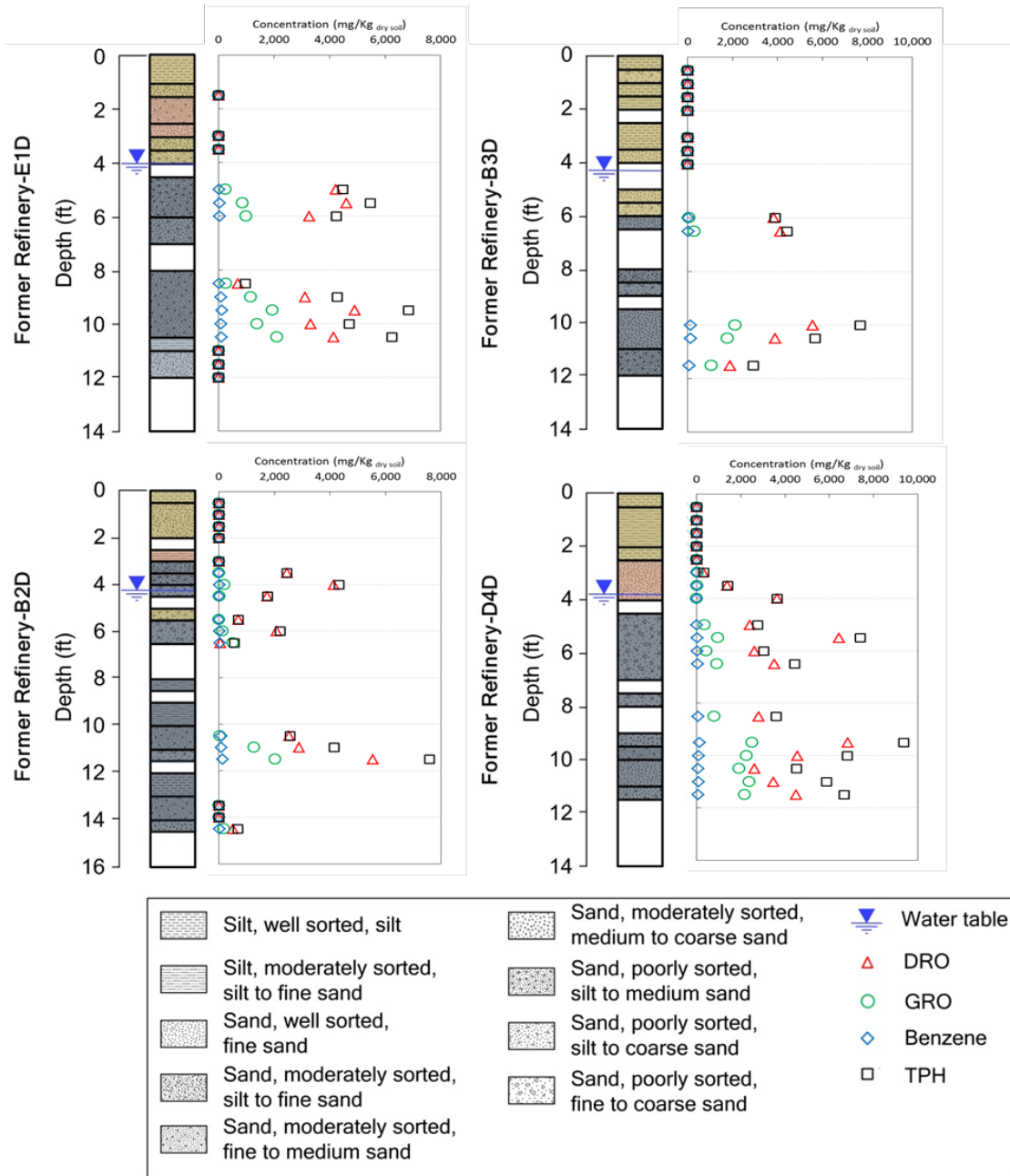


Figure 4-28 – GRO, DRO, and Benzene in Soil at the former refinery.

Chapter 5: High-Throughput Core Analysis 2 – Frozen Core Scanning

An overarching objective of this research is to evaluate methods for high-throughput analysis of the frozen cores. In Chapter 4, advances in sub-sampling and analysis of the frozen cores were described. HTCA represents a good approach to generate comprehensive data in support of managing subsurface releases; however, those methods are labor-intensive and require destruction of the cores. In contrast, geophysical scanning of frozen core represents a potential opportunity to collect data with minimal handling and without destructive sub-sampling. Scanning techniques can potentially be used to provide compositional data on cores (air, water, NAPL and solids concentrations) as well as physical and geochemical data that could be used to direct the sub-sampling process. Techniques that were considered here are focused on detecting the presence of NAPL in samples and included Ultrasound, Resistance Tomography, Computerized Tomography (CT) scanning and Magnetic Resonance Imaging (MRI). Of those techniques, only MRI was successful at detecting NAPL within frozen cores. Work presented in this section was funded by GE.

5.1. Frozen Core Scanning Methods

Test-sample specimens for MRI were prepared using laboratory-grade materials. The methods used for these analyses are presented in this section, and the results are presented in Section 5.2. Since these methods were developed to assess NAPL-impacted media, and no NAPL was presents in the FEW AFB cores, no scanning of the FEW field cores was conducted.

5.1.1 Materials and Sample Preparation

All test-sample cores contained silica sand (20-50 mesh Colorado Silica Sand™) supplied by Premier Silica (Irving, Texas). The measured porosity of the sand was $\phi = 0.30$. For most of the analyses (except as noted below), the sand was saturated with deionized (DI) water. In some cases, the sand/water mixture was spiked with neat TCE (Alfa Aesar, Ward Hill, Massachusetts; 99.5% purity). The sand/water or sand/water/TCE mixtures were homogenized by hand-mixing for about 10 minutes in PTFE bags (12 inch \times 13 inch, thickness = 0.0025 inch) supplied by Welch Fluorocarbon (Dover, New Hampshire). After homogenization, the test-sample specimens were remolded in transparent PVC liners (2-inch OD). Sample lengths varied for the different analyses, as described below). The liners were then sealed with plastic end caps and stored in a freezer at $-20\text{ }^{\circ}\text{C}$ until the time of analysis.

5.1.2 Magnetic Resonance Imaging

MRI has been used as a non-invasive scanning method to characterize physical properties of porous media since 1956 (Brown and Fatt 1956). MRI functions by detecting relaxation of excited protons in a strong magnetic field after radio frequency (RF) pulsing; the resulting data can be used to determine the proton densities spatially throughout the sample. Herein, consideration is given to using the MRI technique to resolve spatial NAPL saturation in frozen cores.

The signals produced by MRI result from the excitation and relaxation of protons (^1H) in liquid phases (aqueous or non-aqueous). Due to the high proton density in water, and high fraction of

volume occupied by water in water-saturated porous media, the MRI signal resulting from water tends to overwhelm signals resulting from NAPLs, especially when NAPL saturation is much less than that of water. Thus, MRI is of limited value to determine NAPL saturations and/or distribution in samples with pores filled primarily with liquid water. To overcome this potential limitation of MRI scanning of cores, our research hypotheses were as follows:

- The water-induced MRI signal could be suppressed by freezing water in the sample – but not the NAPL, and
- NAPL saturations could therefore be measured using MRI techniques for analysis of cryogenically-collected cores.

These hypotheses were tested at Colorado State University.

Preliminary Experiments. Laboratory experiments were conducted to measure NAPL saturation and spatial distribution in frozen-cores using MRI. Test-sample specimens were prepared in 2-inch OD PVC liners as described previously, with 4-inch sample lengths. A summary of prepared samples is shown (Table 5-1).

Table 5-1. Cores prepared for laboratory MRI experiment

Sample	Sample contents	Analysis Temperature (°C)
a	Sand/Water	22
b	Sand/Water	-20
c	Sand/TCE	-20
d	Sand/Water/TCE	-20

MRI Scanning Procedure. The cores were scanned by a magnetic resonance scanner at the Rocky Mountain Magnetic Resonance Center (RMMRC) at Colorado State University (Fort Collins, CO). The scanner was a Bruker (Billerica, MA) Biospin MRI with a magnetic field strength of 2.35 Tesla, equipped with a 6-inch diameter probe that is designed for scanning of small animals. The cores were scanned at ambient temperature (about 22°C) and at -20°C as shown in Table 5-1. To keep the test-sample cores frozen during the scanning, a hollow Styrofoam cylinder (6-inch OD, 2-inch ID, and 6-inch long) was used as insulation (Figure 5-1). The insulation proved to be adequate to keep samples frozen for about 30 minutes to complete an MRI scan.



Figure 5-1. Styrofoam insulation for keeping the core frozen during MRI

Data Processing. For spatial quantification of NAPL distribution in cores, the one-dimensional imaging method of Watson (2013) was applied. This method is based on acquiring simultaneous MRI signals from a reference sample, consisting of pure-phase contaminant, and a core. For implementation of this method, the reference sample and core are both located in the MRI probe (Figure 5-2). Calculating a ratio between integrated intrinsic signal intensities from reference, core, and the mass of reference could quantify the NAPL saturation within the core as follows:

$$m_s = \frac{m_r \int_s I(z) dz}{\int_r I(z) dz} \quad 5-1$$

where r and s are subscripts for reference sample and core, respectively, $I(z)$ is the intrinsic signal intensity predicted from detected free induction decays (FID) of protons while relaxing after radio frequency (RF) pulse is imposed, and m is the mass. Intrinsic intensities of detected signals are a key parameter in quantification. Since the detection coil is not able to collect the signals immediately (at time zero plus) after a RF pulse, a non-parametric regression method (shown in Figure 5-3), is employed to predict the intrinsic signal intensities (Uh 2005; Uh and Watson 2014). Because free induction decay of protons after pulse is not a single exponential decay and the number of exponential terms is unknown, a non-parametric regression method was employed. This method uses a continuous function to represent the FID (Uh 2005; Uh and Watson 2014). A code in MATLAB (Version R2012b) was developed to automate one-dimensional quantification of NAPL saturation in the core. MRI results, which include two-dimensional sample images and quantification, are shown in Section 5.2.3.

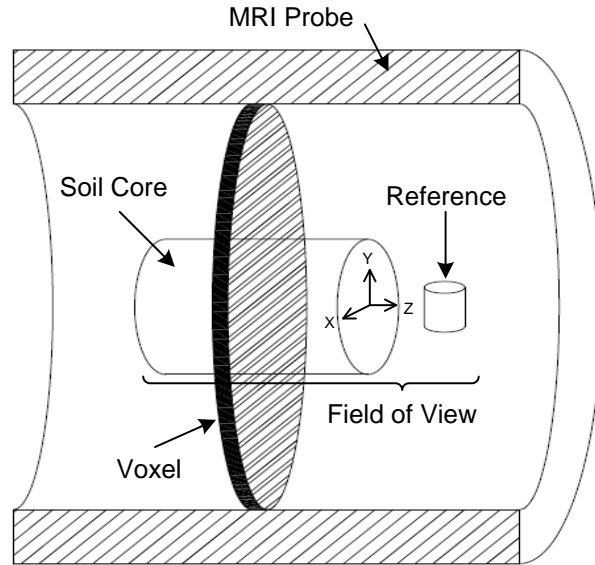


Figure 5-2. Schematic of reference and core setting in mri probe for the one-dimensional quantification

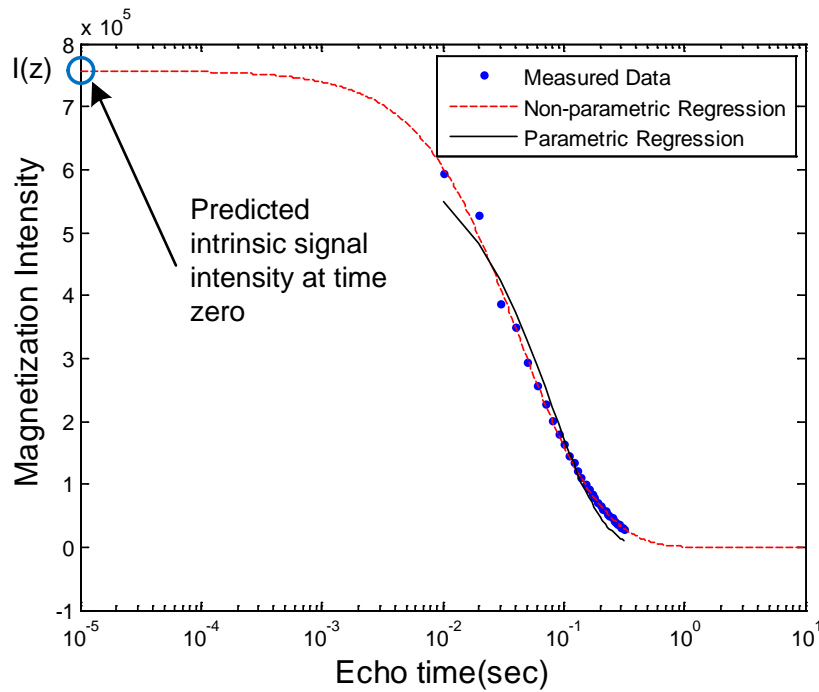


Figure 5-3. Predicted intrinsic signal intensity of measured fid using a regression method

5.2 Frozen Core Scanning Results

Scanning methods were employed to investigate the possibility of obtaining data from frozen cores without destructive and/or time-consuming handling and preparation. MRI results are presented in this section.

5.2.3 Magnetic Resonance Imaging

MRI scanning was conducted on four test-cores. Procedures were described previously (Section 5.1.3). MRI images of the test-cores are shown in Figure 5-4. Quantification analysis is presented subsequently.

Figure 5-4 indicates that in unfrozen cores (at 20°C) saturated with water, a strong MRI signal was detected from water-associated ^1H (Figure 5-4a). Therefore, a method was needed to improve sensitivity of the MRI method to detection of NAPL. To accomplish this sensitivity, the samples were frozen at -20°C to suppress the water signal, while TCE remained in liquid state (the freezing point of TCE is -73°C). In the frozen core saturated with water, the only detected signals were noise (Figure 5-4b). In the absence of water, when only TCE was present in the core, a strong signal was detected even at -20°C (Figure 5-4c). When both water and TCE were present, a much stronger signal was obtained from the phase-separated TCE (Figure 5-4d) than from the frozen water at -20°C (left of the core in Figure 5-4d), illustrating the great potential of this technique for sensitive NAPL detection in frozen cores.

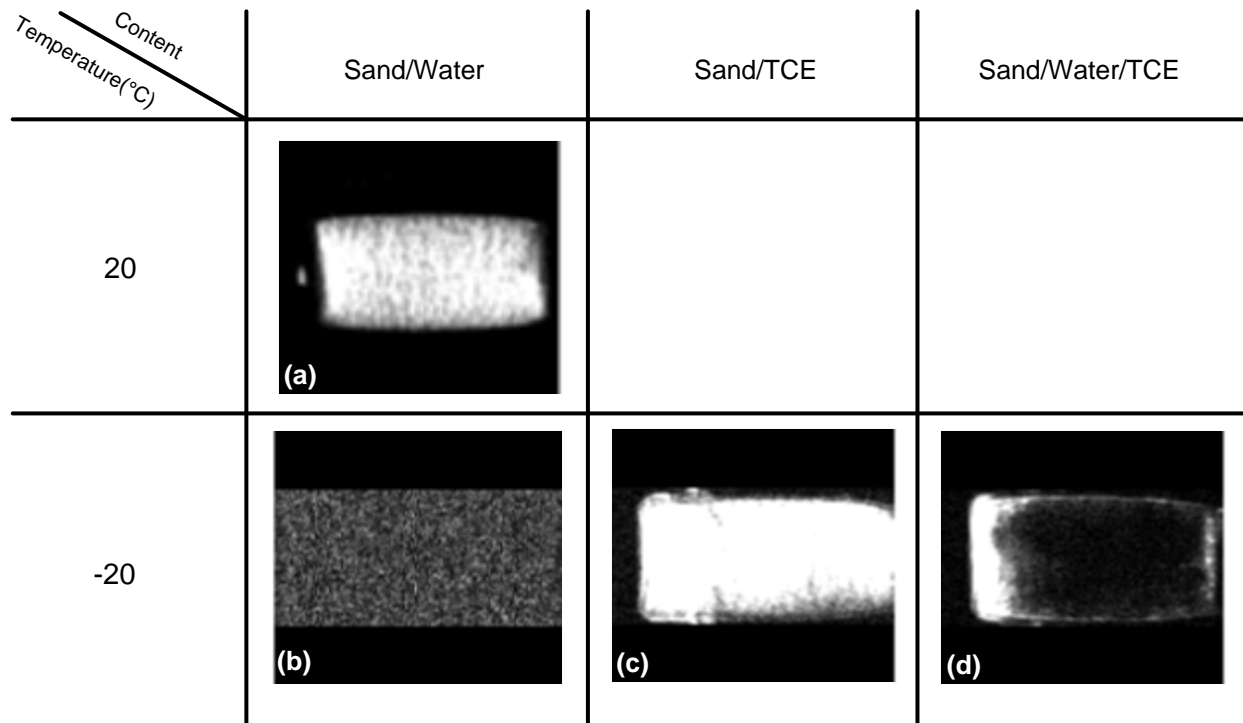


Figure 5-4. MRI images of the scanned cores. (a) sand and water at 20°C, (b) sand and water at -20°C, (c) sand and TCE (100% pore saturation) at -20°C, and (d) sand, water, and TCE (variable pore saturation) at -20°C

The results of one-dimensional quantification of a laboratory core are shown in Figure 5-5. Figure 5-10a shows the raw MRI signal in one dimension. The data were collected by making a series of scans across the column while moving down the length of the column, and scanning a TCE-only reference. This image indicates a stronger TCE signal on the right-hand side of the sample because the core was positioned horizontally in the freezer after fabrication, and some gravity drainage occurred. In Figure 5-10b, the MRI signal has been converted into a NAPL

volume following Equation 5-1. The total detected NAPL volume, following this method, is 26.9 mL. This calculated NAPL volume compared favorably to the actual volume of NAPL in the sample, 29.4 mL (i.e., ~90% of the true volume).

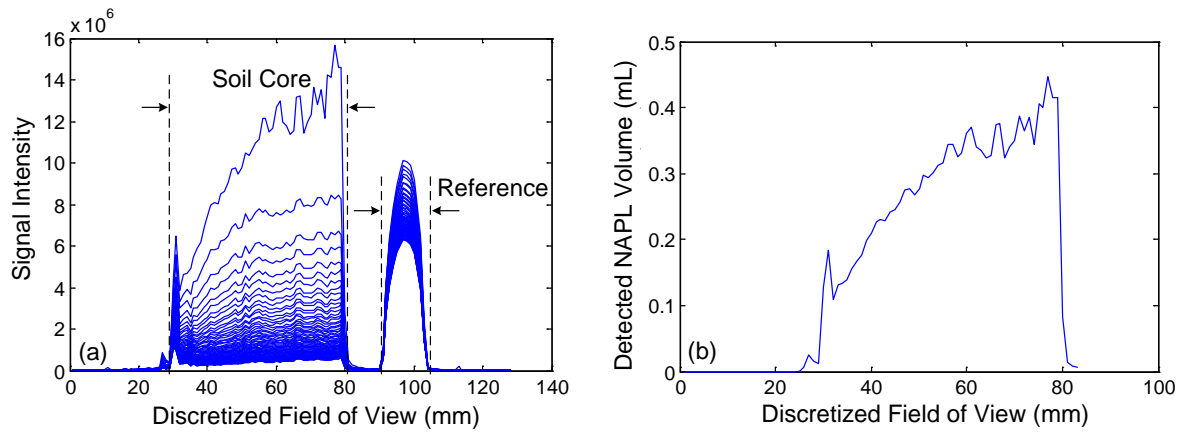


Figure 5-5. One-dimensional quantification results of a TCE-contaminated core. a) detected signals from the field of view b) quantification curve within the core.

Chapter 6: Conclusions and Implications

The overarching objectives of this research were to:

- Demonstrate and document the efficacy of cryogenic core collection and high-throughput core analysis for site characterization.
- Develop standard operating procedure for cryogenic core collection and high-throughput core analysis that will allow its broader application for site characterization.

In addition, biogeochemical data collected from the FE Warren AFB site has been used here to demonstrate how information made available by cryogenic collection of core samples can be utilized to improve our characterization of contaminated groundwater sites.

6.1 Key Findings

The key findings of this project are summarized below:

6.1.1 An efficient method for cryogenic core collection was developed

Through a sequential process of design improvements, freezing times below the water table were reduced from ~50 minutes to about 5 minutes. This had several additional benefits, including significant reduction in the likelihood of freezing augers and core barrel to the formation.

6.1.2 Frozen core recovery was excellent

Even in difficult material (e.g., flowing sands), good recovery was obtained (i.e., >85% of material retained in the core liner). This was largely due to the in situ freezing process, which kept materials from falling from the core during retrieval to ground surface. As with all hollow-stem (and other) auger techniques, hard layers (e.g., caliche) and cobbles can prevent materials from entering the core liner. In these cases, cryogenic core collection does not represent a significant advantage.

6.1.3 Field processing of core samples is simplified

Because the cores are frozen in situ, the only sample processes required prior to shipment are trimming the core liner, capping and labeling. This can represent a significant advantage over other in-the-field-processing techniques which are necessary if measurement of sensitive parameters (e.g., VOCs, ORP, dissolved gases) from field cores is desired.

6.1.4 Intact frozen cores are well-suited for geophysical scanning

We demonstrated a new MRI method for detection of NAPLs in frozen cores that is non-invasive and benefits from the cores being frozen to suppress the water background signal. Other geophysical methods, including CT scanning, could also prove useful for guiding the core sub-sectioning process.

6.1.5 Cores frozen *in situ* provide access to additional analyses

Many analyses of interest are time-sensitive and/or oxygen sensitive (e.g., mRNA, ORP, dissolved gases and bubbles). Freezing cores also allows sub-sampling with techniques that are not available for unfrozen core (e.g., chopping into 1-inch “hockey pucks” and sectioning those disks into quarters with a sterile chisel).

6.1.6 High-throughput core analysis represents a practical approach to obtain a high density of information from cores

The ability to conduct sample processing in the laboratory, rather than the field provides multiple benefits. First, it allows parameters that could not be measured using unfrozen cores to be determined (e.g., dissolved gases and bubbles). Second, it allows core to be efficiently processed in an “assembly line” manner with additional technical staff, access to fume hoods, glove boxes and other laboratory equipment. This process also facilitates performing multiple types of analysis on individual sub-samples.

6.1.7 Data fusion adds value above and beyond the individual analyses

While an increase in the numbers of individual analyses can be important for answering specific questions (e.g., high-resolution vertical contaminant distribution), the combination of an expanded range of types of analyses can allow conclusions to be drawn which would otherwise not be possible. In the context of this work, for example, the inverse relationship between TCE and methane concentrations at FEW AFB almost certainly represents new insight into *in situ* remediation processes.

6.1.8 Confidence in accuracy of the depth interval sampled was significantly improved due to improved recovery

The combination of material sluffing from core liners, poor initial collection into the liner, flowing sands and other factors all contribute to uncertainties regarding the exact depth from which core materials originated (as well as loss of information because no core was recovered). C₃ can potentially address this issue by reducing sluffing and flowing sands. In our experience, this can significantly reduce depth uncertainty.

6.2 Implications for Site Characterization

As discussed in the previous section, the combination of C₃ and HTCP can significantly increase the amount and quality of information available to site investigators. This is briefly re-capped below.

6.2.1 *In situ* frozen core samples can yield more information

Additional site characterization information using C₃ and HTCP comes both from an increase in the range of analysis types. This includes molecular tools analysis, dissolved gases and

gas bubbles, and improved ORP measurements. The combined approach also allows for better sub-sampling of cores, which can yield better depth resolution.

An important aspect of the combined approach that has not been discussed above is that processing of frozen core allows sequential analysis of the core. The HTCA approach described above leaves ~75% of the core unused, but still in pristine condition. If, after initial analyses, additional information between analyzed sections is needed, the remaining core can be processed to obtain that information. This can be of great importance as site conceptual models evolve.

6.2.2 Improved retention of important sample intervals

Flowing sands and geologic interfaces represent critical subsurface intervals that can be difficult to characterize using conventional drilling techniques. We believe that the C₃ method has significant potential to minimize flowing sands and capture interfaces. While our results in this regard are promising, more work is needed.

6.2.3 Improved certainty of depth measurements

Decreased sample loss and decreased flowing sands both contribute to improved certainty of the depth intervals represented by core samples. As an example of this, even in the case where recovery is incomplete, because freezing basically eliminates sluffing from the core liner, the lack of recovery can be clearly identified as failure of the material to initially enter the core, rather than due to losses during retrieval to ground surface. More importantly, consistent complete recovery can provide “inch-scale” confidence in depth measurements.

6.3 Future Work

6.3.1 Improved design of dual-wall cooling cylinder is needed

Both the cooling coil design and the dual-wall cooling cylinder could benefit from improved designs, although it is particularly the case for the dual-wall cylinder. The challenge for the latter is coming up with a design that allows sufficient LN flow, given the geometric constraints of the core barrel. The dual-wall cylinder does have an intrinsic advantage over the coils in that it should facilitate additional delivery of “cooling” to the drive shoe, which we believe will lead to better control of flowing sands.

6.3.2 Control of flowing sands needs additional demonstration and development

As suggested above, while we have some field evidence supporting decreased impact of flowing sands due to freezing, additional demonstration of this important effect is needed. Fortunately, several new SERDP/ESTCP projects will include C₃ and HTCA as part of their scope, and our expectation is that improved insight will come as the result of that work.

6.3.3 Additional high-level thinking about best strategies for utilizing the newly available information is needed

The collection and processing of frozen cores represents a new paradigm for site characterization (hence our use of the term “3G”). New types of data and the fusion of those data will result in new conceptual models for sites. Interpretation of those data, as well as identification of yet more capabilities made available *by in situ* frozen core need to result from high-level thinking about subsurface processes (e.g., the production of peer-reviewed scientific papers).

6.3.4 Application of C₃ at a broader range of sites would improve protocols

The protocols presented here have been tested at multiple field sites. However, all of those sites are located in one geographic area of Colorado and Wyoming. Application of the techniques to other settings will undoubtedly result in changes to those protocols. As the developers of this technology, we hope to play a role in documenting improvements to the protocols. In addition, we anticipate working with SERDP/ESTCP to make those updated protocols widely available (e.g., through the SERDP/ESTCP web site and via social media).

Literature Cited

- Brown, R.J., Fatt, I., (1956). Measurement of fractional wettability of oil field rocks by the nuclear magnetic relaxation method. *Trans. AIME* 207, 262–264.
- Duliu, O.G., (1999). Computer axial tomography in geosciences: an overview, *Earth Sci. Rev.*48, 265–281.
- Durnford, D., Brookman, J., Billica, J., and Milligan, J., (1991). LNAPL distribution in a cohesionless soil: a field investigation and cryogenic sampler. *Ground Water Monitoring and Remediation*, 11(3), 115-122.
- Goldstein, L., Prasher, S.O., and Ghoshal, S. (2007). Three-dimensional visualization and quantification of non-aqueous phase liquid volumes in natural porous media using a medical X-ray computed tomography scanner. *Journal of Contaminant Hydrology*, 93(1), 96-110.
- Irianni Renno, M., Akhbari, D., Olson, M.R., Byrne, A.P., Lefevre, E., Zimbron, J., Lyverse, M., Sale T., and Long, S.K. (2015). Comparison of bacterial and archaeal communities in depth-resolved zones in an LNAPL body. In preparation for submission to *Applied Microbiology and Biotechnology*.
- Johnson, R.L., Simon, H.S., Brow, C.N., and Johnson, R.O.B. (2012). Cryogenic collection of complete subsurface samples for molecular biological analysis. Strategic Environmental Research and Development Program, US DOD, ER-1559.
- Johnson, R.L., Brow, C.N., Johnson, R.O.B., and Simon, H.M. (2013). Cryogenic core collection and preservation of subsurface samples for biomolecular analysis. *Groundwater Monitoring & Remediation*, 33(2), 38-43.
- Li, L., Marica, F., Chen, Q., MacMillan, B., and Balcom, B.J. (2007). Quantitative discrimination of water and hydrocarbons in porous media by magnetization prepared centric-scan SPRITE. *Journal of Magnetic Resonance*, 186(2), 282-292.
- Murphy, F. and Herkelrath, W.N., (1996). A sample-freezing drive shoe for a wire line piston core sampler. *Ground Water Monitoring and Remediation*, 16(3), 86-90.
- Pankow, J.F., and Cherry, J.A., (1996). Dense chlorinated solvents and other DNAPL's in groundwater: history, behavior, and remediation: Portland, OR, Waterloo Press, 522 p.
- Uh, J. (2005). Nuclear magnetic resonance imaging and analysis for determination of porous media properties. PhD dissertation, Texas A&M University.
- Uh, J. and A.T. Watson, (2014) A nonparametric approach for determining NMR relaxation distributions, *Transport in Porous Media*, 105, pp. 141--170.
- Watson, A.T. (2013). Development of one-dimensional imaging. Department of Chemical and Biological Engineering, Colorado State University, Fort Collins, USA.
- Whitby, C. and Lund, S.T. (2009) *Applied microbiology and molecular biology in oil field systems*. Springer, Netherlands.

Yoshimi, Y., Tokimatsu, K., Kaneko, O., and Makihara, Y., (1984). Undrained cyclic shear strength of a dense Niigata sand, soils and foundations, 24(4), 131–145.

Zapico M.M., S. Vales, and J.A. Cherry, (1987). A wireline piston core barrel for sampling cohesionless sand and gravel below the water table. Ground Water Monitoring Review 7, no. 3:74-82.

Appendix A: Performance of Cryogenic Coring Systems – Developmental and Field Studies

Fort Collins Developmental Studies

. Summary of the first DEI demonstration (Fort Collins, CO)

NO.	Depth Interval (ft)	Size of Copper Tube (inch)	Length of Copper Tube (ft)	Length of Coil (ft)	Insulation	Pressure of dewar (psi)	Time to Freeze (minute)	Weight of Consumed LN (lb)	Comment
1	5.0	1/4	50.0	1.5	N/A	110	29	15	The bottom of the core was frozen
2	5.0	1/4	50.0	5.0	3/16" insulation foam covered with butyl acetate	110	32	28	The bottom of the core was frozen
3	5.0	1/4	150.0	5.0	3/16" insulation foam covered with butyl acetate	110	100	22	The top of the core reached not less than 8 °C
4	5.0	3/8	50.0	5.0	Open system	110	16	N/A	The system was not water tight
5	20.0	1/4	150.0	5.0	3/16" insulation foam covered with butyl acetate	230	53	150	The top of the core reached not less than 0.8 °C

Summary of the second DEI demonstration (Fort Collins, CO)

NO.	Depth Interval (ft)	Size of Copper Tube (inch)	Length of Copper Tube (ft)	Length of Coil (ft)	Insulation	Pressure of dewar (psi)	Back pressure (psi)	Time to freeze (minute)	Weight of consumed LN (lb)	Comment
1	5.0	1/4	50.0	1.5	1/4" insulation foam	230	N/A	9	24	The bottom of the core was frozen
2	20.0	1/4	50.0	1.5	1/4" insulation foam	230	N/A	15	23	The bottom of the core was frozen
3	20.0	1/4	50.0	5	1/4" insulation foam	230	N/A	23	28	The top to middle of the core was frozen
4	20.0	1/4	50.0	1.5	Acetate liner, 3/16" white foam, acetate liner, grease	230	N/A	15	27	The bottom of the core was frozen

Summary of the third DEI demonstration (Fort Collins, CO)

NO.	Depth interval (ft)	Size of copper tube (in.)	Length of copper tube (ft)	Length of coil (ft)	Insulation	Pressure of dewar (psi)	Back pressure (psi)	Time to freeze (minute)	Weight of consumed LN (lb)	Comment
1	10.0	1/4	50.0	2.5	1/8" abrasion resistance silicon foam	230	N/A	12	23	Inner stainless steel liner was used. Core stuck in the liner. To create back pressure, 1/8" orifice was used at the vent. The core barrel stuck in the auger
2	15.0	3/8	50.0	2.5	1/8" abrasion resistance silicon foam	230	N/A	9	33	Inner stainless steel liner was used. Core stuck in the liner. To create back pressure, 1/8" orifice was used at the vent. The core barrel stuck in the auger
3	15.0	1/4	50.0	1.5	3/16" closed cell foam	230	N/A	9	21	Inner stainless steel liner was used. Steam wash used

Summary of the pilot experiments at ARDEC (Fort Collins, CO)

NO.	Depth interval (ft)	Size of copper tube (in.)	Length of copper tube (ft)	Length of coil (ft)	Insulation	Pressure of dewar (psi)	Back pressure (psi)	Time to freeze (minute)	Weight of consumed LN (lb)	Comment
1	14.0-19.0	1/4	50.0	1.5	3/16" closed cell foam	160	1/8" orifice	10	46	The core was frozen
2	19.0-24.0	1/4	50.0	1.5	3/16" closed cell foam	180	1/8" orifice	12	50	The core was frozen
3	24.0-26.5	1/4	50.0	1.5	3/16" closed cell foam	170	1/8" orifice	15	38	The core barrel stuck in the auger, Core stuck in the barrel
4	26.5-29.0	1/4	50.0	2.5	3/16" closed cell foam	185	1/8" orifice	12	17	Core stuck in the barrel. Steam wash used
5	29.0-31.5	1/4	50.0	2.5	3/16" closed cell foam	180	1/8" orifice	15	18	Core stuck in the barrel. Steam wash used
6	31.5-34.0	1/4	50.0	2.5	3/16" closed cell foam	175	1/16" orifice	15	13	Core stuck in the barrel. Steam wash used
7	34.0-39.0	1/4	50.0	2.5	3/16" closed cell foam	180	Manual valve and gauge, 40 psi	15	17	Core stuck in the barrel. Steam wash used

Summary of the fourth DEI demonstration (Fort Collins, CO)

NO.	Depth interval (ft)	Size of copper tube (in.)	Length of copper tube (ft)	Length of coil (ft)	Insulation	Pressure of dewar (psi)	Back pressure (psi)	Time to freeze (minute)	Weight of consumed LN (lb)	Comment
1	20.0	Dual-wall cooling cylinder			1/4" Closed cell foam	220	0	43	42	The heat distribution was not uniform through the system
2	5.0	Dual-wall cooling cylinder			1/4" Closed cell foam	190	70	12	14	The test was successful above the water table
3	20.0	3/8	50.0	2.5	1/8" electric insulation plus 1/8" closed cell foam	190	70	7	23	Core stuck in the barrel/steam wash used

FEW AFB Field Studies

Summary of cryogenic coring at MW38C, FEW AFB.

The water table at this location was 14.0 feet. The cryogenic system consisted of 50.0 feet of $3/8$ -inch copper tube coiled over 2.5 feet.

NO.	Depth interval (ft)	Copper coil specifications (diameter and coil length)	Pressure of dewar (psi) (psi)	Back pressure (psi)	Recovery (%)	Time of LN injection (minute)	Comment
1	9.00-11.50	3/8" tube 2-1/2 feet	220	60	100	5	The core was frozen
2	11.50-14.00	3/8" tube 2-1/2 feet	150-180	90	100	5	The core was frozen
3	14.00-16.50	3/8" tube 2-1/2 feet	150	100	50	6	The core was frozen
4	17.50-19.00	3/8" tube 2-1/2 feet	150	125	100	6	The core was frozen
5	19.00-21.50	3/8" tube 2-1/2 feet	140	100	100	6	The core was frozen
6	21.50-22.75	3/8" tube 2-1/2 feet	140	80	100	6.5	The core was frozen

Summary of cryogenic coring at MW700, FEW AFB.
The water table at this location was 11.5 feet.

NO.	Depth interval (ft)	Copper coil specifications (diameter and coil length)	Pressure of dewar (psi)	Back pressure (psi)	Recovery (%)	Time of LN Injection (minute)	Comment
1	9.00-11.50	3/8" tube 2-1/2 feet	180-220	0	100	12	The core was frozen
2	11.50-14.00	3/8" tube 2-1/2 feet	160-170	85-100	100	5	The core was frozen
3	14.00-16.50	3/8" tube 2-1/2 feet	150	115	84	5	The core was frozen
4	16.50-17.50	3/8" tube 2-1/2 feet	140	90	100	5	The core was frozen

Summary of cryogenic coring at MW173C, FEW AFB.

The water table at this location was 25.0 feet. The cryogenic system consisted of 50.0 feet of 3/8-inch copper tube coiled over 2.5 feet.

NO.	Depth interval (ft)	Copper coil specifications (diameter and coil length)	Pressure of dewar (psi)	Back pressure (psi)	Recovery (%)	Time of LN Injection (minute)	Comment
1	14.00-16.50	3/8" tube 2-1/2 feet	180	50	100	5	The core was frozen
2	16.90-19.25	3/8" tube 2-1/2 feet	160	110	100	5	The core was frozen
3	19.25-21.75	3/8" tube 2-1/2 feet	155	70	96	4.5	The core was frozen
4	21.75-24.25	3/8" tube 2-1/2 feet	140	50-75	100	5	The core was frozen
5	24.25-26.75	3/8" tube 2-1/2 feet	200	60-100	100	4.5	The core was frozen
6	26.75-29.25	3/8" tube 2-1/2 feet	150	100	100	4.5	The core was frozen
7	29.25-31.75	3/8" tube 2-1/2 feet	200	100	100	5	The core was frozen
8	31.75-33.25	3/8" tube 2-1/2 feet	190	100	100	5.5	The core was frozen
9	33.25-35.75	3/8" tube 2-1/2 feet	180	110	100	5.5	The core was frozen
10	35.75-38.25	3/8" tube 2-1/2 feet	160	100	100	6	The core was frozen

Former Refinery Field Studies

Summary of cryogenic coring at location A3A, former refinery.

The water table at this location is 7.0 feet. The cryogenic system consisted of 50.0 feet of $\frac{3}{8}$ -inch copper tube coiled over 2.5 feet.

NO.	Depth Interval (ft)	Copper Coil Specifications (diameter and coil length)	Pressure of dewar (psi)	Back Pressure (psi)	Recovery (%)	Time of LN Injection (minute)	Comment
1	0.00-4.00	$\frac{3}{8}$ " tube 2-1/2 feet	145-260	60-100	95	4	The core was frozen
2	4.00-9.00	$\frac{3}{8}$ " tube 2-1/2 feet	150	100	100	4	The core was frozen
3	9.00-11.50	$\frac{3}{8}$ " tube 2-1/2 feet	135	100	100	5.5	The core was frozen
4	14.00-16.50	$\frac{3}{8}$ " tube 2-1/2 feet	135	70	71	7	The core was frozen

Summary of cryogenic coring at location C2C, former refinery.

The water table at this location was 7.0 feet. The coil cooling system cryogenic system consisted of 50.0 feet of 3/8-inch copper tube coiled over 2.5 feet.

NO.	Depth interval (ft)	Copper coil specifications (diameter and coil length)	Pressure of dewar (psi)	Back pressure (psi)	Recovery (%)	Time of LN Injection (minute)	Comment
1	0.00-2.50	Dual Wall Cooling Barrel 2-1/2 feet	140	90	86	10	The core was frozen
2	2.50-4.00	Dual Wall Cooling Barrel 2-1/2 feet	130	60	50 Gravel	8.5	The core was frozen
3	4.00-6.50	Dual Wall Cooling Barrel 2-1/2 feet	120	50	70 Gravel	20 Low Pressure on dewar	The core was frozen
4	6.50-9.00	Dual Wall Cooling Barrel 2-1/2 feet	120	0	20 Rock in Core Barrel	20 Low Pressure on dewar	The core was frozen
5	9.00-11.50	3/8" tube 2-1/2 feet	110	75	60	10	The core was frozen
6	11.50-14.00	3/8" tube 2-1/2 feet	200	100	83	6.5	The core was frozen
7	14.00-16.50	3/8" tube 2-1/2 feet	200	100	78	4.5	The core was frozen

Appendix B: Protocol for Cryogenic Core Collection

Introduction

The protocol outlined below describes the steps involved in collecting cryogenic cores using a CME hollow-stem auger. The tooling needed to accomplish core collection is described in the report on cryogenic core collection as part of SERDP ER-1740.

The protocol steps outlined below are designed to cover assembly of the core barrel, making connection between the liquid nitrogen (LN) tank, freezing of the core, removal of the core from the core barrel, and packing the core. A protocol has been developed for laboratory analysis of those cores and is discussed in Appendix C.

At the conclusion of the protocol steps there is a brief section on troubleshooting. The primary function of this section is to deal with freezing of components of the system (e.g., cooling tubes, core barrel in auger, and core liner in core barrel). We believe that both the protocols and the troubleshooting tips will provide sufficient insight to allow an experienced driller to collect cryogenic cores.

1. Prepare the cooling system
 - a. Place the tube retrieval rods into the core barrel.
 - i. These are two 6-foot $\frac{1}{4}$ " OD rods with Swagelok nuts on the ends.
 - ii. They are fed through the holes in the core barrel top in order to pull the cooling coils/cylinder into the core barrel.



- b. Attach the tube retrieval rods to the cooling coils
 - i. The rods feed through the core barrel and connect to the tops of the cooling coil tubes



- c. Pull/push the cooling coil/cylinder into core barrel



- d. Insert the core liner into the core barrel.



- e. Screw the drive shoe onto the core barrel



- f. Connect core barrel to hex rod



- g. Connect LN riser tubes to the cooling coil tubes



- h. Attach the LN riser tubes to the hex rod
- i. Lower hex rod assembly 5 feet
- j. Repeat “g-i” until core barrel is at the sampling depth
- k. Add one length of hex rod above ground surface, as well as lengths of LN riser tube
- l. Attach an additional auger flight



- m. Attach the auger string to the drill rig and advance the drill string 2 to 5 feet, depending on the length of core desired.
- n. Disconnect auger from drill rig



- o. Connect to the LN inlet riser tube to LN supply



- p. Attach the LN effluent pressure control assembly to the LN outlet riser tube
 - i. The solenoid valve should be in the normally open position (not powered)
 - ii. If a manual valve is used, it should be in the open position.
 - iii. NOTE: it is important that the valve used in this application be designed for cryogenic service.



- q. Turn on the LN at the tank
 - i. LN should be discharged from the solenoid valve.
- r. When the temperature at the vent reaches 0 °C the valve should be closed and at that point all of the flow should be out of the orifice (1/8 inch)
- s. After 5-7 minutes of cooling, the LN is turned off, the LN tank line and the pressure manifold are disconnected from the LN riser tubes and the core sample is recovered from the ground.



- t. During core extraction to ground surface the LN riser tubes and the hex rod must be sequentially removed. (Note: depending on the depth, 20-foot sections of the hex rod and riser tubes may be taken off at a time to speed the process.)



- u. Loosen and remove the drive shoe



- v. Remove the core liner from the core barrel
 - i. Note: the liner can become frozen in the core barrel. If necessary, hot water can be circulated through the cooling coils for <1 min to free the core liner from the core barrel.



- w. Cut the core as desired, cap both ends, and label the core.



- x. Pack core in dry ice for shipment to the lab.



- y. Insert a new core liner in the core barrel and return to step “e”

Troubleshooting

- a. Plugging of the LN lines and coil
 - a. During the core recovery process it is possible to get water and other materials in the cooling pipes and coil. Generally this material will be blown out by nitrogen vapor at the beginning of cooling cycle. If not, water may freeze in the lines and plug the flow. In this case it will be necessary to warm the pipes until the water melts and the cooling process can be tried again.
- b. Freezing of the core barrel in the auger
 - a. This sometimes occurs with longer freezing times. In all cases the driller was able to unfreeze the barrel with a combination of downward pressure on the augers, upward pull on the hex rod with the wench, and on rare occasions hitting the hex rod with a large hammer.
- c. Freezing of the core liner in the core barrel
 - a. If freezing times are long, there is a greater risk of freezing the sample in the core barrel. The strategy we have used to free the liner is to flush hot water through the cooling coils just until the liner releases from the coils (usually less than 20 seconds). In our experience, this did not result in appreciable thawing of the core sample.

- b. Following this process there is an increased chance that water remaining in the lines will freeze. So, care should be taken to remove water prior to the next freezing cycle.



- d. Freezing of the auger flights in the ground
 - a. In some cases the augers can become frozen and are not readily retrieved. In all cases the drillers employed a combination of “tricks” to free the augers. Freezing of the augers is not common in our experience when LN delivery times are kept <~5 min. Breaking the augers free rarely required more than 5 minutes.

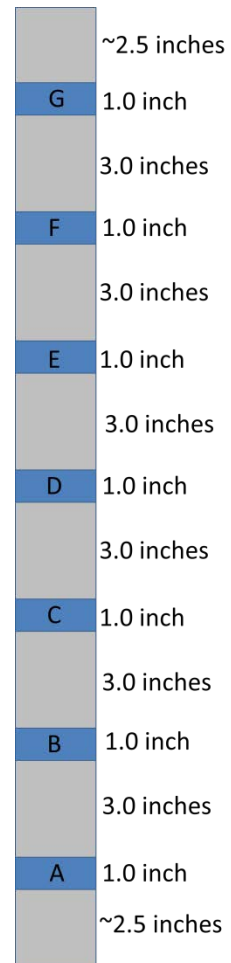
Appendix C: Protocol for High-Throughput Core Analysis

This section presents a protocol developed for High-Throughput Core Analysis by the project team. The procedures were developed to generate data on frozen cores collected using Cryogenic Core Collection techniques. This protocol is designed for cores that were cryogenically collected and maintained in a frozen state during storage.

Cutting of Cores (day 1)

Frozen core sections are removed from a frozen environment (i.e., either in a freezer or on dry ice), one section at a time, immediately prior to processing. This procedure describes cutting of full length (typically 30-inches) cores into samples for subsequent extraction and analyses.

- Materials and equipment
 - Saw (cut-off saw with 14-inch diameter, 1/8-inch thick blade)
 - Scale (up to 1 kg, 1 decimal)
 - Aluminum foil
 - 1-qt zip lock bags
 - Sample log sheet (see below)
- Preparation
 - Aluminum foil into small squares (8-inch)
 - Label small and large zip lock bags
- Methods
 - Remove one section of core (30-inch) from freezer
 - Cut into sections (see figure →)
 - Small pieces (“hockey pucks”): process each piece, immediately after cutting, as described in the next section
 - Wrap 3-inch non-sampled core section in aluminum foil and place in zip lock baggies; these “waste” sections are returned to the freezer
- Results
 - 1-inch core sub-segments processed as described in next phase
 - 3-inch core sub-segments returned to freezer

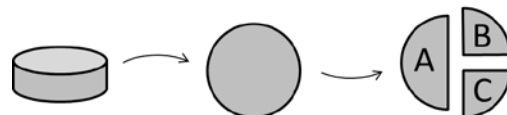


Core Sample Processing (day 1 – immediately after cutting core)

This procedure describes processing of the 1-inch-thick frozen-core samples (i.e., “hockey pucks”) generated in the previous task. These processing steps are completed for each sample

immediately after being generated, while samples remain frozen. As described herein, the samples are subdivided for subsequent extractions and analysis.

- Materials and equipment
 - Dremmel tool
 - Small vice (portable, used in hood)
 - Big hammer (4-lb.)
 - Chisel (4-inch wide by 7 ½-inch long tile chisel)
 - Hard plate
 - Ring (3-inch PVC, cut to size, with notch in one side to make room for chisel)
 - Sample jars: methanol extract (4-oz glass jars with PTFE-lined, closed caps)
 - Sample jars: water extract (4-oz glass jars with PTFE-lined, septum caps)
- Preparation
 - Methanol extraction
 - Label jars
 - Measure out 80 mL of methanol into each jar and close lid
 - Record weight
 - Water extraction
 - A sufficient quantity of deionized water is equilibrated in an anaerobic chamber (for about 2 days)
 - Label 4-oz glass septa-cap jars
 - In anaerobic chamber, fill each jar to the top with de-aired, de-ionized water
 - Record weight of each jar with water
 - Store jars in anaerobic chamber until use
 - Biological analytical sample
 - Cut 6-inch aluminum-foil squares, label
- Methods
 - Collect freshly cut “hockey puck” from saw
 - Use Dremmel tool to cut through plastic casing, remove the plastic casing
 - Place puck inside PVC ring, on hard plate
 - Split down middle with hammer and chisel
(see figure →)
 - Collect one half for bio analysis
 - Wrap with aluminum foil, place in Ziploc[®] back, and return to freezer (or on dry ice) immediately
 - Split other half in half again (i.e., quarters)



- One quarter in methanol, other quarter in water
 - Methanol extraction
 - Place sample in methanol jar and close cap immediately
 - Record weight
 - Perform enhanced extraction procedures (i.e., vortex shaking and/or sonication)
 - Store at about 4 °C
 - Water extraction
 - Before sampling, place sample container in plastic bowl, and place on scale
 - Tare the scale with bowl and water-filled water-extract jar
 - Remove lid, and carefully add sample to water extract jar, thus displacing water from the extract jar into the plastic bowl (notes: (a) while adding the sample, be careful to not splash water; (b) make sure water level remains level with the top so there is no headspace after re-sealing)
 - Carefully replace cap on sampling container, such that little-to-no headspace is present in the jar
 - Record weight of plastic bowl with water-extract jar and excess water (if properly tared, the scale will directly read the total sample mass)
 - Tumble or vortex to mix
 - Store at about 4 °C for one-or-more days, allowing for solids to settle
 - Subsequent processing of methanol- and water-extract samples is described in the following sections
- Results
 - End product – extraction jars with sample submersed in methanol or water, stored at 4 °C
 - Continue processing over the next few days

Methanol-Extract: Processing (day 2-5)

This procedure describes transfer of liquid extract from the methanol-extract jar into a GC vial to analyze for halogenated organic compounds, particularly TCE and PCE.

- Materials and equipment
 - 2-mL GC analytical vials
 - 1-mL pipette
- Methods

- Transfer methanol extract phase into GC vial for analysis
- Analyze extract on gas chromatograph with electron capture detector (GC/ECD) for halogenated organic compounds
- Results
 - GC/ECD data for TCE and PCE

Water-Extract: Primary Processing (day 2-5)

This procedure describes transfer of an aqueous subsample from the water-extract jar into a headspace vial to analyze for organic compounds. Following this procedure, the transfer occurs with no exposure of the aqueous sample to the atmosphere, thus reducing the chances for loss of organics due to volatilization. Once transferred to the headspace vial, the sample can be analyzed for gas-phase organics (e.g., methane and ethane) and volatile organic compounds (e.g., TCE and PCE).

- Materials and equipment
 - 20-mL headspace analytical vials with crimp-seal PTFE-lined septa caps
 - 5-mL syringe
 - DA/DI water in tedlar bag with Luer fitting (female, so syringe can attach)
 - Needle assembly (see figure →)
 - 20-mL headspace vials with PTFE-lined septa caps
 - Extra 27-gauge by ½-inch-long needles
- Preparation
 - Crimp caps on empty headspace vials (anaerobic)
 - Label headspace vials
 - Construct two or more needle assemblies, such that one can be decontaminated while another is being used
 - Record empty weights of crimp-sealed headspace vials
- Methods
 - Note: due to potential instability of chemical concentrations in the the headspace vials, the transfers described herein should only be conducted on the day in which they will be analyzed. The analytical method we used required about 25 minutes per sample
 - Attach water-extract jar to headspace vial via assembly (see figure →)
 - Collect >5 mL of DA/DI water in syringe; attach ½-inch × 27-gauge needle to syringe; purge water upward to purge air until syringe-plunger is at 5-mL mark
 - Inject 5 mL of DA/DI water into extract vial, thus displacing water into headspace vial



- While holding syringe-plunger in place, clamp tubing on needle assembly. Release plunger on syringe to relieve pressure in the water-extraction vial. Remove headspace vial (note: vial is under pressure)
- Remove all needles from water-extract jar.
- After sample collection complete, store headspace vials upside down, until analysis; return water-extracton vial to 4 °C storage to preserve for other analyses (e.g., anions and cations)
- Within 24 hours of transfer to headspace vial
 - Analyze headspace vials on gas chromatograph with flame ionization detector (GC/FID) with headspace autosampler; use GC method for PCE, TCE, down to ethene, ethane, and methane (analytical method details are described in the companion SERDP ER-1740 project report)
- Results
 - Water-extraction results for chlorinated and non-chlorinated compounds
 - Convert data back to dry-weight concentration basis

Water Extract: Secondary Processing (days 5-7)

Methods are presented here to analyze aqueous extract remaining after transfer for headspace analysis. The water extract could be analyzed for any number of parameters; analytical methods are presented herein for ferrous iron (Fe^{2+}), dissolved ions (anions or cations), pH, and ORP.

- Materials and equipment
 - Hach (Loveland, CO) Ferrous Iron Reagent Pillow
 - Spectrophotometric cuvettes (2-mL)
 - Ion chromatography vials
 - 5-mL pipette
 - ORP and pH probes
- Preparation
 - Calibrate pH meter
 - Dissolve Ferrous Iron Reagent in DI water to create stock reagent solution: 1 pillow per 4.167 mL water
- Methods
 - Ferrous iron
 - Transfer 1800 μL water extract into 2-mL cuvette
 - Add 200 μL ferrous iron reagent stock solution to sample (this provides reagent at the same ratio as 1 pillow per 25 mL, as specified in Hach method 8146)
 - Analyze on a spectrophotometer at a wavelength of 510 nm
 - Dissolved ions

- Using pipette, transfer 10 mL (or another amount, as required per instrument-specific analysis) into an IC vial
 - Analyze on IC
 - pH and ORP
 - Calibrate pH probe
 - Submerge probes into samples and record values
- Results
 - Fe²⁺, dissolved iron, pH, and ORP data

Date: _____ Time: _____

Core location: _____

Core depth interval: _____

Core length, measured: _____

Core recovery: _____

Sample numbers



Notes:

Date: _____ Time: _____

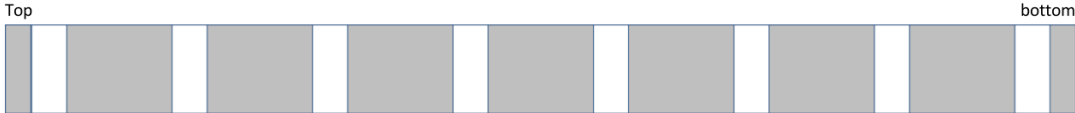
Core location: _____

Core depth interval: _____

Core length, measured: _____

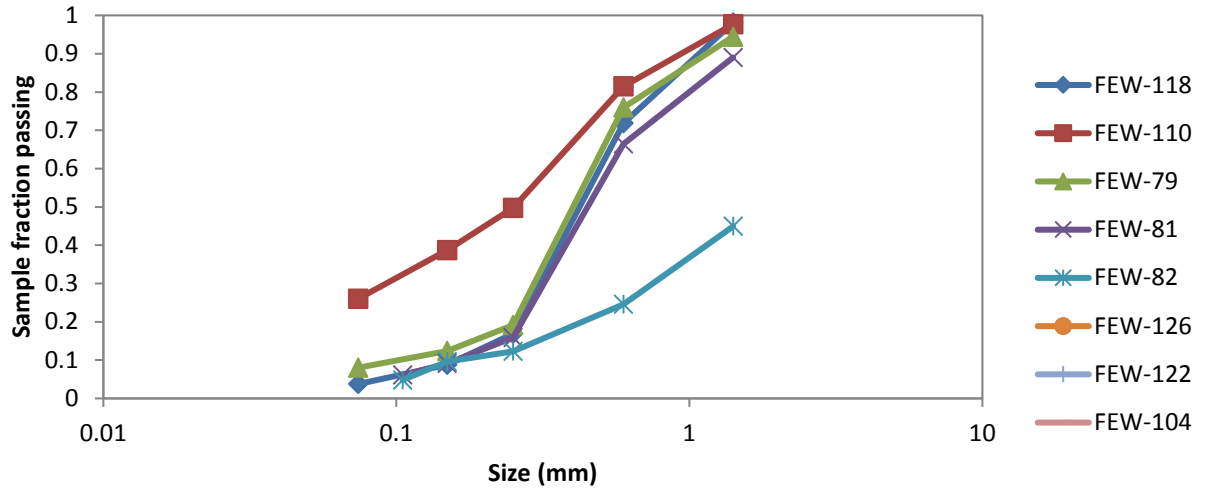
Core recovery: _____

Sample numbers



Notes:

Appendix D: K-Testing Particle Size Distribution Curves



Appendix E: Geologic Log Data Table

Sample No	Core location	calc depth (ft)	Size			Sorting			description				NAPL			color					Cementation			Comments* *mineralogical abbreviations defined at bottom of table		
			sand	silt	clay	well	moderate	poor	-silt	-fine	-medium	-coarse	mobil	residual	sheen	black	red	tan	light brwn	grey	white	well	moderate		poor	
9	MW173F	14.082	x			x					x							x						x		
10	MW173F	14.4428	x			x					x							x						x		
11	MW173F	14.8036	x			x					x							x						x		
12	MW173F	15.1644	x			x					x							x						x		
13	MW173F	15.5252	x			x					x							x						x		mv
14	MW173F	15.886	x			x					x							x						x		
1	MW173F	16.982	x				x				x	x						x						x		
2	MW173F	17.31	x				x				x	x						x						x		
3	MW173F	17.638	x				x				x	x						x						x		
4	MW173F	17.966		x		x					x							x						x		
5	MW173F	18.294	x				x				x	x						x							x	mv
6	MW173F	18.622	x				x				x	x						x							x	
7	MW173F	18.95		x			x				x	x						x		x					x	
8	MW173F	19.278	x			x						x						x							x	
43	MW173F	19.414		x		x					x							x		x					x	
44	MW173F	19.7748		x			x				x	x						x		x					x	
45	MW173F	20.1356		x			x				x	x						x		x					x	
46	MW173F	20.4964	x				x				x	x						x		x					x	
47	MW173F	20.8572	x			x						x														x
48	MW173F	21.218	x					x			x	x	x					x							x	

Sample No	Core location	calc depth (ft)	Size			Sorting			description				NAPL			color					Cementation			Comments* *mineralogical abbreviations defined at bottom of table				
			sand	silt	clay	well	moderate	poor	-silt	-fine	-medium	-coarse	mobil	residual	sheen	black	red	tan	light brwn	grey	white	well	moderate		poor			
24	MW173F	30.0536	x					x		x	x							x								x	q,fs,mc	
25	MW173F	30.4144	x				x			x								x									x	
26	MW173F	30.7752	x				x			x								x									x	
27	MW173F	31.136	x				x			x								x									x	
28	MW173F	31.4968	x				x		x	x								x									x	
36	MW173F	31.832	xx				x			x	x							x								x		
37	MW173F	32.1928	x			x				x								x									x	
38	MW173F	32.5536	x			x				x								x									x	
39	MW173F	32.9144	x			x				x								x									x	
40	MW173F	33.2752	x			x				x								x									x	
41	MW173F	33.636	x			x				x								x									x	q,fs,hb
42	MW173F	33.9968		x		x				x								x									x	q,fs,hb
15	MW173F	34.332	x			x				x								x								x		q,hb
16	MW173F	34.6928	x			x				x								x								x		q,hb
17	MW173F	35.0536	x			x				x								x								x		q,hb
18	MW173F	35.4144	x			x				x								x								x		q,hb
19	MW173F	35.7752	x			x				x								x								x		q,hb
20	MW173F	36.136	x			x				x								x								x		q,hb
21	MW173F	36.4968	x			x				x								x								x		q,hb
57	MW173F	36.832	x			x				x								x									x	
58	MW173F	37.1928	x			x				x								x									x	
59	MW173F	37.5536	x			x				x								x									x	
60	MW173F	37.9144	x			x				x								x									x	
61	MW173F	38.2752	x			x				x								x									x	

Sample No	Core location	calc depth (ft)	Size			Sorting			description				NAPL			color					Cementation			Comments* *mineralogical abbreviations defined at bottom of table	
			sand	silt	clay	well	moderate	poor	-silt	-fine	-medium	-coarse	mobil	residual	sheen	black	red	tan	light brwn	grey	white	well	moderate		poor
62	MW173F	38.636	x			x				x							x							x	
63	MW173F	38.9968	x			x				x							x							x	
96	MW38C	9.082	x			x				x							x						x	q,fs,hb	
97	MW38C	9.4428	x			x				x							x						x		
98	MW38C	9.8036	x			x				x							x						x	q,fs,mv	
99	MW38C	10.1644	x			x				x							x						x	q,fs,mv	
100	MW38C	10.5252	x			x				x							x						x	q,fs,mv	
101	MW38C	10.886	x			x				x							x						x	q,fs,mv	
102	MW38C	11.2468	x			x				x							x						x	q,fs,mv	
103	MW38C	11.582	x				x			x	x						x						x	q,fs,mc,mv	
104	MW38C	11.9428	x			x				x							x						x		
105	MW38C	12.3036	x						x	x	x						x						x	q,fs,hb	
106	MW38C	12.6644	x						x	x	x						x						x	q,fs,hb	
107	MW38C	13.0252	x				x			x	x						x						x	q,fs,hb	
108	MW38C	13.386	x			x				x							x						x	q,fs,mc,hb	
109	MW38C	14.984		x			x			x	x						x						x		
110	MW38C	15.3448		x		x				x							x						x		
111	MW38C	15.7056	x				x			x	x						x						x	q,fs,mc,hb	
112	MW38C	16.0664	x			x				x							x					x			
113	MW38C	17.582		x		x				x							x						x		
114	MW38C	17.9428	x						x	x	x						x						x	q,fs,hb,mc	
115	MW38C	18.3036	x						x	x	x						x						x	q,fs,hb,mc	
116	MW38C	18.6644	x						x	x	x						x						x	q,fs,hb,mc	
117	MW38C	18.9596	x			x				x							x						x		

Sample No	Core location	calc depth (ft)	Size			Sorting			description				NAPL			color					Cementation			Comments* *mineralogical abbreviations defined at bottom of table			
			sand	silt	clay	well	moderate	poor	-silt	-fine	-medium	-coarse	mobil	residual	sheen	black	red	tan	light brwn	grey	white	well	moderate		poor		
118	MW38C	19.082	x				x			x	x						x	x							x	q,fs,hb,mc	
119	MW38C	19.4428	x					x	x									x							x		
120	MW38C	19.8036		x		x												x							x		
121	MW38C	20.1644	x					x										x	x						x	q,fs	
122	MW38C	20.5252		x			x										x		x						x		
123	MW38C	20.886	x					x									x		x						x	q,fs,mv	
124	MW38C	21.2468	x					x									x		x						x	q,fs,mv	
125	MW38C	21.582	x					x									x	x							x	q,fs,hb	
126	MW38C	21.9428		x			x											x							x		
127	MW38C	22.3036		x			x										x		x						x	q,hb	
128	MW38C	22.6644		x			x										x		x						x	q,hb	
77	MW700C	9.082	x			x				x											x					x	
78	MW700C	9.4428	x			x				x											x					x	
79	MW700C	9.8036	x			x				x											x					x	
80	MW700C	10.1644	x					x	x	x											x						q,fs,mv
81	MW700C	10.5252	x					x		x	x										x						q,fs,hb,mv
82	MW700C	10.886	x				x			x	x										x					x	
83	MW700C	11.2468	x				x			x	x										x					x	with pebble (granite)
84	MW700C	11.582		x			x			x	x										x					x	
85	MW700C	11.9428		x			x			x	x										x					x	
86	MW700C	12.3036		x			x			x	x										x					x	
87	MW700C	12.6644		x			x			x	x										x					x	
89	MW700C	13.5572	x			x				x									x	x						x	organics
88	MW700C	13.918	x			x				x																x	root

Sample No	Core location	calc depth (ft)	Size			Sorting			description				NAPL			color					Cementation			Comments* *mineralogical abbreviations defined at bottom of table			
			sand	silt	clay	well	moderate	poor	-silt	-fine	-medium	-coarse	mobil	residual	sheen	black	red	tan	light brwn	grey	white	well	moderate		poor		
90	MW700C	14.41	x			x				x							x		x							x	
91	MW700C	14.7708	x			x				x							x		x							x	
92	MW700C	15.1316	x			x				x								x								x	q,fs,hb
93	MW700C	15.4924	x			x				x								x								x	q,fs,hb
94	MW700C	15.8532	x			x				x								x								x	q,fs,hb
95	MW700C	16.214	x			x				x								x								x	q,fs,hb
71	MW700C	16.582	x				x			x	x							x								x	q,fs,mc
72	MW700C	16.664	x				x			x	x							x								x	q,fs,mc
73	MW700C	16.746	x			x				x								x							x		q,fs,mc
74	MW700C	16.828	x			x				x								x							x		q,fs,mc
75	MW700C	16.91	x			x				x								x							x		q,fs,mc
76	MW700C	16.992	x			x				x								x							x		q,fs,mc

fs = feldspar, hb = horn blend, mc = microcline, mv = muscovite, q = quartz

Appendix F. Calculation of Dissolved TCE Concentrations

Sample ID	Core location	calc depth (ft)	porosity	dry bulk density (g/mL)	foc	Kd (L/kg)	TCE conc (µg/kg)	TCE water conc (µg/L)	TCE sorbed conc (µg/kg)
1	MW173F	16.98	0.20	2.27	0.00%	0.000	9.3	105.3	0.0
2	MW173F	17.31	0.37	1.89	0.00%	0.000	20.5	105.3	0.0
3	MW173F	17.64	0.31	1.67	0.00%	0.000	20.8	110.8	0.0
4	MW173F	17.97	0.47	1.46	0.01%	0.006	40.5	122.8	0.8
5	MW173F	18.29	0.44	1.55	0.07%	0.066	21.4	57.7	3.8
6	MW173F	18.62	0.30	1.74	0.08%	0.077	23.2	85.9	6.6
7	MW173F	18.95	0.48	1.48	0.01%	0.011	44.9	132.7	1.5
8	MW173F	19.28	0.49	1.47	0.05%	0.045	82.7	209.8	9.5
9	MW173F	14.08	0.37	1.71	0.07%	0.070	35.8	116.7	8.1
10	MW173F	14.44	0.36	1.77	0.11%	0.107	66.1	193.9	20.7
11	MW173F	14.80	0.40	1.66	0.11%	0.102	49.2	130.6	13.3
12	MW173F	15.16	0.18	2.23	0.03%	0.028	16.2	136.4	3.8
13	MW173F	15.53	0.45	1.48	0.04%	0.037	49.8	142.5	5.2
14	MW173F	15.89	0.40	1.69	0.07%	0.063	32.7	102.4	6.5
15	MW173F	34.33	0.36	1.75	0.09%	0.089	25.3	78.0	7.0
16	MW173F	34.69	0.41	1.73	0.06%	0.062	18.0	56.6	3.5
17	MW173F	35.05	0.37	1.77	0.09%	0.090	11.9	36.9	3.3
18	MW173F	35.41	0.36	1.75	0.12%	0.113	7.9	22.5	2.5
19	MW173F	35.78	0.38	1.66	0.06%	0.056	11.3	37.4	2.1
20	MW173F	36.14	0.33	2.11	0.08%	0.082	15.4	58.3	4.8
21	MW173F	36.50	0.42	2.00	0.05%	0.051	24.9	90.0	4.6

22	MW173F	29.33	0.36	1.89	0.02%	0.024	20.5	92.7	2.2
23	MW173F	29.69	0.31	1.76	0.00%	0.000	12.7	72.7	0.0
24	MW173F	30.05	0.37	1.76	0.03%	0.026	19.8	81.1	2.1
25	MW173F	30.41	0.40	1.58	0.03%	0.032	31.0	105.8	3.4
26	MW173F	30.78	0.46	1.48	0.08%	0.073	79.5	194.6	14.3
27	MW173F	31.14	0.35	1.81	0.04%	0.037	90.8	375.3	13.7
28	MW173F	31.50	0.35	1.80	0.04%	0.038	91.0	377.7	14.4
29	MW173F	24.33	0.17	2.35	0.00%	0.000	8.6	115.8	0.0
30	MW173F	24.69	0.25	2.11	0.09%	0.087	12.5	53.6	4.7
31	MW173F	25.05	0.32	1.59	0.12%	0.117	16.7	47.4	5.6
32	MW173F	25.41	0.27	2.06	0.03%	0.031	18.4	105.7	3.3
33	MW173F	25.78	0.36	1.65	0.00%	0.000	15.8	72.5	0.0
34	MW173F	26.14	0.38	1.77	0.18%	0.173	17.2	39.3	6.8
35	MW173F	26.50	0.39	1.78	0.07%	0.072	13.0	41.8	3.0
36	MW173F	31.83	0.43	1.57	0.11%	0.102	21.4	52.3	5.3
37	MW173F	32.19	0.44	1.51	0.13%	0.129	108.2	235.7	30.3
38	MW173F	32.55	0.41	1.60	0.06%	0.055	97.3	298.7	16.5
39	MW173F	32.91	0.37	2.44	0.05%	0.051	96.5	440.1	22.4
40	MW173F	33.28	0.36	1.78	0.06%	0.054	85.9	317.1	17.2
41	MW173F	33.64	0.30	1.78	0.10%	0.094	60.6	207.0	19.4
42	MW173F	34.00	0.30	1.91	0.06%	0.057	44.5	193.0	10.9
43	MW173F	19.41	0.43	1.59	0.10%	0.092	63.4	162.7	15.0
44	MW173F	19.77	0.45	1.62	0.05%	0.048	61.1	180.9	8.7
45	MW173F	20.14	0.30	1.85	0.08%	0.073	57.2	222.9	16.3
46	MW173F	20.50	0.28	1.98	0.04%	0.035	10.4	55.0	1.9
47	MW173F	20.86	0.28	1.97	0.04%	0.042	10.9	54.8	2.3
48	MW173F	21.22	0.29	1.99	0.03%	0.031	23.5	127.3	3.9

49	MW173F	21.41	0.28	1.87	0.04%	0.035	25.5	129.3	4.5
50	MW173F	26.83	0.33	1.82	0.31%	0.302	39.4	68.6	20.7
51	MW173F	27.19	0.30	1.89	0.22%	0.217	55.7	126.2	27.4
52	MW173F	27.55	0.22	2.14	0.00%	0.000	44.7	431.1	0.0
53	MW173F	27.91	0.18	2.30	0.00%	0.000	14.8	187.5	0.0
54	MW173F	28.28	0.27	2.06	0.00%	0.000	7.4	56.3	0.0
55	MW173F	28.64	0.26	2.05	0.00%	0.000	7.7	59.5	0.0
56	MW173F	29.00	0.20	2.17	0.07%	0.068	6.8	37.1	2.5
57	MW173F	36.83	0.34	1.80	0.05%	0.052	41.7	162.3	8.5
58	MW173F	37.19	0.41	1.61	0.04%	0.043	66.4	212.3	9.1
59	MW173F	37.55	0.37	1.74	0.04%	0.041	90.4	343.5	13.9
60	MW173F	37.91	0.38	1.71	0.04%	0.040	88.6	322.4	13.0
61	MW173F	38.28	0.37	1.68	0.05%	0.048	96.8	344.5	16.5
62	MW173F	38.64	0.36	1.72	0.05%	0.051	96.0	346.4	17.8
63	MW173F	39.00	0.38	1.70	0.04%	0.035	93.4	343.9	12.0
64	MW173F	21.83	0.32	1.76	0.08%	0.073	15.9	57.0	4.2
65	MW173F	22.19	0.33	1.81	0.05%	0.051	11.5	46.1	2.3
66	MW173F	22.55	0.25	2.10	0.03%	0.030	12.1	77.3	2.3
67	MW173F	22.91	0.30	1.77	0.00%	0.000	7.7	45.7	0.0
68	MW173F	23.28	0.38	1.71	0.00%	0.000	11.1	49.8	0.0
69	MW173F	23.64	0.24	2.13	0.00%	0.000	5.0	44.1	0.0
70	MW173F	24.00	0.20	2.25	0.08%	0.073	7.0	37.7	2.8
71	MW700C	16.58	0.44	1.54	0.03%	0.028	69.3	214.8	6.1
72	MW700C	16.66	0.41	1.54	0.18%	0.174	97.3	196.5	34.1
73	MW700C	16.75	0.40	1.09	0.08%	0.075	114.7	246.5	18.5
74	MW700C	16.83	0.46	1.57	0.18%	0.179	82.4	156.7	28.0
75	MW700C	16.91	0.45	1.58	0.24%	0.232	176.8	302.0	70.2

76	MW700C	16.99	0.33	1.85	0.06%	0.057	106.3	421.1	24.0
77	MW700C	9.08	0.58	1.14	0.34%	0.329	54.6	58.5	19.2
78	MW700C	9.44	0.47	1.44	0.21%	0.207	9.8	16.5	3.4
79	MW700C	9.80	0.39	1.61	0.10%	0.099	6.5	17.6	1.7
80	MW700C	10.16	0.43	1.59	0.14%	0.133	6.1	13.8	1.8
81	MW700C	10.53	0.32	1.86	0.05%	0.050	6.6	27.6	1.4
82	MW700C	10.89	0.29	2.09	0.09%	0.084	7.7	31.3	2.6
83	MW700C	11.25	0.28	1.96	0.19%	0.181	17.3	45.8	8.3
84	MW700C	11.58	0.48	1.53	0.39%	0.374	33.6	42.2	15.8
85	MW700C	11.94	0.37	1.78	0.17%	0.165	9.0	21.2	3.5
86	MW700C	12.30	0.41	1.57	0.22%	0.209	10.9	20.4	4.3
87	MW700C	12.66	0.37	1.75	0.10%	0.093	12.5	37.6	3.5
88	MW700C	13.92	0.35	1.83	0.06%	0.062	233.5	849.7	52.6
89	MW700C	13.56	0.48	1.42	0.12%	0.116	17.8	36.3	4.2
90	MW700C	14.41	0.38	1.67	0.13%	0.128	400.1	1021.8	131.0
91	MW700C	14.77	0.37	1.71	0.09%	0.089	365.2	1112.9	98.6
92	MW700C	15.13	0.35	1.79	0.08%	0.074	271.8	927.3	68.8
93	MW700C	15.49	0.34	1.87	0.06%	0.055	249.6	991.5	54.7
94	MW700C	15.85	0.34	1.85	0.07%	0.067	222.1	814.7	55.0
95	MW700C	16.21	0.34	1.81	0.11%	0.111	210.7	635.4	70.5
96	MW38C	9.08	0.20	2.31	4.03%	3.913	18.4	3.6	13.9
97	MW38C	9.44	0.34	1.85	0.06%	0.055	36.2	140.7	7.7
98	MW38C	9.80	0.34	1.75	0.10%	0.093	53.3	167.7	15.6
99	MW38C	10.16	0.33	1.86	0.03%	0.031	38.5	175.5	5.4
100	MW38C	10.53	0.30	2.07	0.03%	0.025	23.3	131.7	3.2
101	MW38C	10.89	0.33	2.00	0.01%	0.013	41.3	230.4	2.9
102	MW38C	11.25	0.32	1.70	0.00%	0.000	34.0	182.7	0.0

103	MW38C	11.58	0.31	1.88	0.05%	0.053	14.6	62.5	3.3
104	MW38C	11.94	0.32	1.92	0.05%	0.046	34.3	153.3	7.1
105	MW38C	12.30	0.27	1.98	0.00%	0.000	30.2	218.2	0.0
106	MW38C	12.66	0.33	2.05	0.26%	0.249	20.9	43.2	10.8
107	MW38C	13.03	0.25	2.06	0.32%	0.306	29.0	56.1	17.2
108	MW38C	13.39	0.31	1.93	0.00%	0.000	34.1	212.9	0.0
109	MW38C	14.98	0.30	2.00	0.05%	0.049	26.2	121.5	6.0
110	MW38C	15.34	0.36	1.73	0.26%	0.257	41.2	76.0	19.5
111	MW38C	15.71	0.29	2.05	0.01%	0.014	33.7	209.2	2.9
112	MW38C	16.07	0.24	2.13	0.05%	0.050	26.7	148.7	7.5
113	MW38C	17.58	0.44	1.87	0.12%	0.112	24.9	65.4	7.3
114	MW38C	17.94	0.32	1.87	0.00%	0.000	19.3	112.7	0.0
115	MW38C	18.30	0.33	1.84	0.00%	0.000	11.3	63.2	0.0
116	MW38C	18.66	0.32	1.90	0.00%	0.000	4.9	28.9	0.0
117	MW38C	18.96	0.37	1.72	0.00%	0.001	8.5	39.1	0.0
118	MW38C	19.08	0.34	1.81	0.08%	0.077	6.4	22.1	1.7
119	MW38C	19.44	0.42	1.60	0.02%	0.020	6.1	20.9	0.4
120	MW38C	19.80	0.47	1.45	0.43%	0.412	18.4	21.3	8.8
121	MW38C	20.16	0.35	1.77	0.02%	0.021	15.7	69.9	1.4
122	MW38C	20.53	0.47	1.46	0.00%	0.000	8.5	26.4	0.0
123	MW38C	20.89	0.34	1.83	0.00%	0.000	14.8	80.4	0.0
124	MW38C	21.25	0.26	2.06	0.07%	0.071	9.5	43.4	3.1
125	MW38C	21.58	0.28	2.14	0.08%	0.079	8.8	37.9	3.0
126	MW38C	21.94	0.33	1.84	0.14%	0.139	11.1	31.0	4.3
127	MW38C	22.30	0.53	1.22	0.35%	0.343	6.8	7.7	2.6
128	MW38C	22.66	0.31	1.98	0.02%	0.021	20.8	113.3	2.4

